DISSERTATIONES
MEDICINAE
UNIVERSITATIS
TARTUENSIS
255

KALEV NÕUPUU

Autosomal-recessive Stargardt disease: phenotypic heterogeneity and genotype-phenotype associations

DISSERTATIONES MEDICINAE UNIVERSITATIS TARTUENSIS
255

DISSERTATIONES MEDICINAE UNIVERSITATIS TARTUENSIS
255

KALEV NÕUPUU

Autosomal-recessive Stargardt disease: phenotypic heterogeneity and genotype-phenotype associations

UNIVERSITY OF TARTU
Press

Department of Ophthalmology, University of Tartu, Estonia

This dissertation has been accepted for the commencement of the degree of Doctor of Philosophy (Medicine) on the 15th of March, 2017 by the Council of the Faculty of Medicine, University of Tartu, Estonia

Supervisors: Kuldar Kaljurand, MD, PhD, Department of Ophthalmology, Faculty of Medicine, University of Tartu, Estonia

Professor Rando Allikmets, PhD, Department of Ophthalmology and Department of Pathology & Cell Biology, Columbia University, USA

Reviewers: Professor Pille Taba, MD, PhD, Department of Neurology and Neurosurgery, University of Tartu, Estonia

Professor Katrin Õunap, MD, PhD, Department of Clinical Genetics, University of Tartu, Estonia

Opponent: Associate Professor Bart Peter Leroy, MD, PhD, Department of Ophthalmology and Center of Medical Genetics, Ghent University Hospital& Ghent University, Belgium.

Chairman and Head of Department, Department of Ophthalmology, Ghent University Hospital & Ghent University, Belgium.

Attending Physician, Ophthalmic Genetics and Visual Electrophysiology, Division of Ophthalmology and Center for Cellular and Molecular Therapeutics, The Children's Hospital of Philadelphia, USA.

Commencement: June 14th, 2017

This study was supported by grants from the National Eye Institute/National Institutes of Health (Bethesda, MD, USA) EY021163, EY019861, and EY019007 (Core Support for Vision Research), Foundation Fighting Blindness (Owings Mills, MD, USA), and an unrestricted funds from Research to Prevent Blindness (New York, NY, USA) to the Department of Ophthalmology, Columbia University.

ISSN 1024–395X
ISBN 978-9949-77-423-4 (print)
ISBN 978-9949-77-424-1 (pdf)

University of Tartu Press
www.tyk.ee

TABLE OF CONTENTS

LIST OF ORIGINAL PUBLICATIONS

Paper I:
Lee, W*., Nõupuu, K*., Oll, M., Duncker, T., Burke, T., Zernant, J., Bearelly, S., Tsang, S. H., Sparrow, J. R., Allikmets, R. 2014. The External Limiting Membrane in Early-Onset Stargardt Disease. *Invest Ophthalmol Vis Sci,* 55, 6139–49.

Paper II
Nõupuu, K., Lee, W., Zernant, J., Tsang, S. H., Allikmets, R. 2014. Structural and Genetic Assessment of the *ABCA4*-Associated Optical Gap Phenotype. *Invest Ophthalmol Vis Sci,* 55, 7217–26.

Paper III
Nõupuu, K., Lee, W., Zernant, J., Greenstein, V. C., Tsang, S. H., Allikmets, R. 2016. Recessive Stargardt Disease Phenocopying Hydroxychloroquine Retinopathy. Graefes Arch Clin Exp Ophthalmol, 254, 865–72.

* These authors contributed equally to this work.

Contribution of the author to the preparation of the original publications:

Paper I: Working with clinical and genetic databases, participation in the design of the study, patient recruitment, retinal imaging, data analysis and interpretation as well as participation in the manuscript writing process.

Paper II: Participation in the patient recruitment and retinal imaging, working with clinical and genetic databases, proposing the research idea, planning the study design, analyzing the phenotypic and clinical data, proposing the phenotype grading system and detecting the genotype-phenotype association, preparing the figures and writing the first manuscript draft.

Paper III: Participation in the patient recruitment and retinal imaging, working with clinical and genetic databases, presenting the research idea, designing the study, analyzing the data (images and clinical data), preparing the figures and writing the first manuscript draft.

ABBREVIATIONS

ABCA4	Retinal-specific ATP-binding cassette transporter
ABCA4	A gene which encodes the ABCA4 transporter
AF	Autofluorescence
AMD	Age-related macular degeneration
ATP	Adenosine triphosphate
A2E	N-retinylidene-N-retinylethanolamine
BCVA	Best-corrected visual acuity
BEM	Bull's eye maculopathy
cSLO	Confocal scanning laser ophthalmoscope
ECD	Exocytoplamatic domain
ELM	External limiting membrane
EZ	Ellipsoid zone
(ff)ERG	(Full-filed) electroretinography
FAF	Fundus autofluorescence
GCL	Ganglion cell layer
HCQ	Hydroxychloroquine (Plaquenil)
ICC	Intraclass correlation coefficient
ILM	Internal limiting membrane
INL	Inner nuclear layer
IPL	Inner plexiform layer
IS	Inner segment
IZ	Interdigitation zone
mfERG	Multifocal electroretinography
NBD	Nucleotide binding domain
NGS	Next-generation sequencing
ONL	Outer nuclear layer
OPL	Outer plexiform layer
OS	Outer segment
PERG	Pattern electoretinography
RPE	Retinal pigment epithelium
RDH8	Retinol dehydrogenase 8
(SD)-OCT	(Spectral-domain) optical coherence tomography
STGD1	Stargardt disease
TMD	Transmembrane domain

1. INTRODUCTION

Stargardt disease (STGD1) is the most common form of juvenile-onset macular dystrophy with the estimated prevalence between 1:8000 to 1:10 000 worldwide (Michaelides et al., 2003). Although it is not a very common disease, it causes progressive visual loss from childhood or early adolescence affecting substantially a person's everyday life.

The disease is caused by mutations in the *ABCA4* gene, which encodes the photoreceptor specific transporter vital in the visual cycle (Allikmets et al., 1997b). The dysfunctional transporter leads to photoreceptor degeneration and visual deterioration (Molday and Zhang, 2010). To date, more than 1000 disease causing mutations have been described resulting in remarkable allelic and phenotypic heterogeneity (Zernant et al., 2014b).

The modern imaging methods enable to detect and assess phenotypic expression on the histological level providing further insights into the pathophysiology of the disease. Furthermore, multimodal imaging enables to expand the phenotypic spectrum permitting to detect new genotype-phenotype associations. New insights into the pathophysiology, phenotypes and genotype-phenotype correlations are essential in the light of ongoing research on gene- and stem cell therapy in STGD1. Therefore, the present study was designed to research the phenotypes and possible phenotype-genotype associations in STGD1 using multimodal imaging. We assessed and analyzed early stage retinal structural changes in young patients with STGD1 and provided further insight into the pathophysiology of the disease. In addition, we acquired some new diagnostic information that may facilitate early diagnosis of STGD1.

2. LITERATURE REVIEW

2.1. Topographic anatomy of the retina

Retina is a light-sensitive neural tissue in the inner surface of the eye responsible for converting light into electrical signals, a process called phototransduction (Sung and Chuang, 2010). It is part of the central nervous system, as it is embryonically derived from the forebrain (Purves et al., 2004). Direct connection with the brain is ensured by the retinal ganglion cell axons which form the optic nerve and transmit the visual impulses to the brain. The optic nerve head, also called optic disc, could be visualized with the ophthalmoscope. It does not contain any photoreceptors and is an entry site for the major retinal blood vessels **(Figure 1)**.

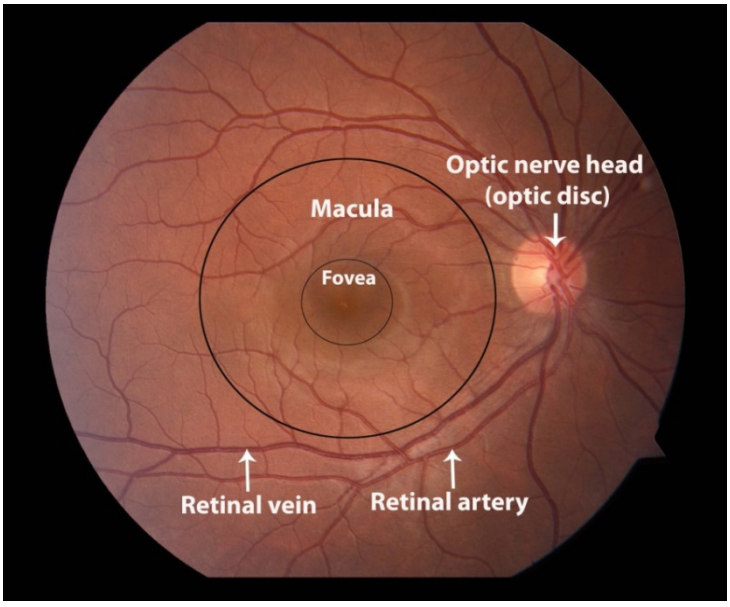

Figure 1. Topography of the fundus. The optic nerve head, also called optic disc, is formed by axons of the ganglion cells. It is an entrance site for major retinal blood vessels. Macula situates between the retinal temporal arcades and is centered by fovea. The center of the macula is cone-dominated and the peripheral retina is rod-dominated.

Topographically, retina can be divided into the central and peripheral retina. The central retina is called macula and it is located between the retinal temporal arteries covering a diameter of approximately 5.5 mm. The macula has central depression with the diameter of 1.5 mm called fovea (Yanoff and Duker, 2004). Ophthalmoscopically, fovea is recognized by the foveal reflex. The loss of foveal reflex could be an early sign of various retinal diseases, including STGD1 (Reynolds and Olitsky, 2011). The bottom of the fovea is called foveola with the diameter of 350 μm. It has the highest concentration of cone photoreceptors

providing the highest visual acuity and resolution as well as color vision (Yanoff and Duker, 2004, Reynolds and Olitsky, 2011). The peripheral retina is rod-dominated and runs from the temporal retinal arteries to the *ora serrata* (Ross and Pawlina, 2011). The main function of the peripheral retina is peripheral and night vision (Yanoff and Duker, 2004).

2.2. Histological layers and different cell types in the retina

2.2.1. Histological layers of the retina

The retina has a laminate structure with anatomically distinct layers and different cell types (Ross and Pawlina, 2011). There are 10 distinct histological layers in the retina: the pigment epithelium layer (RPE), the photoreceptor layer, the external limiting membrane (ELM), the outer nuclear layer (ONL), the outer plexiform layer (OPL), the inner nuclear layer (INL), the inner plexiform layer (IPL), the ganglion cell layer, the nerve fiber layer and the inner limiting membrane (ILM) (Ross and Pawlina, 2011) **(Figure 2)**.

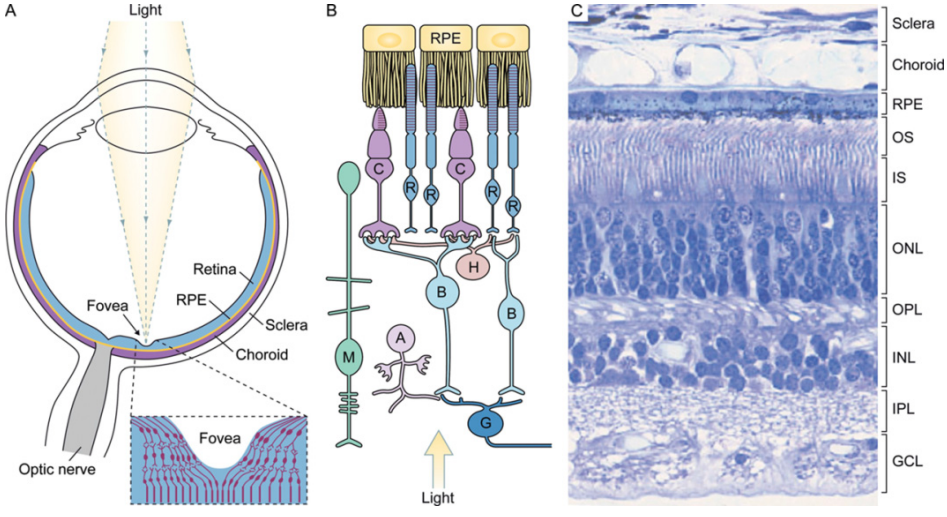

Figure 2. Retina is a light- sensitive tissue lining the inner surface of the eye (A: blue). It contains a variety of cells responsible for visual phototransduction, processing and transmission (B: cones (C) and rods (R), bipolar cells (B), horizontal cells (H), amacrine cells (A), Müller cells (M) and ganglion cells (G)). These cells and their axons form distinct histological layers within the retina (C): pigment epithelium layer (RPE), photoreceptor layer (OS, IS), external limiting membrane (not marked), outer nuclear layer (ONL), outer plexiform layer (OPL), inner nuclear layer (INL), inner plexiform layer (IPL), ganglion cell layer (GCL), nerve fiber layer (not marked) and inner limiting membrane (not marked) (Sung and Chuang, 2010) (with permission from the Rockefeller University Press).

The outermost layer is the RPE layer, which separates the neural retina from the choroid (Ross and Pawlina, 2011). It is a monolayer of RPE cells on the 1–4 μm elastic membrane called Bruch's membrane (Reynolds and Olitsky, 2011). Due to the close affinity to each other, a term RPE-Bruch's membrane complex is sometimes used (Karampelas et al., 2013).

The layer next to the RPE cells is the photoreceptor layer, which consists of photoreceptor light sensitive outer segments (OS), responsible of phototransduction, and inner segments (IS) (Ross and Pawlina, 2011). The nuclei of the photoreceptors form the outer nuclear layer, which is separated from the photoreceptor layer by the external limiting membrane (Ross and Pawlina, 2011). The ELM is formed by the apical ends of Müller cells forming junctional complexes between each other and photoreceptors (Bringmann et al., 2006, Reichenbach and Bringmann, 2013), preventing the passage of large molecules into the inner parts of the retina (Ross and Pawlina, 2011). Each photoreceptor cell body has an axon with synaptic terminal connections with interneuron cells. These connections form the outer plexiform layer responsible for visual impulse transmission. Interneuron cells which have direct connections with photoreceptors are bipolar- and horizontal cells, while additional interneurons responsible for visual processing are amacrine and interplexiform cells (Reynolds and Olitsky, 2011, Ross and Pawlina, 2011). Nuclei of the interneurons and Müller cells are in the inner nuclear layer and more connections between interneurons (amacrine, bipolar, interplexiform) and ganglion cells are formed in the inner plexiform layer. Visual impulses are processed and transferred to ganglion cells, which are situated in the ganglion cell layer. The axons of the ganglion cells form the nerve fiber layer and the optic nerve, which transmit the visual impulse to the brain (Purves et al., 2004, Ross and Pawlina, 2011). The innermost layer is called the internal limiting membrane and it consists of flattened processes of Müller cells (Ross and Pawlina, 2011).

2.2.2. Main cell types in the retina

Retinal pigment epithelium (RPE)

Retinal pigment epithelial cells are melanin containing cells that form the outer blood retinal barrier and separate choriocapillaris from the photoreceptors (Reynolds and Olitsky, 2011). These cells form tight junctions between each other preventing free flow of molecules between neural retina and choroid. Instead, they facilitate active transport which is essential for the photoreceptor and RPE metabolism (Marmor and Wolfensberger, 1998, Strauss, 2005). The retinal pigment epithelial cell layer is vital for photoreceptor functioning and survival and, in addition to outer blood-retinal barrier function, it serves as a pump, keeping the subretinal space dehydrated and neural retina attached to the RPE. Furthermore, it supports the retinal development by secreting growth factors and cytokines (Strauss, 2005). Different antioxidants in the RPE cells protect cells from oxidative damage (Boulton and Dayhaw-Barker, 2001). The retinal

pigment epithelium is vital in the visual cycle and retinoid metabolism. It participates in the regeneration of chromophores and provides the visual cycle with additional retinol by absorbing it from the choroidal circulation (Marmor and Wolfensberger, 1998, Strauss, 2005, Simo et al., 2010).

Photoreceptors are non-dividing cells in an environment of potentially harmful free radicals, therefore regular renewal and turnover is essential for photoreceptor proper functioning (Sung and Chuang, 2010, Molday and Zhang, 2010). This reparation mechanism is ensured by the RPE cells, which constantly phagocytose photoreceptor outer segment tips, while new ones are formed and replaced by the photoreceptors. In fact, 10% of outer segment tips are replaced daily (Tsybovsky et al., 2010). In the process of regular turnover of photoreceptor outer segments, there is a progressive accumulation of lipofuscin pigment to the RPE cells. This pigment is an end-product of outer photoreceptor segment degradation that accumulates gradually with age (Kennedy et al., 1995). Chemically, it is a heterogeneous mixture of lipids, proteins and different fluorescent compounds (Kennedy et al., 1995). Lipofuscin is a fluorescent pigment enabling to visualize the RPE cells with autofluorescence (AF) imaging (Delori et al., 1995). Excessive lipofuscin is toxic to the RPE cells and it has a fundamental role in the pathophysiology of STGD1 (Cideciyan et al., 2004, Sparrow et al., 2000, Sparrow and Boulton, 2005). Another pigment in the RPE is melanin, which serves as a free radical stabilizer and a light absorber lowering the glare (Simo et al., 2010).

Photoreceptor cells

There are two types of photoreceptor cells in the retina: cones and rods. Cones are less numerous than rods, accounting for 3–5% of photoreceptors, but they are the major photoreceptor type in the fovea and the only one present in the foveola (Sung and Chuang, 2010, Mustafi et al., 2009). Cones are responsible of color and high resolution vision in bright light. Rods, on the other hand, dominate the rest of the retina and are responsible for vision in low light intensity (Sung and Chuang, 2010).

The photoreceptor cell consists of the outer segment, the connecting cilia, the inner segment, the nucleus and the axon with synaptic terminal (Sung and Chuang, 2010, Ross and Pawlina, 2011) **(Figure 3)**. Outer segments in both, cones and rods, are cylindrically modified cilia which contain flattened, lamellar-shaped membrane discs, arrayed perpendicular to the axis of the outer segments (Sung and Chuang, 2010). The lipid membrane of these discs contains various molecules essential in visual function, including visual pigments and the ABCA4 transporter (Ross and Pawlina, 2011, Mustafi et al., 2009). The outer segment is connected with the inner segment via the connecting cilia. The inner segment has two parts: an outer ellipsoid and inner myeloid part. The myeloid region is mainly responsible for protein synthesis, containing Golgi apparatus, endoplasmic reticulum and free ribosomes, whereas the ellipsoid region contains numerous mitochondria that provide photoreceptors with the adenosine

triphosphate (ATP) energy (Ross and Pawlina, 2011, Reynolds and Olitsky, 2011). A photoreceptor signal is transmitted to the outer plexiform layer via the axon and synaptic terminal (Reynolds and Olitsky, 2011).

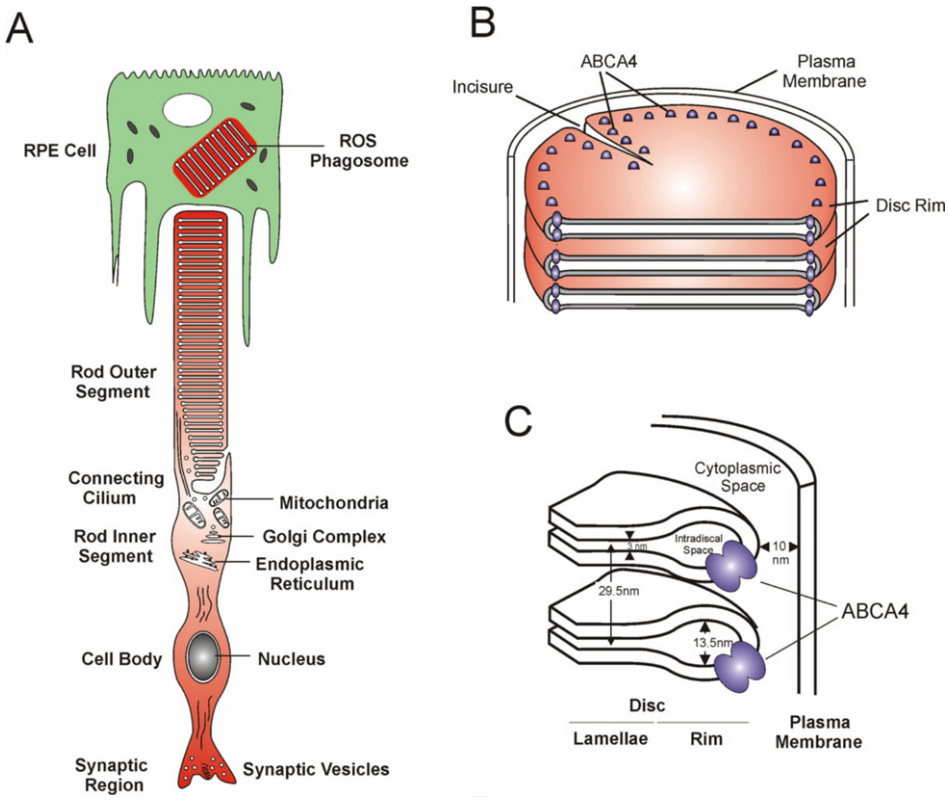

Figure 3. Structure of the rod photoreceptor. Photoreceptors consist of the outer-and inner segment, connected with the connecting cilium, the nucleus and synaptic terminal (A). The outer segment contains the outer segment discs and inner segment contains various organelles vital for photoreceptor functioning (A). The RPE cells participate in the outer segment renewal by phagocytosing the tips of the outer segments (A). Outer segment contains lamellar discs surrounded by cytoplasm and plasma membrane (B). The disc membrane contains various molecules important in phototransduction and the visual cycle, including photopigment (not shown) and ABCA4 transporter (C) (Molday and Zhang, 2010) (with permission from Elsevier).

Interneuron cells

The cell bodies of the interneurons are located in the inner nuclear layer. There are four types of interneurons responsible for visual signal transmission and image processing: bipolar, horizontal, amacrine and interplexiform cells (Ross and Pawlina, 2011, Reynolds and Olitsky, 2011). These cells form complex neuroretinal circuitries in the OPL and IPL through synapses with photo-receptors and ganglion cells (Ross and Pawlina, 2011).

Ganglion cells

Ganglion cells are located in the GCL forming contacts with the bipolar and amacrine cells (Reynolds and Olitsky, 2011). The axons of the ganglion cells form NFL and the optic nerve. The main function of these cells is to conduct visual impulses to the brain via the optic nerve. However, there is a small sub-group of photoreceptive ganglion cells that express photopigment melanopsin. These intrinsic photosensitive retinal ganglion cells are non-image-forming, but they influence circadian rhythms, pupillary light reflex and sleep (Hattar et al., 2002, Schmidt et al., 2011, O'Brien et al., 2002).

Glial cells in the retina

There are three types of glial cells in the retina: Müller cells, astrocytes and microglia (Fischer et al., 2010). Müller cells are the major type of glial cells in the retina spanning their processes throughout the entire retina filling the most of the extracellular space (Bringmann et al., 2006, Reichenbach and Bringmann, 2013). The nuclei of Müller cells are located in the INL and their basal and apical ends form the inner and outer limiting membranes, respectively (Ross and Pawlina, 2011). Müller cells provide structural support as well as metabolic support to the other retinal cells (Bringmann et al., 2006, Reichenbach and Bringmann, 2013). They are able to phagocytose fragments of retinal cells and protect photoreceptors from damage by releasing neurotrophic factors and antioxidants (Reichenbach and Bringmann, 2013, Bringmann et al., 2006). Furthermore, Müller cells participate in the formation and conduction of visual impulse by participating in the cone visual cycle and regulating synaptic activity in the retina (Reichenbach and Bringmann, 2013, Wang and Kefalov, 2011). Müller cells have been shown to act like optical fibers, guiding light through the inner retinal layers minimizing the light scattering and improving the quality of vision (Franze et al., 2007).

Astrocytes enter the developing retina via the optic nerve and are mostly located in the nerve fiber layer where they envelope the axons of the ganglion cells and retinal blood vessels (Chan-Ling, 1994). Astrocytes participate in the formation of retinal vessels, the blood-retina barrier and they provide neuro-tropic as well as mechanical support for degenerating axons (Vecino et al., 2016).

Microglial cells are tissue-resident phagocytosing cells situating mostly in the inner retinal layers. In normal conditions microglia is important in maintaining retinal homeostasis. They phagocytose cell debris and secrete growth factors (Vecino et al., 2016). However, it has been shown that in various pathological conditions, including retinal degenerative diseases like age-related macular degeneration (AMD) and retinitis pigmentosa, extensive microglia activation leads to inflammation, which adds its detrimental effect on photoreceptors health (Vecino et al., 2016, Ma et al., 2009, Ma et al., 2012, Langmann, 2007). In fact, it has been shown in a retinitis pigmentosa rat model, that suppressing microglial activation may delay photoreceptor death (Noailles et al., 2014).

2.3. Physiology of the retina

2.3.1. Phototransduction cascade

The process where energy of light is converted into electrical neural signal is called phototransduction (Roosing et al., 2014). The process takes place in the photoreceptor outer segments via the activation of the visual pigment (Sung and Chuang, 2010). The visual pigment is a compound molecule of light sensitive chromophore and opsin molecule located in the lipid membrane of outer segment discs (Wang and Kefalov, 2011, Palczewski, 2012). The photo-sensitive chromophore is vitamin A aldehyde 11-cis retinal and the molecule is the same in both rods and cones. However, there are 4 types of opsin molecules depending on the absorption peak (Reynolds and Olitsky, 2011). The visual pigment in rods is called rhodopsin and in cones, there are 3 types of cone visual pigments with different absorption maxima (Mustafi et al., 2009). The mixture of different cones with different visual pigments and absorption peaks result in the ability to detect colors (Mustafi et al., 2009). The rods, on the other hand, have only one type of visual pigment which is responsible for achromatic vision in dim light (Mustafi et al., 2009).

The visual cascade starts with the capture of a photon and isomerization of 11-cis retinal to all-trans retinal. This reaction changes the conformation of the opsin molecule and activates the photopigment. In the cytosolic side of the disc membrane opsin is combined with a G-protein called transducin, which activates the enzyme cGMP phosphodiesterase (PDE). This activation reduces the cGMP concentration in the cytoplasm resulting in closure of cGMP-gated cation channels located in the photoreceptor outer segment plasma membrane. The closure of these channels leads to photoreceptor hyperpolarization resulting in reduced neurotransmitter glutamate secretion in the synaptic terminal (Palczewski, 2012, Yau, 1994, Yau and Hardie, 2009).

The restoration of the visual pigment is thereafter crucial. The chromophore is restored in the visual cycle and the visual pigment is rebuilt. Deactivation of the phototransduction cascade and restoring the photoreceptor sensibility is ensured by a cascade of enzymatic reactions (Lamb and Pugh, 2006).

2.3.2. Visual cycle and chromophore restoration

Phototransduction cascade is dependent on the visual cycle, responsible for recycling the all-trans-retinal to 11-cis-retinal vital for restoring the visual pigment (Palczewski, 2012). This continuous process takes place in the photoreceptor outer segments and the RPE cells. In cone system, additional Müller cell-based visual cycle has been reported (Reichenbach and Bringmann, 2013, Wang and Kefalov, 2011).

Absorption of photon by visual chromophore isomerizes 11-cis retinal to all-trans retinal, which is released to the disc lumen. Free all-trans retinal diffuses to the cytoplasmatic leaflet of the disk membrane, where NADHPH-dependent

retinol dehydrogenase (RDH8) reduces all-trans retinal to all-trans retinol (Palczewski, 2012). A fraction of all-trans retinal and 11-cis retinal form compounds with the disk membrane phospholipids which cannot diffuse freely across the disk membrane (Quazi et al., 2012, Quazi and Molday, 2014). These compounds are flipped out from the disk lumen by ABCA4 transporter after which they can be reduced to retinol (Quazi et al., 2012, Quazi and Molday, 2014). All-trans retinol is transferred out of the photoreceptors to the extracellular compartment, where it binds to the inter-photoreceptor retinoid binding protein (IRBP) and is transported to the RPE cells (Wang and Kefalov, 2011, Saari, 2012). In the RPE it binds to cellular retinol-binding protein type 1 (CRBP1) and is esterified by lecithin retinol acyltransferase (LRAT) to all-trans retinyl ester (Saari, 2012). This ester is further hydrolyzed and isomerized by RPE65 to 11-cis retinol. 11-cis retinol is bound to cellular retinaldehyde-binding protein (CRALBP) and oxidized to 11-cis retinal by 11-cis retinol dehydrogenase after which 11-cis retinal is transported back to the photoreceptors with IRBP to regenerate the visual pigment (Saari, 2012). Additional retinol is constantly added from the choroid blood circulation by the RPE cells (Chen and Heller, 1977).

2.4. Stargardt retinal dystrophy

Stargardt disease is the most common form of inherited macular dystrophy with the estimated prevalence of 1:8000 to 1: 10 000 (Michaelides et al., 2003). The disease is caused by mutations in the *ABCA4* gene, which is on chromosome 1 and encodes the ABCA4 transporter (Allikmets et al., 1997b). The transporter is vital in the visual cycle and the dysfunctional protein leads to lipofuscin overaccumulation in the RPE cells resulting in RPE and photoreceptor degeneration (Sparrow and Boulton, 2005, Cideciyan et al., 2004). The symptoms usually start in the first or second decade with progressive visual deterioration (Michaelides et al., 2003). Lipofuscin accumulation is responsible for STGD1-associated features such as increased fundus autofluorescence (FAF) (Cideciyan et al., 2004, Boon et al., 2008), yellow pisciform flecks, and progressive atrophy of the outer retinal layers. Early clinical signs of STGD1 are atrophic changes in the macula and yellowish flecks, but there is remarkable phenotypic heterogeneity within the clinical spectrum of STGD1 (Fishman et al., 1999, Fishman, 1976, Fujinami et al., 2013d, Cella et al., 2009, Lois et al., 2001, Westenengvan Haaften et al., 2012). Distinguishing STGD1 from other phenotypically similar diseases is often difficult with just a clinical exam, therefore *ABCA4* genetic screening and application of several imaging methods, such as SD-OCT and FAF imaging, are important **(Figure 4)**.

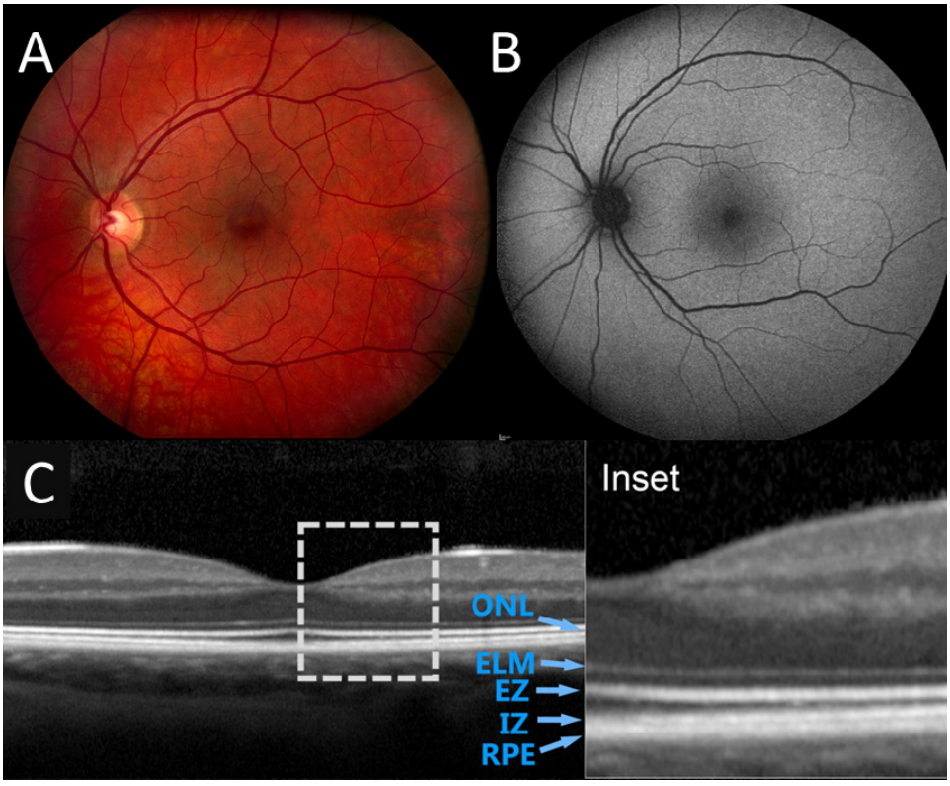

Figure 4. Different imaging methods of the retina in the healthy eye: color photo (A), an autofluorescence image (B) and an optical coherence tomography image (C). The SD-OCT enables to visualize different retinal layers (inset): outer retinal layers are retinal pigment epithelium (RPE), the interdigitation zone (IZ), the ellipsoid zone (EZ), the external limiting membrane (ELM) and the outer nuclear layer (ONL) (from Edward S. Harkness Eye Institute).

Stargardt disease is autosomal recessive dystrophy requiring mutations on both chromosomes to cause the disease (Allikmets et al., 1997b), however, complete sequencing of *ABCA4* coding and intron-exon boundaries reveal two *ABCA4* mutations in only 65–70% of patients and one *ABCA4* mutation in 15–20% of patients (Zernant et al., 2011). Detection of only one *ABCA4* mutation with "typical" STGD1 phenotype could be explained from both genetic and clinical aspects. The second mutation could be large deletion, insertion or deep intronic variant, which all elude the routinely used screening methods, such as direct PCR-based sequencing, or the phenotype could be a phenocopy caused by mutation(s) in other genes (Zernant et al., 2011, Zernant et al., 2014b). Furthermore, the second mutation could be present in modifier genes or in promoter/enhancer regions near the *ABCA4* gene which influence the *ABCA4* expression (Zernant et al., 2011, Westeneng-van Haaften et al., 2012).

2.4.1. ABCA4 function in visual cycle and pathogenesis of STGD1

ABCA4 is a photoreceptor specific transporter vital for the visual cycle. It is a member of the ATP-binding cassette transporter superfamily and has two nucleotide binding domains (NBD) for ATP binding and hydrolyzing, two transmembrane domains (TMD) and two exocytoplasmatic domains (ECD) for substrate binding and transportation (Molday and Zhang, 2010). The protein is encoded by the *ABCA4* gene on chromosome 1 and is located in the outer segment disc rims of rods and cones (Sun and Nathans, 1997, Molday et al., 2000) (**Figure 3**).

In the process of photo-transduction, all-trans retinal is released. The molecule contains an aldehyde group, which makes it highly reactive and potentially harmful to the photoreceptors. Therefore all-trans retinal needs to be detoxified and reduced to all-trans retinol (Quazi and Molday, 2014, Quazi et al., 2012). The enzyme essential for this reaction is retinol dehydrogenase 8 (RDH8) in the cytoplasm of the photoreceptor outer segments (Rattner et al., 2000). Therefore, all-trans retinal has to get out from the disc lumen to be accessible to the RDH8. Most of the all-trans retinal diffuses freely across the lipid bilayer but a fraction form compounds with the membrane phospholipid called phosphatidylethanolamine. The formed compound is called N-retinylidene-phosphatidylethanolamine and it cannot diffuse across disc membrane by itself, but employs the ABCA4 transporter for that purpose (Quazi et al., 2012). The ABCA4 transporter flips N-retinylidene-phosphatidylethanolamine from the lumen to the cytoplasmatic leaflet of the disc membranes where it diffuses back to phosphatidylethanolamine and all-trans-retinal (Quazi et al., 2012). Thereafter the all-trans retinal can be reduced to all-trans retinol by RDH8. In addition, ABCA4 transports free phosphatidylethanolamine in the same direction (Quazi et al., 2012). Recently it has been showed that similar process is true for 11-cis retinal, where excess 11-cis retinal may form compounds with phosphatidylethanolamine and ABCA4 transports N-11-retinylidene-phosphatidylethanolamine out from the disc lumen (Quazi and Molday, 2014). Therefore, ABCA4 transporter helps to clear the photoreceptors from the excessive 11-cis and all-trans retinal, both highly reactive and potentially toxic molecules to the photoreceptors (Quazi et al., 2012, Quazi and Molday, 2014).

Mutations in the *ABCA4* gene lead to dysfunctional ABCA4 transporter resulting in N-retinylidene-phosphatidylethanolamine accumulation and formation of bisretinoid complexes in the lumen side of disc membrane (Molday and Zhang, 2010). There is constant renewal of the photoreceptor outer segments by the RPE cell phagocytosis. During the process these diretinoid complexes deposit to the lysosomes of the RPE cells where major lipofuscin fluorophore, A2E (N-retinylidene-N-retinylethanolamine) is formed and deposited (Sparrow et al., 2008, Tsybovsky et al., 2010, Ben-Shabat et al., 2002). A2E containing lipofuscin has harmful effects on the RPE cell functioning via various effects. These include lysosomal dysfunction (Holz et al., 1999), membrane disruption (Sparrow et al., 1999), loss of antioxidant effectivity

(Shamsi and Boulton, 2001), photo-toxicity (Schutt et al., 2000, Sparrow et al., 2000), immune dysregulation (Zhou et al., 2009, Zhou et al., 2006) and DNA damage (Sparrow et al., 2003). As the RPE cells are vital in photoreceptor function, progressive RPE cell degeneration leads to photoreceptor death.

The excessive lipofuscin accumulation is believed to be the hallmark of the pathogenesis in STGD1 (Sparrow and Boulton, 2005, Cideciyan et al., 2004, Burke et al., 2014), however, there is increasing evidence that neuro-inflammation in the retina plays also an important role in the pathogenesis of retinal degenerations (Zhou et al., 2009, Kohno et al., 2013, Xu et al., 2009, Radu et al., 2011, Ma et al., 2012, Langmann, 2007, Zhou et al., 2006). Photo-exposure to A2E and all-trans retinal dimers leads to formation of photo-oxidation products which are capable of activating complement and induce low-grade inflammation (Zhou et al., 2009, Zhou et al., 2006, Sparrow et al., 2000, Schutt et al., 2000). Furthermore, the migration of microglia and macrophages into subretinal space has been described in $Abca^{-/-}$ mice (Radu et al., 2011, Kohno et al., 2013) and it has been demonstrated that the deposition of A2E to the RPE cells and microglia increases microglial activation and alters the complement regulation in vitro as well as in vivo (Ma et al., 2013, Kohno et al., 2013, Zhou et al., 2009, Zhou et al., 2006). Microglia accumulates the bisretinoids and lipofuscin primary by phagocytosing surrounding degenerating photoreceptors and RPE cells (Ma et al., 2013, Lei et al., 2012, Kohno et al., 2013, Xu et al., 2009). In addition, the RPE cells themselves modulate microglia by producing chemokines after phagocytosing the photoreceptor outer segments (Kohno et al., 2013)**.** Therefore, the activation of immune cascade affects the environment and different cell types in the outer retina contributing to the pathogenesis of STGD1.

Furthermore, it has been shown that excess all-trans retinal and possibly 11-cis retinal can cause photoreceptor damage directly (Maeda et al., 2009, Maeda et al., 2014, Maeda et al., 2012, Chen et al., 2012). However, there is still debate whether the primary cells affected in STGD1 are RPE cells or photoreceptors (Sparrow and Boulton, 2005, Cideciyan et al., 2004, Duncker et al., 2014, Gomes et al., 2009, Burke et al., 2011).

2.4.2. Structural and functional assessment of the retina in STGD1

Spectral-domain optical coherence tomography and retinal structural changes in STGD1

Optical coherence tomography (OCT) is a non-invasive imaging method enabling to create cross sectional retinal images *in vivo* (Sakata et al., 2009) It uses light waves to measure their reflection time delay and intensity from different retinal structures by comparing it with the reference reflection path (Drexler and Fujimoto, 2008). This enables to visualize different retinal layers correlating with retinal histology and detect even minor disease-associated structural changes (Spaide and Curcio, 2011, Staurenghi et al., 2014). The image quality and resolution of OCT has improved substantially within the last

decade providing researches new perspectives in terms of clinical research and understanding of the retinal diseases.

The spectral-domain optical coherence tomography (SD-OCT) retinal images exhibit different intensity bands correlating with the anatomical layers of the retina (Spaide and Curcio, 2011, Staurenghi et al., 2014). Four distinct hyper-reflective fine bands are visualized in the outer retina associated with Müller cells, photoreceptors and RPE cells (Spaide and Curcio, 2011) **(Figure 4, C)**. The outermost hyper-reflective band represents RPE/Bruch`s membrane complex formed mainly by the RPE cells. Anteriorly, a fine elusive band is attached to the RPE layer. The band is called the interdigitation zone and is possibly formed by the RPE apical processes enveloping cone outer segment tips. The third band is called the ellipsoid zone, thought to represent the ellipsoid zone of the photoreceptor inner segment just above the cilia. The hyper-reflectivity is thought to be caused by intensely packed mitochondria in this region (Spaide and Curcio, 2011, Staurenghi et al., 2014). Disappearance of this band represents photoreceptors integrity loss correlating well with visual acuity decline (Wong et al., 2012, Testa et al., 2012). The innermost hyper-reflective band represents the external limiting membrane formed by junctional complexes of Müller cell apical ends to each other and with photoreceptors (Spaide and Curcio, 2011, Staurenghi et al., 2014).

Stargardt disease is retinal dystrophy affecting mostly the outer retina layers: the RPE and the photoreceptor associated layers (Burke et al., 2011, Duncker et al., 2014, Park et al., 2015, Ergun et al., 2005) **(Figure 5)**. It has been shown that greater photoreceptor loss on OCT imaging corresponds to lower visual acuity (Ergun et al., 2005), furthermore, the ellipsoid zone integrity correlates also well with other studies which assess photoreceptor health including multifocal electro-retinography (mfERG), full-field electroretinography (ffERG) and microperi-metry (Testa et al., 2012). However, changes in retinal thickness have also been detected in the inner retinal layers. Extrafoveal inner nuclear layer thickening associated with the regions of outer nuclear layer thinning have been noted, probably due to the retinal remodeling following the photoreceptor loss (Huang et al., 2014). Furthermore, changes in peripapillary nerve fiber layer thickness in STGD1 have been demonstrated (Genead et al., 2011, Pasadhika et al., 2009). These findings confirm that retina is a complex tissue with vigorous commu-nication between different cell types and changes in the outer retina lead to inner retina remodeling and laminopathy (Huang et al., 2014).

Choroidal thickness measurements in STGD1 have revealed that the mean subfoveal total choroidal thickness as well as subfoveal large choroidal vessel thickness is significantly reduced in STGD1 (Adhi et al., 2015).

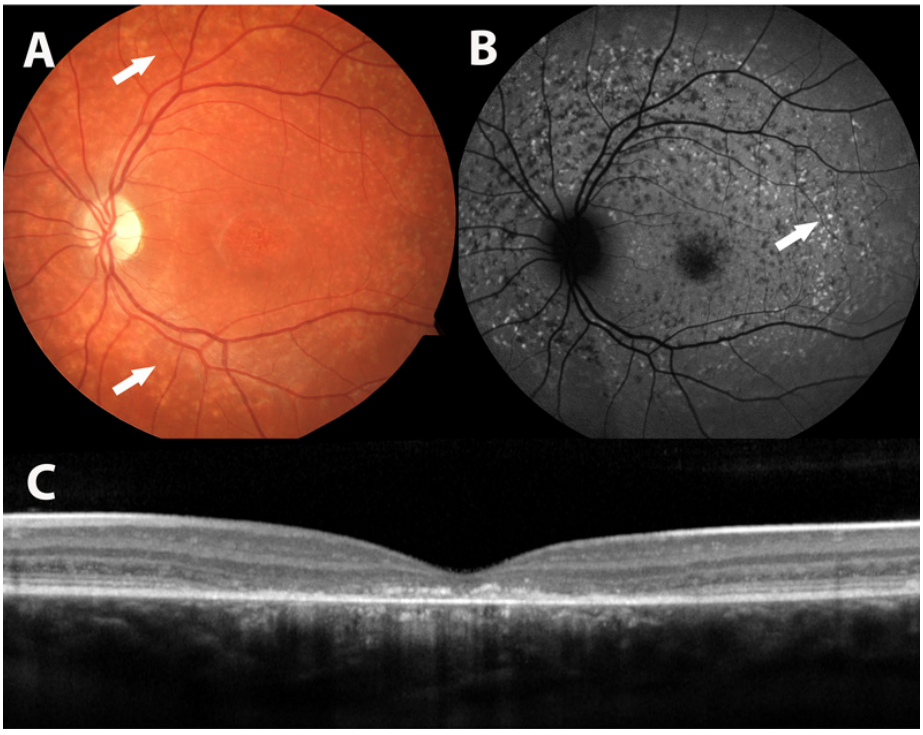

Figure 5. "Classical" phenotype in STGD1. The color photo of the fundus exhibits bull's-eye like atrophic lesion in the macula and yellowish flecks throughout the entire fundus (A, arrows). Macular atrophy corresponds to hypo-autofluorescent central lesion on the fundus autofluorescence image due to the atrophy of the RPE layer. Hyper-AF dots are seen throughout the fundus (white arrow), representing flecks. Hypo-autofluorescent dots are seen on the nasal side representing resorbed flecks (B). Disruption and atrophy of the outer retinal layers are seen in the macula on SD-OCT image (C) (from Edward S. Harkness Eye Institute).

Fundus autofluorescence imaging in STGD1

The major source for short-wavelength FAF signal is lipofuscin which is accumulated in the RPE cells (Delori et al., 1995, Sparrow and Boulton, 2005). Lipofuscin contains a mixture of fluorophores, which could be excited with a light source. After the excitation it emits back signal with longer wave length, which can be detected and recorded. The signal is generated by illuminating the fundus with an argon laser source within blue spectrum (488 nm) and the resultant FAF signal is recorded with confocal scanning laser ophthalmoscope (cSLO) with bandpass filter having short wavelength cutoff 495 nm (Keane and Sadda, 2014, Schmitz-Valckenberg et al., 2008).

The lipofuscin concentration in the RPE cells increase with age, but in STGD1 it is pathologically extensive (Delori et al., 2001, Burke et al., 2014), therefore FAF imaging enables to detect early stage pathological changes in

STGD1, including an increased FAF signal and characteristic fleck patterns (Cideciyan et al., 2004, Lois et al., 2004, Fujinami et al., 2013b, Burke et al., 2014). As FAF imaging provides information about the health and integrity of the RPE cells, absence of or the reduced FAF signal indicates mostly to RPE atrophy or death (Holz et al., 2001, Boon et al., 2008).

Cideciyan et al proposed a model of ABCA4 disease sequence where initially there is an accumulation of lipofuscin leading to a progressive increase in the FAF signal and hyper-AF fleck formation in the posterior pole followed by FAF signal reduction and loss in later stages due to the RPE dysfunction and death accompanied by slowing of the retinoid cycle and increasing photoreceptor degeneration (Cideciyan et al., 2004).

As STGD1 cases have very variable phenotype, different FAF patterns have been described, whereas the most typical is central hypo-autofluorescent (hypo-AF) lesion reflecting chorioretinal macular atrophy surrounded by small hyper-autofluorescent (hyper-AF) pisciform flecks (Boon et al., 2008) **(Figure 5)**. Measurements of FAF signal intensity in STGD1 with quantitative AF demonstrate that different genotypes provide different fluorescence levels and certain genotype-phenotype associations are possible (Duncker et al., 2014).

Functional assessment of the retina with electroretinography in STGD1

Retinal function is assessable with many different methods, while one of the most objective methods is electroretinography (ERG). Full-field ERG enables to assess the general function of the photoreceptors as well as the function of other retinal cells in the inner nuclear layer (Holder et al., 2010). Depending on the stimuli and background illumination it is possible to record the function of cone and rod photoreceptors separately. The full-field ERG generates mass response of the cones, rods or both, therefore in isolated macular disease the full-field ERG is usually normal (Holder et al., 2010). Consequently, multifocal ERG (mfERG) or pattern ERG (PERG) is essential in assessing the macular function (Holder et al., 2010).

Multifocal ERG examines the spatial aspect of the cone system function in the central retina mapping the electrical activity of cones in the central visual field (Holder et al., 2010, Kretschmann et al., 1998). Pattern ERG, on the other hand, does not use light stimulus, but black and white checkerboard instead, assessing the central retinal photoreceptor function as well as ganglion cell function (Holder et al., 2010).

Stargardt disease is macular dystrophy suggesting that there should be abnormalities in the PERG and mfERG, but normal full-field ERG. However, STGD1 shows a wide range of full-field ERG abnormalities (Fishman, 1976, Lois et al., 2001, Zahid et al., 2013, Fujinami et al., 2013a), based on which the disease could be divided into 3 separate groups: Group 1 exhibits PERG abnormalities, but normal full-field photopic and scotopic responses, Group 2, in addition to PERG abnormality, exhibits changes in photopic ERG and Group 3 exhibits decreased responses in both photopic and scotopic ERG responses (Lois et al., 2001).

Furthermore, the differences in groups are not explained on the basis of differences in age of onset and duration of the disease, suggesting that these could be separate phenotypic subgroups rather than different stages of the disease progression (Lois et al., 2001). Indeed, it would be reasonable to assume that the phenotype might predict cone-rod function on full-field ERG, meaning that lesions confined to the macula have normal ERG, while more wide-spread disease has more affected ERG, (Fishman, 1976, Zahid et al., 2013, Cella et al., 2009) but it is not always the case. The retinal phenotype with macular lesion could have very prominent changes in full-field ERG and more prominent fundus changes could have normal full-field ERG (Oh et al., 2004, Lois et al., 2001).

Full-field ERG may have prognostic value in terms of STGD1 progression since it has been shown that abnormalities in maximum stimulation A-and B-wave amplitudes have significantly higher average rate of scotoma progression compared with the patients with normal full-field ERG (Zahid et al., 2013). Fujinami et al showed that patients with STGD1 who present initially with normal full-field ERG (Group1) have most favorable prognosis, as only 22% of patients have ERG deterioration, while in patients in ERG groups 2 or 3 have ERG deterioration in 65% and 100% of patients, respectively. Association between best-corrected visual acuity (BCVA) and ERG as well as between ERG and age of onset was also detected, meaning that lower BCVA was associated with more affected ERG and the earlier the onset, the more affected was the ERG (Fujinami et al., 2013a).

Multifocal ERG is a sensible tool for detecting early functional abnormalities of the macula in STGD1 even before apparent morphological macular change or visual acuity loss, furthermore, the area of dysfunction is usually larger than predicted by morphological studies (Kretschmann et al., 1998).

2.4.3. Phenotypic heterogeneity in STGD1

The clinical expression of the disease was first described by a German ophthalmologist Karl Stargardt in 1909, but the association with the *ABCA4* gene was discovered almost 90 years later (Allikmets et al., 1997b, Stargardt, 1909). Since then, more than 1000 disease causing mutations in the *ABCA4* gene have been found resulting in remarkable phenotypic and genotypic heterogeneity in ABCA4-associated retinopathies (Zernant et al., 2014b). In addition to phenotypic heterogeneity in STGD1 in terms of clinical expression, fundus and electroretinography findings as well as in age of onset, mutations in *ABCA4* have also been reported in cone-rod dystrophy (Cremers et al., 1998, Maugeri et al., 2000), autosomal recessive retinitis pigmentosa (Cremers et al., 1998, Martinez-Mir et al., 1998) and AMD (Allikmets et al., 1997a). However, it has to be noted that autosomal-recessive cone-rod dystrophy is also considered as a phenotypic version of STGD1 (Lois et al., 2001). Sometimes the term *fundus flavimaculatus* is used in a subgroup of patients, with widespread fundus flecks without apparent macular atrophy, but currently it is considered as a phenotypic

variant of the STGD1 rather than a separate entity (Fishman, 1976, Franceschetti and Francois, 1965, Michaelides et al., 2003). Overall, STGD1 typically begins with early macular atrophic changes and yellowish flecks at the posterior pole, but there is remarkable phenotypic heterogeneity with variable age of onset and clinical expression (Michaelides et al., 2003). Most of STGD1 patients have the disease onset in the first two decades of life (Michaelides et al., 2003) with the central visual loss, reduced dark adaption (Fishman et al., 1991) and disturbances in the color vision (Mantyjarvi and Tuppurainen, 1992, Vandenbroucke et al., 2015), but it could vary largely (Westeneng-van Haaften et al., 2012).

Based on disease onset, STGD1 has been divided into early-onset and late-onset disease (Westeneng-van Haaften et al., 2012, Yatsenko et al., 2001, Lambertus et al., 2015) or childhood-onset and adult-onset STGD1 (Fujinami et al., 2015). Phenotypes in early-onset STGD1 are more severe compared with the late-onset STGD1 (Fujinami et al., 2015, Lambertus et al., 2015). It has been shown that childhood-onset STGD1 is associated with more severe and faster visual acuity deterioration and more common generalized cone and rod system dysfunction compared with adult-onset STGD1 (Fujinami et al., 2015). Late-onset STGD1 patients have usually milder phenotype with adult or even elderly age of onset, better visual acuity and slower progression (Westeneng-van Haaften et al., 2012). Many late-onset patients exhibit foveal sparing phenotype (Westeneng-van Haaften et al., 2012).

Foveal sparing is a sub-phenotype where foveal region remains relatively intact maintaining partial or full function despite relatively advanced disease (Fujinami et al., 2013d, van Huet et al., 2014). The foveal sparing phenotype is not specific to STGD1, but it has been described in other retinal degenerations as well (Duncker et al., 2015, Querques et al., 2016, Forte et al., 2013). In STGD1, there has been a report of tendency to higher frequency of p.R2030Q and lower incidence of p.G1961E variant (Fujinami et al., 2013d), however another study did not confirm the association (van Huet et al., 2014).

A less common phenotype in STGD1 is optical gap, also known as foveal cavitation or optically empty lesion (Cella et al., 2009, Leng et al., 2012, Ritter et al., 2013). The phenotype is detectable on SD-OCT as focal subfoveal loss of ellipsoid zone reflectivity, representing subfoveal photoreceptor loss leaving an optically empty space (Leng et al., 2012). The phenotype is not specific to STGD1; it has also been described in solar retinopathy (Jain et al., 2009), laser induced retinal injury (Zhang et al., 2016), rod monochromatism (Greenberg et al., 2014) and *RP1L1* maculopathy (Park et al., 2010).

Based on phenotypic expression, multiple grading systems for the disease have been suggested. Fishman et al divided STGD1 patients into 4 phenotypic stages: Stage 1 disease represents central macular atrophy with para- or perifoveal flecks; Stage 2 represents flecks throughout the entire posterior pole often extending anterior to the vascular arcades and/or nasal to the optic disc, Stage 3 presents with mostly resorbed flecks and Stage 4 represents widespread RPE and chorioretinal atrophy throughout the fundus (Fishman, 1976).

Electrophysiological abnormalities were noted from Stage 3 indicating that phenotype affects the ERG. Lois et al, on the other hand, did not find that ERG abnormalities correlated with age of onset or disease duration, suggesting that there could be distinct ERG phenotypes depending on abnormalities in cone and rod function (Lois et al., 2001).

Flecks in STGD1 are not universal, but may develop later in the disease course (Fujinami et al., 2015, Lambertus et al., 2015). In some patients with childhood-onset STGD1, fine macular dots have been described (Fujinami et al., 2015).

2.4.4. Genotype-phenotype associations in STGD1

Genotype-phenotype associations are difficult to determine due to extensive allelic heterogeneity. Furthermore, determining the severity of specific allele is impeded because compound heterozygous patients harbor two different alleles and the number of patients sharing the same allelic combinations is generally low. The phenotypic expression of the same genotype may vary between different cases or even within the same pedigree, indicating a possibility of modifying genes and environmental factors (Lois et al., 1999, Schindler et al., 2010, Michaelides et al., 2007). Previous studies have hypothesized that phenotype severity, including age of onset, is determined by mutations effect on ABCA4 activity, meaning that the lower the ABCA4 residual activity the more severe is the phenotype (Sun et al., 2000, Shroyer et al., 1999, van Driel et al., 1998). Missense mutations mapping outside the functional ABCA4 region, probably retaining partial ABCA4 activity, have shown to be associated with milder disease and later-onset STGD1 (Yatsenko et al., 2001), while mutations abolishing ABCA4 function, exhibit severe phenotype with early-onset pan-retinal disease (Cremers et al., 1998, Wiszniewski et al., 2005, Fujinami et al., 2013a, Fujinami et al., 2015). Fujinami et al demonstrated further that childhood-onset STGD1 have higher portion of deleterious *ABCA4* variants compared with adult-onset STGD1 and 71% patients with two deleterious *ABCA4* variants in childhood-onset STGD1 were in the ERG Group 3 (Fujinami et al., 2015).

Mutations in the *ABCA4* gene may phenotypically express as STGD1, cone-rod dystrophy (Cremers et al., 1998, Maugeri et al., 2000) or retinitis pigmentosa-like disease (Cremers et al., 1998, Martinez-Mir et al., 1998). It has been shown that the most severe mutations abolishing the ABCA4 function result in retinitis pigmentosa-like dystrophy, while milder mutations result in cone-rod dystrophy or STGD1 (Heathfield et al., 2013). It has to be noted that autosomal recessive cone-rod dystrophy caused by ABCA4 dysfunction has also been classified as a phenotypic variant of STGD1 belonging to ERG Group 3 (Lois et al., 2001, Fishman, 1976, Fujinami et al., 2013a). Moreover the “classical” STGD1 may progress to retina-wide disease, affecting both rod and cone induced full-field ERG responses, diagnostic to cone-rod dystrophy (Fujinami et

al., 2013a). However, some studies have shown that the ABCA4 function hypothesis does not always apply, and probably some additional factors contribute to the phenotypic expression (Cideciyan et al., 2009, Burke et al., 2012b).

Probably the most studied variant in STGD1 is the p.G1961E allele. This is not unexpected, as the p.G1961E mutation is the most frequent disease-causing *ABCA4* allele seen in approximately 10% of STGD1 patients of European origin (Burke et al., 2012a). The p.G1961E allele has been associated with bull's eye maculopathy and milder phenotypes in STGD1 (Cella et al., 2009, Fishman et al., 1999, Fujinami et al., 2013c). Cella et al studied a cohort of patients with at least one p.G1961E allele and none of the patients exhibited generalized cone or rod function loss (Cella et al., 2009). All patients presented with bull's eye maculopathy without flecks. They concluded that the p.G196E allele in either homozygosity or compound heterozygosity confers a milder phenotype with bull's eye lesion, later disease onset and absence of generalized retinal dysfunction (Cella et al., 2009). However, a larger study with patients homozygous for p.G1961E demonstrated that it is not always the case and exceptions are possible (Burke et al., 2012a). Furthermore, it is believed that p.G1961E has a "dominant" effect over the other allele in *trans*, because even if the second mutation is "severe", the phenotype tends to be "milder" (Burke and Allikmets, 2013, Burke et al., 2014). Additionally, patients carrying the p.G1961E allele have lower FAF signal level and absence of the dark choroid phenomenon indicating lower lipofuscin accumulation with this allele (Burke et al., 2014, Fishman et al., 1999).

2.4.5. Differential diagnosis of STGD1

It is often difficult to distinguish STGD1 by an ophthalmic examination from other phenotypically similar retinopathies, especially if these exhibit similar hyper-AF flecks. One example is multifocal patter dystrophy which frequently simulates STGD1 (Duncker et al., 2015, Boon et al., 2007). It is an autosomal dominant dystrophy caused by mutations in the *PRPH2* gene (Boon et al., 2007). Two other autosomal dominant Stargardt-like macular dystrophies (STGD3 and STGD4), caused by mutations in *ELOVL4* and *PROM1* genes, respectively, have been described (Palejwala et al., 2016, Zhang et al., 2001, Kniazeva et al., 1999).

Stargardt disease could exhibit bull's eye macular lesion even without characteristic flecks (Cella et al., 2009, Fujinami et al., 2015), therefore all conditions exhibiting bull's eye maculopathy should be considered as a differential diagnosis. These include cone (rod) dystrophy, central areolar choroidal dystrophy, age-related macular degeneration, chronic macular hole, chloroquine/ hydroxychloroquine (HCQ) retinopathy, olivopontocerebellar atrophy and ceroid lipofuscinosis (Regillo et al., 2007). Cone (rod) dystrophy is a diagnosis made via ERG and can be caused by many genes, including *ABCA4* (Cremers et al., 1998, Maugeri et al., 2000), which is/are mostly considered as phenotypic variant(s) of STGD1 (Lois et al., 2001). Central areolar choroidal dystrophy has

autosomal dominant inheritance, adult onset and is caused by mutation in *PRPH2* (Hoyng et al., 1996)**.** Late-onset STGD1 is sometimes confused with AMD (Westeneng-van Haaften et al., 2012, Burke et al., 2012a), while bull's eye maculopathy in younger individuals with neurologic deficit could suggest olivopontocerebellar atrophy or lipofuscinosis (Wright et al., 2006).

Hydroxychloroquine is an anti-malaria drug commonly used in the treatment of various systemic autoimmune disorders which may cause retinopathy with bull's eye lesion exhibiting "flying-saucer" sign on SD-OCT (Chen et al., 2010). The term "flying-saucer" sign is a variant of foveal sparing, referring to abrupt disruption of the EZ band in the parafoveal region and thinning of the outer nuclear layer, forming a so-called "flying saucer" configuration (Chen et al., 2010, Marmor, 2012, Ascaso et al., 2013, Tailor et al., 2012).

3. AIMS OF THE STUDY

1) To assess and analyze early stage retinal structural changes in young patients with STGD1 (Paper I).
2) To find, describe and analyze uncommon SD-OCT phenotypes in STGD1 and to assess retinal function in these patients (Papers II, III).
3) To detect possible genotype-phenotype associations in STGD1 (Paper II).

4. MATERIALS AND METHODS

4.1. Study subjects and clinical evaluation

All studies were conducted at the Department of Ophthalmology of the Columbia University, using clinical and genetic database involving patients with clinical diagnosis and genetic confirmation of STGD1 found to have one or two disease causing mutations in the *ABCA4* gene. Within this cohort, SD-OCT and FAF (AF; 488 nm) images were available for 179 patients in Paper I and Paper II. New patients with STGD1 were constantly added to the database and followed and re-imaged once a year, therefore, for Paper III, 200 patients with the set of imaging data were available.

Each patient underwent a complete ophthalmic examination by a retinal specialist, including slit-lamp examination and dilated fundus examination. The function of the retina was assessed with full-field and multifocal ERG, while the structure was examined using color fundus photography, FAF imaging and SD-OCT. The best corrected visual acuity (BCVA) was detected in all patients, except for only one patient in Paper I, where data about BCVA were not available.

The estimated disease duration was defined to be the period from the reported age of symptomatic onset to the age at first examination.

Phenotypic expression and outer retinal abnormalities in young patients with STGD1 (Paper I)

Due to our clinical observation that the abnormalities in the ELM develop in younger patients who in general have shorter disease duration and earlier disease stage, we included all patients with STGD1 from the group of 179 patients who presented to the Retina Division for SD-OCT and FAF imaging before the age of 20. Therefore, these patients were imaged relatively soon after the disease onset (mean disease duration was 3.2 years). A total of 26 STGD1 patients (mean age, 12.9 years; range, 5–19 years) satisfied the inclusion criteria. The thickness and reflectivity of the ELM and EZ were measured and the data were compared with the data obtained from the SD-OCT-s from 30 age-matched controls (age range, 4–20 years; mean age, 12.5 years). Full-field ERG recordings were available and analyzed in 19 patients.

Structural and Genetic Assessment of the ABCA4-Associated Optical Gap Phenotype (Paper II)

Spectral-domain OCT images of 179 STGD1 patients were analyzed and 15 patients with the optical gap phenotype were identified and included to the study. Phenotypic staging was carried out and defined by two independent graders for each patient. Clinical characteristics and *ABCA4* mutation profile were described and analyzed for all patients.

Recessive Stargardt disease phenocopying hydroxychloroquine retinopathy (Paper III)

Spectral-domain OCT images of 200 patients with STGD1 were retrospectively assessed and 8 patients with a variant of foveal sparing SD-OCT phenotype usually associated with hydroxychloroquine (HCQ) retinopathy were detected. Clinical characteristics and genetic profile of the STGD1 patients with the SD-OCT phenotype were described and analyzed.

4.2. Retinal imaging

Spectral-domain OCT scans, FAF and near-infrared reflectance images were acquired using the Spectralis HRA+OCT device (Heidelberg Engineering, Heidelberg, Germany). Fundus autofluorescence images were acquired by illuminating the fundus with an argon laser source (488 nm) and viewing the resultant fluorescence through a band-pass filter with a short wavelength cutoff at 495 nm. Color fundus photos were obtained with an FF 450plus Fundus Camera (Carl Zeiss Meditec AG, Jena, Germany). Foveal fixation in Paper II was assessed using fundus camera with fixation needle.

Quantitative image analysis

In Paper I, quantitative analyses of the ELM and EZ were conducted on high-resolution SD-OCT scans of the right eye of 24 STGD1 patients (mean age, 12.9 years; range, 5–19 years) and 30 age- matched controls (mean age, 12.5 years; range, 4–20 years).

The sampling area for each measurement was assigned to a position half the distance between the foveal center and the nasal edge of the optic disc, a location measured with the ruler tool within the ophthalmic software (Heidelberg Explorer Software; Heidelberg Engineering **(Figure 6, A).** Analysis of the designated area in the macula was not possible for two patients (P10, P23) due to progressed outer retina atrophy. Thickness and reflectivity values were averages between measurements made manually by two independent observers with the ophthalmic software (Heidelberg Engineering) (**Figure 6, B and C**).

Reflectivity of the ELM and EZ on SD-OCT was assessed by obtaining the maximum pixel gray values (peaks) corresponding to the ELM and EZ of a vertically positioned pixel intensity profile (reflectivity profile) perpendicular to the RPE layer. Pixel intensity profiles were generated and analyzed with ImageJ software (http://imagej.nih.gov/ij/; available in the public domain of the National Institutes of Health, Bethesda, MD, USA) **(Figure 6, C).** Longitudinal changes were analyzed and described where possible.

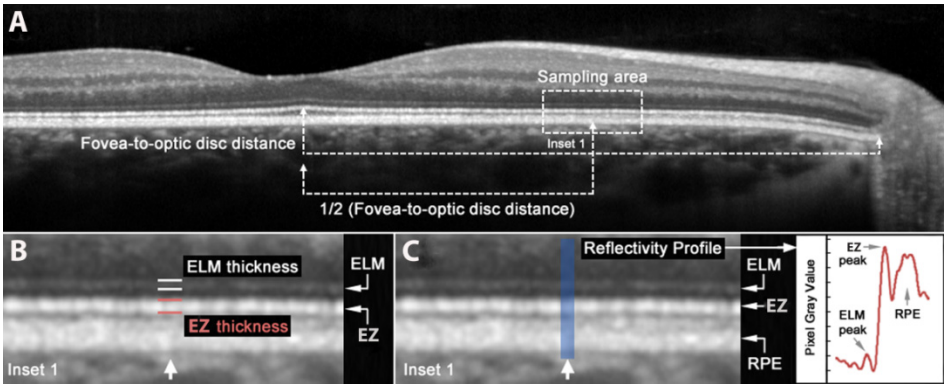

Figure 6. Quantitative analyses of ELM and EZ thickness and reflectivity on SD-OCT. (A) The sampling area for each measurement was assigned to half the distance between the foveal center and the nasal edge of the optic disc. (B) Thickness measurements where made manually by two independent observers. (C) Comparative band reflectivity values were obtained from the maximum pixel gray values (peaks) corresponding to the ELM and EZ of a vertically positioned pixel intensity profile (reflectivity profile).

4.3. Electrophysiology

Full-field scotopic and photopic electroretinograms were obtained according to the International Society for Clinical Electrophysiology of Vision (ISCEV) standards (Marmor et al., 2009) using the Espion visual electrophysiology system (Diagnosys LLC, Littleton, MA, USA) and silver-impregnated fiber electrodes (DTL; Diagnosys LLC, Littleton, MA, USA).

Multifocal ERG in Paper 2 was recorded and analyzed with the VERIS system (VERIS EDI, San Mateo, CA, USA) using Burian-Allen contact electrode. Test was performed according to the standards and guidelines of the International Society for Clinical Electrophysiology of Vision (Hood et al., 2012).

Based on the full-field ERG findings, patients were divided into 3 groups: Group1 exhibited pattern electroretinography abnormalities, but normal full field photopic and scotopic responses, Group 2 exhibited changes in isolated photopic function and Group 3 exhibited significant dysfunction in both the scotopic and photopic systems (Lois et al., 2001).

4.4. Genetic analyses

In Paper I, *ABCA4* screening was first performed with the ABCA4 microarray for all patients. If none or one *ABCA4* mutations were identified, then further screening was performed with next-generation sequencing (NGS).

In Papers II and III all patients were screened for *ABCA4* variants by complete sequencing of all coding and intron/exon boundaries of the gene by either Sanger sequencing or by NGS. The next-generation sequencing was performed either with Fluidigm Custom Amplicon protocol (Access Array; Fluidigm,

South San Francisco, CA; http://www.fluidigm.com/products/access-array.htnl) followed by sequencing on 454 GS-FLX Fluidigm sequencer as described before (Zernant et al., 2011) or with the Illumina TruSeq Custom Amplicon protocol (Illumina, San Diego, CA), followed by sequencing on Illumina MiSeq platform (Illumina MiSeq; Illumina, Inc). The next-generation sequencing reads were analyzed and compared to the reference genome GRCh37/hg19, using the variant discovery software NextGENe (SoftGenetics LLC, State College, PA).

All detected possibly disease-associated variants were confirmed by Sanger sequencing and analyzed with the Alamut software (http://www.interactive-biosoftware.com). Segregation of the variants with the disease was analyzed if family members were available. The allele frequencies of all variants were compared to the Exome Variant Server (EVS) dataset, NHLBI Exome Sequencing Project, Seattle, WA, USA (http://snp.gs.washington.edu/EVS/; accessed March 2014).

4.5. Statistics

The utilized statistical software was SPSS Statistics 16.0 for Windows (SPSS, Inc.; Chicago, IL, USA) and the data compared in the studies were deemed statistically significant when $p < 0.05$.

In Paper I, the statistical comparisons of the ELM and EZ measurements between study subjects and age–matched controls were done by unpaired Student t-tests (two-tailed). Agreement on manual measurements of the ELM and EZ was assessed between two independent observers with intraclass correlation coefficients (ICC).

The statistical comparison of the age at time of examination, age of onset and estimated disease duration between the p.G1961E and non-p.G1961E patients in Paper II was performed by unpaired Student t-test (two-tailed). Pearson's chi-square test was used to analyze the significance of the presence of the p.G1961E allele in patients with the optical gap phenotype.

4.6. Ethics

All patients were enrolled in the study after consenting under the protocol #AAAI9906. The protocol was approved by the Institutional Review Board at Columbia University and adhered to the tenets set out in the Declaration of Helsinki. Each subject signed the informed consent.

5. RESULTS

5.1. Phenotypic expression and outer retinal abnormalities in young patients with STGD1 (Paper I)

The study cohort consisted of 26 young patients with early-onset STGD1 imaged before age 20 years.

5.1.1. Clinical and genetic evaluation of the young STGD1 patients

The mean disease duration was 3.2 years, ranging between 0.5 to 8 years. In 7 patients the data about disease duration was not available, because the patients did not remember the age when the symptoms started or the disease was detected accidentally. Best-corrected visual acuities ranged from 20/20 to 20/400 in both eyes. At least two (expected) disease-causing mutations in *ABCA4* gene were identified in all patients, except one sibling pair (P2 and P3) and P20 in whom only one disease associated allele was found **(Table 1).**

5.1.2. Phenotypic evaluation of the young STGD1 patients

At the time of examination 54% of patients exhibited central macular atrophy with or without perifoveal flecks (Fishman stage 1), while 46% of patients exhibited more widespread flecks often extending anterior to the vascular arcades (Fishman stage 2). P12 presented asymptomatically with no apparent changes on funduscopy and was discovered through an affected sibling. Eight patients (31%) presented with bull's eye maculopathy phenotype. 18 patients (69%) patients presented either initially with, or eventually developed yellow pisciform flecks. Fundus autofluorescence imaging revealed the presence of "fine macular dots" in 14 patients (54%). Qualitative thickening of the ELM on SD-OCT was noted in all patients. Full-field ERG results were available for 19 patients, of which 13(68%) exhibited normal generalized scotopic and photopic function (Group 1) and six (32%) had amplitudinal reduction and implict time delays in the photopic system (Group 2). Patients were grouped into Group 1 or Group 2 accordingly (Lois et al., 2001).

Table 1. Summary of clinical and genetic characteristics of young STGD1 patients.

Patient	Age (y)	BCVA Snellen		Fishman Stage	ffERG Group	Estimated Disease Duration, y†	*ABCA4* Mutation	
		OD	OS				Allele 1	Allele 2
P1	10	20/30	20/25	1	1	1	p.E160*	p.R1108C
P2	10	20/70	20/80	2	2	0.5	p.[L541P;A1038V]	
P3	7	20/40	20/30	1	1	ND	p.[L541P;A1038V]	
P4	13	20/80	20/50	2	1	ND	p.P1380L	c.5714+5G>A
P5	14	20/200	20/150	1	1	0.5	p.P1380L	c.5714+5G>A
P6	13	20/40	20/50	2	1	ND	p.[L541P;A1038V]	p.L2027F
P7	8	*n/a*	*n/a*	1	*n/a*	ND	p.[L541P;A1038V]	p.L2027F
P8	10	20/40	20/80	1	1	1	p.R1108C	p.Q1412*
P9	14	20/100	20/100	2	1	0.5	p.T972N	p.L2027F
P10	9	20/150	20/400	2	1	ND	c.5312+1G>A	p.R2030*
P11	15	20/200	20/200	2	2	3	p.L2027F	p.R2077W
P12	5	20/30	20/40	1	*n/a*	ND	c.5018+2T>C	p.G1961E
P13	10	20/200	20/200	2	2	4	p.[L541P;A1038V]	p.R1640W
P14	12	20/200	20/200	2	2	6	p.[L541P;A1038V]	p.R1640W
P15	16	20/200	20/200	2	*n/a*	8	p.K346T	p.T1117I
P16	9	20/150	20/150	1	*n/a*	1	p.P1380L	p.G1961E
P17	18	20/40	20/150	1	1	3	p.P1380L	p.G1961E
P18	18	20/150	20/150	2	1	4	p.[L541P;A1038V]	p.L2027F
P19	16	20/150	20/150	1	*n/a*	6	p.G863A	p.[W1408R;R1640W]
P20	18	20/125	20/50	2	2	5	p.R1640W	p.V1693I (benign)
P21	12	20/50	20/50	1	1	6	p.W821R	p.C2150Y
P22	17	20/40	20/100	1	*n/a*	3	p.G1961E	c.6729+4_+18del
P23	10	20/400	20/400	2	2	3	c.885delC	p.R537C
P24	19	20/20	20/20	1	*n/a*	ND	p.G863A	c.5898+1G>A
P25	16	20/80	20/100	1	1	4	p.A1773V	p.G1961E
P26	17	20/150	20/200	1	1	2	p.K1547*	p.R2030Q

ND, not determined; n/a, not available.
† Estimated disease duration is defined as age of first examination minus reported age of onset.

5.1.3. Longitudinal changes in the cohort

Progression data following two or more time points, one year apart, revealed variable changes in each patient. Out of 17 patients who initially presented with yellow pisciform flecks, two (P2, P9) had very fast progression from small hyper-AF flecks around the fovea to partially resorbed flecks beyond the vascular arcades; two others (P11, P15) presented with larger hyper-AF flecks throughout the macula and developed flecks beyond the vascular arcades, exhibiting partial darkening and resorption of some flecks; and one (P8) appeared unaffected and developed small hyper-AF flecks around the fovea. Serial SD-OCT imaging revealed a receding EZ and apparent RPE thinning over time at the leading edge of the central lesion of atrophy. No apparent changes to the ELM were observed in this time period; however, a consistent discordance between the position of EZ loss and ELM loss was noted. In almost all observed cases, the EZ appeared to recede earlier than the ELM on SD-OCT.

5.1.4. Quantitative analysis of outer retinal layers in young STGD1 patients

The ELM and EZ thickness as well as reflectivity was measured and compared with the age-matched control subjects**.** The measurements of ELM and EZ thickness as well as reflectivity of the bands were done by two independent observers and the calculated ICCs revealed acceptable agreement between both observers for each measurement **(Table 2).**

Table 2. Intraclass correlation coefficients of SD-OCT measurements.

	STGD1 Patients	**Unaffected Individuals**
Sampled ELM Thickness (μm)	0.948 (0.782–0.982)	0.836 (0.659–0.922)
Sampled ELM Reflectivity (gray value)	0.938 (0.861–0.973)	0.920 (0.830–0.962)
Sampled EZ Thickness (μm)	0.796 (0.472–0.915)	0.874 (0.738–0.940)
Sampled EZ Reflectivity (gray value)	0.857 (0.675–0.937)	0.876 (0.736–0.941)

The 95% confidence intervals are in parentheses; SD-OCT, spectral domain-optical coherence tomography; ELM, external limiting membrane; EZ, ellipsoid zone; STGD1, Stargardt disease.

Qualitative and quantitative analyses of the ELM and EZ bands on SD-OCT revealed consistent and significant difference between STGD1 patients and age-matched controls. The thickness of the ELM band in the measured area was significantly greater (mean = 17.69 μm, SD = 4.23) in STGD1 patients, particularly in the three younger patients (P3, P10, P16), compared with unaffected individuals (mean = 11.45 μm, SD = 1.08, $p < 0.0001$; **Table 3 and Figure 7, A).** A mild downward trend in ELM thickness with age was noted ($r^2 = 0.21$), while ELM thickness appeared to be relatively constant in the control group.

We also measured the EZ thickness in the same area and detected that STGD1 patients exhibited a thinner (mean = 16.65 μm, SD = 2.34, $p < 0.0001$) EZ compared with unaffected individuals (mean = 20.64 μm, SD = 1.34, $p < 0.0001$; **Table 3 and Figure 7, B)**.

To assess the thickness of the ELM relative to the EZ, the calculated ratios of ELM/EZ in the patients were compared with the control ratios. Ratios of ELM/EZ in unaffected individuals fell consistently within the 0.5 range, indicating a 1-to-2 relationship between the thickness of the ELM and EZ on SD-OCT. Thickness ratios of ELM/EZ in STGD1 patients, while more variable, were significantly greater ($p < 0.0001$) than the control group (**Table 3 and Figure 7, C**).

Band reflectance on SD-OCT was assessed by comparing the brightest pixel (vertical gray value profile peak) of the ELM and EZ bands **(Table 3**). To compare patients while accounting for scan normalization, reflectance values were compared as ratios for each patient. The reflectance ratios in STGD1 patients were significantly greater ($p < 0.0001$) than those of the control group **(Table 3 and Figure 7, D)**. Quantitation in two patients, P10 and P23, was impossible due to progressed atrophy in the measurement area; however, the ELM thickening and increased reflectivity was qualitatively observed in their respective SD-OCT scans in less-affected areas of the macula.

Table 3. Quantitative thickness and reflectivity sampling in SD-OCT scans.

	SD-OCT Thickness (μm)				**SD-OCT Reflectivity (gray value)**			
	EZ		**ELM**		**EZ**		**ELM**	
Mean Measurements	**STGD1**	**Control**	**STGD1**	**Control**	**STGD1**	**Control**	**STGD1**	**Control**
Mean	16.65	20.64	17.69	11.45	170.40	210.58	139.5	81.15
Standard deviation	2.34	1.34	4.23	1.08	19.24	31.32	24.40	22.76
Standard error	0.48	0.24	0.86	0.20	3.98	5.72	4.98	4.16
	SD-OCT Thickness (μm)				**SD-OCT Reflectivity**			
Unpaired *t*-test	EZ: STGD vs control		ELM: STGD1 vs. control		ELM-EZ ratio: STGD1 vs control			
p-value	< 0.0001		< 0.0001		< 0.0001			
	ELM-EZ ratio: STGD1 vs. control < 0.0001							

SD-OCT, spectral-domain optical coherence tomography; ELM, external limiting membrane; EZ, ellipsoid zone; STGD1, Stargardt disease.

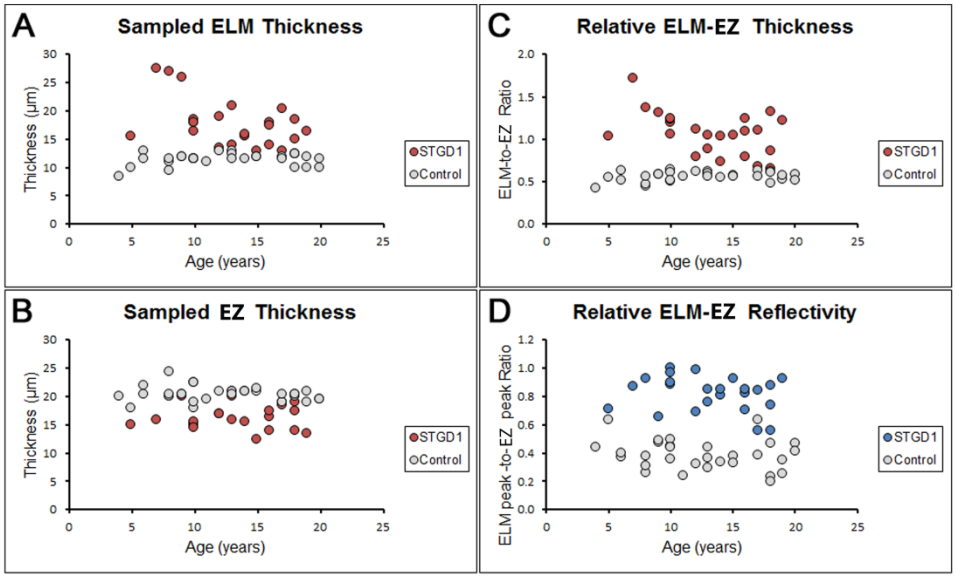

Figure 7. Quantitative analyses of the ELM and EZ band thickness and reflectivity on SD-OCT. Thickness (µm) of the ELM and EZ were measured at a consistent position within the macula in 24 STGD1 patients (red circles) and 30 age-matched controls (gray circles). Analysis of the designated area of the macula was not possible in two patients (P10, P23) due to progressed atrophy. (A) Thickness of the ELM in the measured areas was significantly greater ($p < 0.0001$) in STGD1 patients compared with unaffected individuals, (B) whereas the thickness of the EZ at the same location was thinner in STGD1 ($p < 0.0001$). (C) The relative ELM/EZ thickness (calculated as the ratio between the ELM and the EZ) within normal subjects consistently fell within 0.5 (EZ band is approximately two times thicker than the ELM band); an overall larger and more variable relative ELM/EZ thickness ($p < 0.0001$)was observed in STGD1 patients. (D) Relative reflectivities of the ELM-to-EZ bands where significantly more intense ($p < 0.0001$) in STGD1 patients compared with normal controls.

5.2. Optical gap phenotype in STGD1 (Paper II)

The optical gap, also referred as optically empty lesion or foveal cavitation (Leng et al., 2012), is a retinal phenotype representing a focal loss of subfoveal photoreceptors detectable on SD-OCT as a focal loss of ellipsoid reflectivity leaving an optically empty space under the fovea (Leng et al., 2012).

We detected the optical gap phenotype in 15 STGD1 patients from the cohort of 179 patients with the available SD-OCT images and characterized the optical gap phenotype in STGD1 according to its developmental stages. We investigated the mutations in the *ABCA4* gene in these patients and detected a phenotype-genotype association.

5.2.1. Clinical and phenotypic evaluation of STGD1 patients with the optical gap phenotype

Fifteen patients were detected and evaluated from a cohort of 179 patients **(Table 4)**. The mean age of the patients with the optical gap phenotype was 23.5 years (range, 12–30 years) and the reported age of the disease onset was in the second and third decades of life (mean age of onset of 19.4 years) corresponding to the mean symptomatic disease duration of 4 years. One patient (P1) was asymptomatic at the time of presentation.

Thirteen patients exhibited a bull's eye-like phenotype on color fundus photos. Parafoveal flecks were observed in 6 patients (12 eyes). Fixation was assessed at the first visit in 10 patients. Eighteen eyes from 10 patients had extrafoveal fixation, while P10 and P11 had preserved central fixation in the right eye only due to the eccentric localization of the optical gap and preserved ellipsoid zone in the center.

All except two patients (P1, P2) had undergone full-field ERG at initial visit and were categorized to Group 1 (Lois et al., 2001) having age-matched normal scotopic and maximal responses. Multifocal ERG data were available in six patients, while half of them had data available only for the right eye. Each patient had decreased responses in the central 5° to 15° on mf ERG, showing much larger affected area than SD-OCT and FAF images predicted.

5.2.2. Structural staging of the optical gap phenotype with SD-OCT

Based on clinical observation and follow-up data from SD-OCT images we staged the optical gap phenotype and divided the patients into three disease development groups (**Figure 8**).

Stage 1: Moderate ellipsoid zone disruptions.
The initial stage represented distinctive structural breaks in the EZ and degradation of photoreceptors in the foveal outer retina on SD-OCT forming an optically empty zone fulfilled with remnants of the ellipsoid **(Figure 8, P2).** The ONL thinning in the macula was present in all patients, while the ELM and the RPE were intact. Five patients (10 eyes) of the 15 patients presented with this, Stage 1, disease.

Best corrected visual acuity was relatively mildly affected ranging from 20/25 to 20/60 (mean 20/40) and appeared to be dependent on the degree of EZ band loss.

Fundus autofluorescence images showed a dark roundish lesion with reduced FAF signal in 4 patients, while one patient exhibited a more horizontally-elongated lesion.

Table 4. Summary of demographic and clinical data of *ABCA4*-associated optical gap patients.

Patient #, Gender	Age (yrs)	BCVA Snellen		Age of Onset (yrs)	Optical Gap Staging				ERG Group	Lesion shape on AF		Fixation	
					Initial		*Current*						
		OD	*OS*		*OD*	*OS*	*OD*	*OS*		*Ellip-tical*	*Circu-lar*	*OD*	*OS*
P1, F	22	20/40	20/50	Unknown	1	1	1	1	N/A	–	+	N/A	N/A
P2, F	25	20/40	20/30	24	1	1	1	1	N/A	–	+	Eccentric	Eccentric
P3, M	30	20/30	20/30	25	1	1	1	1	G1	–	+	N/A	N/A
P4, M	30	20/25	20/25	25	1	1	1	1	G1	–	+	N/A	N/A
P5, F	18	20/60	20/60	14	0	0	1	1	G1	+	–	Eccentric	Eccentric
P6, F	24	20/150	20/150	14	2	2	2	2	G1	Speckled		N/A	N/A
P7, F	22	20/100	20/100	17	2	2	2	2	G1	+	–	Eccentric	Eccentric
P8, F	19	20/80	20/80	15	2	2	2	2	G1	+	–	Eccentric	Eccentric
P9, F	25	20/100	20/150	15	2	2	2	2	G1	+	–	Eccentric	Eccentric
P10, F	23	20/40	20/30	18	2	2	2	2	G1	+	–	Foveal	Eccentric
P11, M	23	20/40	20/30	22	2	2	2	2	G1	–	+	Foveal	Eccentric
P12, F	22	20/50	20/70	21	2	2	2	2	G1	+	–	N/A	N/A
P13, M	12	20/50	20/50	10	2	2	2	2	G1	+	–	Eccentric	Eccentric
P14, F	30	20/100	20/100	25	Atrophy	2	Atrophy	3	G1	+*	–	Eccentric	Eccentric
P15, F	28	20/30	20/30	26	3	3	Atrophy	Atrophy	G1	+	–	Eccentric	Eccentric

F, female; M, male; N/A, not available.
* left eye only.

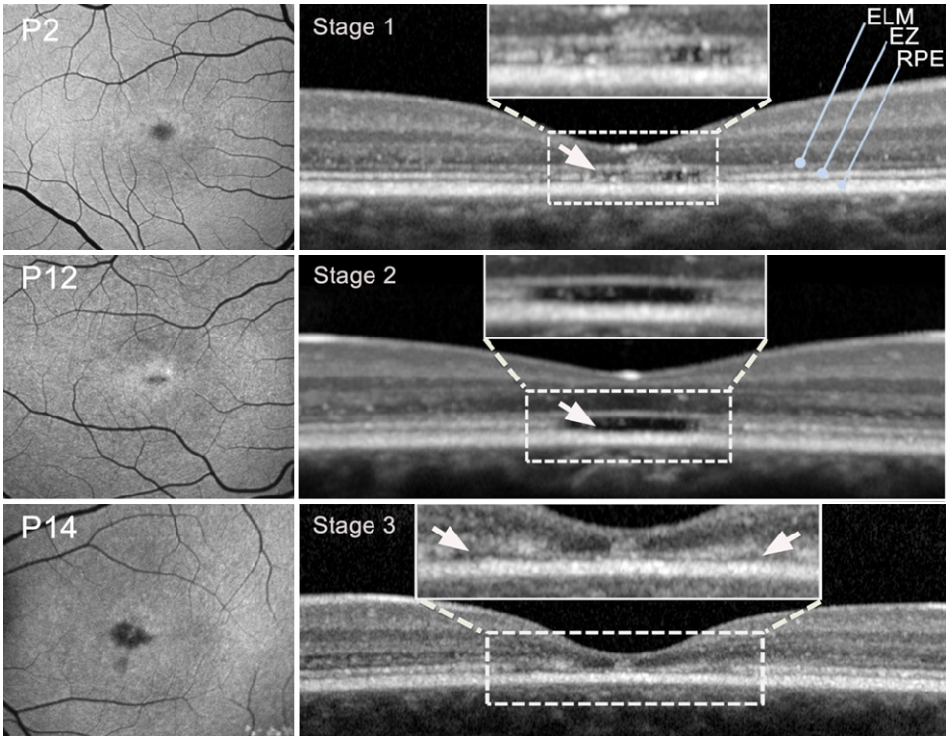

Figure 8. Developmental stages of the optical gap lesion in STGD1.

Stage 2: Expanded foveal cavitation.
A widened empty cavity characterized by total absence of the EZ was observed on SD-OCT in eight patients **(Figure 8, P12).** Some granular deposits or residual debris were attached to the concavely arched ELM in the lesion. A relatively larger, horizontally-elongated lesion resembling an elliptical bull's eye lesion within a hyper-AF halo was observed on FAF imaging in six patients, while P6 had speckled macular appearance on FAF image, which corresponded with fleck-like deposits in the central macula.

Mean visual acuity in Stage 2 patients was 20/80 spanning a spectrum from 20/30 to 20/150. In two patients (P10, P11) the optical gap lesion was atypically eccentrically off-centered, preserving the EZ at the fixation point. Therefore, these patients maintained the BCVA of 20/40 and 20/30 in the right and left eyes, respectively and central fixation in the right eye.

Stage 3: Inner retinal collapse.
A structural collapse of the inner retinal layers into the vacant ellipsoid space with residual spaces along the edge of the previously occupied gap lesion was observed in P14 **(Figure 8, P14**), where we had clear evidence on OCT images showing transition from stage 2 to stage 3. In the retrospective review of the whole cohort, we detected another patient with similar structure with the residual gap spaces along the edges of the lesion, P15.

Visual acuities appeared similar to stage 2 patients, while the BCVA of P15 was relatively preserved at 20/30 in both eyes, possibly explained by relatively spared outer retina fragment in the foveal center seen on FAF and SD-OCT images.

5.2.3. Longitudinal analysis of the optical gap phenotype in STGD1

The longitudinal data enabled us to understand how the optical gap structure behaves over the time and made possible to create the staging system for the optical gap phenotype.

Longitudinal data and images were available and analyzed in 8 patients (P5-P8 and P12-P15). The initial and current stage is presented in Table 4.

Inter-stage progression was observed in patients P5, P14 and P15, while other patients for whom the data were available remained Stage 2 within 1.5 to 3 years follow-up (**Figure 9**). P5 initially presented with mild photoreceptor disorganization and Stage 1 optical gap was detected after one year. The BCVA progressed from 20/30 and 20/25 to 20/60 in both eyes. Her older sibling (P6) exhibited a more advanced Stage 2 optical gap lesion. P14 progressed from Stage 2 to Stage 3 within 2 years retaining a stable BCVA of 20/100 in both eyes. Progression of Stage 3 gap to progressive atrophy within 1 year was seen in P15.

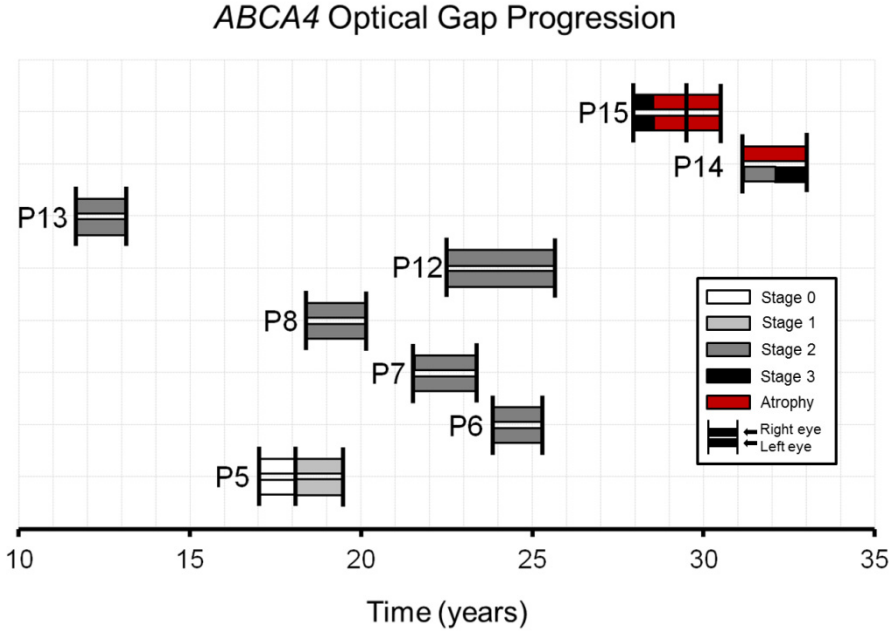

Figure 9. Gantt chart summarizing the *ABCA4*-associated optical gap stage progression and duration. Longitudinal OCT imaging was available for eight patients in the study cohort. Patient 5 presented with minor EZ changes (Stage 0) and progressed bilaterally to Stage 1 optical gap a year after initial examination. Patients 6, 7, 8, 12 and 13 initially presented and remained in Stage 2 over a range of 1.5 to 3 years. Patients 15 progressed to an atrophic stage following Stage 3, while P14 exhibited unilateral progression from Stage 2 to Stage 3 in the left eye.

5.2.4. Phenotype-genotype association in STGD1 with the optical gap phenotype

The cohort of 15 patients included 11 unrelated cases and four sibling pairs. Segregation analysis was available for 11 patients. At least two (expected) disease-causing variants were identified in each patient. In unrelated cases, 91% were compound heterozygous for the p.G1961E variant (**Table 5**). With the exception of P13, the optical gap was not observed in the SD-OCT scans of any other non-p.G1961E patients (n = 131) whose age at time of examination, age of onset and estimated disease duration were not statistically different from those of p.G1961E (n = 48) patients (**Table 6**). The allele frequency of p.G1961E allele in patients with the optical gap phenotype was 46.7%, while in the entire STGD1 cohort of 179 patients (157 unrelated individuals) it was 13.4%, showing statistically highly significant difference ($p < 0.0001$).

Table 5. Summary of genetic data of *ABCA4*-associated optical gap patients.

Patient #, Gender	***ABCA4* Mutations**	
	DNA level	***Protein level***
1, F†*	c.[286A>G];[5882G>A]	p.[(N96D)];[(G1961E)]
P2, F†*	c.[286A>G];[5882G>A]	p.[(N96D)];[(G1961E)]
P3, M†	c.[1622T>C(;)3113C>T(;)5882G>A]	p.[(L541P(;)A1038V(;)G1961E)]
P4, M†	c.[1622T>C(;)3113C>T(;)5882G>A]	p.[(L541P(;)A1038V(;)G1961E)]
P5, F†*	c.[1622T>C;3113C>T];[5882G>A]	p.[(L541P;A1038V)];[(G1961E)]
P6, F†*	c.[1622T>C;3113C>T];[5882G>A]	p.[(L541P;A1038V)];[(G1961E)]
P7, F†*	c.[1622T>C];[5882G>A]	p.[(L541P)];[(G1961E)]
P8, F†*	c.[1622T>C];[5882G>A]	p.[(L541P)];[(G1961E)]
P9, F*	c.[5882G>A];[6448T>C]	p.[(G1961E)];[(C2150R)]
P10, F*	c.[4139C>T];[5882G>A]	p.[(P1380L)];[(G1961E)]
P11, M	c.[5318C>T(;)5882G>A]	p.[(A1773V(;)G1961E)]
P12, F*	c.[5196+1056A>G];[5882G>A]	p.[?];[(G1961E)]
P13, M*	c.[2461T>A];[6449G>A]	p.[(W821R)];[(C2150Y)]
P14, F	c.[5882G>A(;)6229C>T]	p.[(G1961E(;)R2077W)]
P15, F*	c.[1622T>C;4328G>A];[5882G>A]	p.[(L541P;R1443H)];[(G1961E)]

†Sibling pairs: P1and P2, P3 and P4, P5 and P6, P7 and P8.
*The variants are confirmed on different chromosomes.

Table 6. Comparison of clinical data between p.G1961E and non-p.G1961E patients from the entire STGD1 cohort of 179 patients.

	p.G1961E mutation(s) n: 48				**Other *ABCA4* mutations n: 131**				
Clinical data	Mean	SD	Median	Range	Mean	SD	Median	Range	***p-value***
Age	34.5	18.6	28.5	5 to 78	36.9	17.8	37.6	7 to 83	> 0.4
Age of Onset	20	10.1	17.5	2 to 55	19.4	12.1	16.5	4 to 52	> 0.7
Disease Duration	15.6	17.8	8.5	0.1 to 71	17.8	14.9	14.3	0.2 to 63	> 0.4
Fundus phenotype	**Patients (n)**				**Patients (n)**				
BEM	39				42				
Other†	9				89				
Optical Gap	14				1				

Statistical comparison is made by unpaired Student t-test (two-tailed); *p*-value is calculated between p.G1961E and non-p.G1961E patients;
SD, standard deviation; BEM, bull's eye maculopathy; † Other than bull's eye lesion (minor macular changes to more advanced atrophy).

5.3. A subtype of foveal sparing phenotype in STGD1 resembling HCQ retinopathy (Paper III)

We detected and analyzed 8 unrelated patients with STGD1 from the cohort of 200 STGD1 patients who exhibited a variant of foveal sparing phenotype on SD-OCT described previously with HCQ retinopathy. This transient HCQ retinopathy SD-OCT phenotype represents an outer retinal thinning in the parafoveal region with the relative sparing of the foveal region, colloquially termed the „flying saucer" sign (Chen et al., 2010)**.** A retrospective clinical and genetic evaluation of these patients was done and structural analysis of the retina was carried out. Three patients with STGD1 were having classical bull's eye lesion similar to HCQ retinopathy.

5.3.1. Clinical and genetic evaluation of the patients

The cohort (age range, 10–57 years) consisted of ethnically diverse individuals who presented to the Retina Clinic for a retinal evaluation. All patients presented to the clinic without a medical history of HCQ use **(Table 7).** Five patients (P2, P4, P5, P6 and P7) reported no visual symptoms but were referred for a retinal evaluation after routine optometric visits, while P3 complained of mild bilateral

metamorphopsia and P8 complained of halos in front of both eyes. The majority of the patients had 20/20 vision **(Table 7).** Full-field ERG results showed no generalized rod or cone dysfunction.

Genetic screening of both the *ABCA4* and *PRPH2* genes by complete sequencing of the coding regions confirmed two (expected) disease-causing *ABCA4* mutations in five patients and one mutation in the remaining three patients. No mutations in the *PRPH2* gene were found.

Table 7. Clinical and genetics characteristics of the study cohort.

Patient	**Age, Gender**	**Snellen BCVA**		**Fundus Appearance**		***ABCA4* Mutation(s)**
		OD	*OS*	*Color*	*FAF*	
P1	53, M	20/20	20/20	Mottling + Flecks	Mottling + Flecks	c.[5461-10T>C]
P2	55, F	20/20	20/20	Mottling + Flecks	Mottling + Flecks	p. [A1357V] ; [G1961E]
P3	57, M	20/20	20/20	BEM + Flecks	BEM + Flecks	p. [R2107H]
P4	10, F	20/30	20/25	BEM + Flecks	BEM + Flecks	p. [E160*] ; [R1108C]
P5	26, F	20/30	20/20	Mottling + Flecks	Mottling + Flecks	p. [R2107H] ; [E526A]
P6	19, F	20/25	20/25	BEM	BEM	p. [R602W]
P7	26, M	20/20	20/20	BEM	BEM	p. [R1300*] ; [R2106C]
P8	25, M	20/20	20/40	BEM	BEM	p. [Q1003*] ; [G1961E]

M, male; F, female; BCVA, best-corrected visual acuity; OD, right eye; OS, left eye; BEM, bull's eye maculopathy.

5.3.2. Structural analysis of the retina

Fundus photos and FAF imaging

All patients exhibited either a confined or bull's eye maculopathy (BEM)-type lesion restricted within the vascular arcades on fundus photos (**Figures 10 and 11**). Yellow fleck deposits around the central lesions were observed in five patients (P1–5). Accompanying macular lesions in FAF imaging varied among patients. Round or elliptical BEM lesions with a dark center and hyper-AF border were noted in P6, P7 and P8, while mottled fleck patterns where observed in P1–5 (**Figures 10 and 11**). Patients 3 and 4 also exhibited a ring of fluorescent granular deposits surrounding the hypo-AF ovoid foveal lesion (**Figures 10 and 11, P3 and P4**).

Structural analysis of the retina on SD-OCT

Single horizontal line scans through the fovea and volume SD-OCT scans in each patient revealed an abrupt disruption of the EZ band in the parafoveal region and thinning of the outer nuclear layer (ONL), with relative sparing of the central foveal region. Posterior displacement of the parafoveal inner retinal layers and relatively spared fovea with slightly anteriorly bowing ELM and EZ bands forming a so-called „flying saucer“ configuration associated with HCQ-induced retinal toxicity was evident in all patients (see **Figures 10 and 11**).

Despite the apparent sparing of the fovea, SD-OCT scans showed some abnormalities within this region in all patients. All patients had loss of the IZ and thinning of ONL and EZ, except P3, who exhibited normal apparent thickness of all retinal layers, and P1, who showed no apparent decrease in ONL thickness in the fovea **(Figures 10 and 11).** Thinning of the RPE-Bruch's membrane complex in the fovea was observed in three patients (P2, P7 and P8). Patient 4 exhibited a thickened ELM protuberance that delimited a thin layer of spared EZ in the fovea.

The degree of outer retina involvement in the parafoveal region was variable. Three patients (P1–3) showed discontinuity/disruption of the EZ band and thinning of ONL preserving the ELM. Ellipsoid zone disruption in P1 was seen throughout a speckled FAF lesion. Total loss of parafoveal EZ was seen in P4–8, while P7 and P8 had the most prominent changes, resembling most advanced parafoveal atrophy with the ELM loss and the RPE thinning (**Figure 11, P7 and P8**). The RPE thinning in this region also was noted in P1 and P2, while P2 had a very confined area of geographic atrophy in the nasal side of the fovea (**Figure 10, P2**). Interdigitation zone loss was present in all patients, becoming visible in parafoveal region in three patients (P2, P7 and P8).

5.3.3. Lesion formation

A preceding stage of the transient HCQ retinopathy phenotype in STGD1 was observed in P6, who exhibited EZ band loss (optically empty space) in the parafoveal region around the central island of preserved and hyper-reflective photoreceptor layer (**Figure 12, c**). Seven months later, the optically empty space appeared to collapse, forming a lesion resembling the transient HCQ-induced retinal toxicity SD-OCT phenotype (**Figure 12, f)**

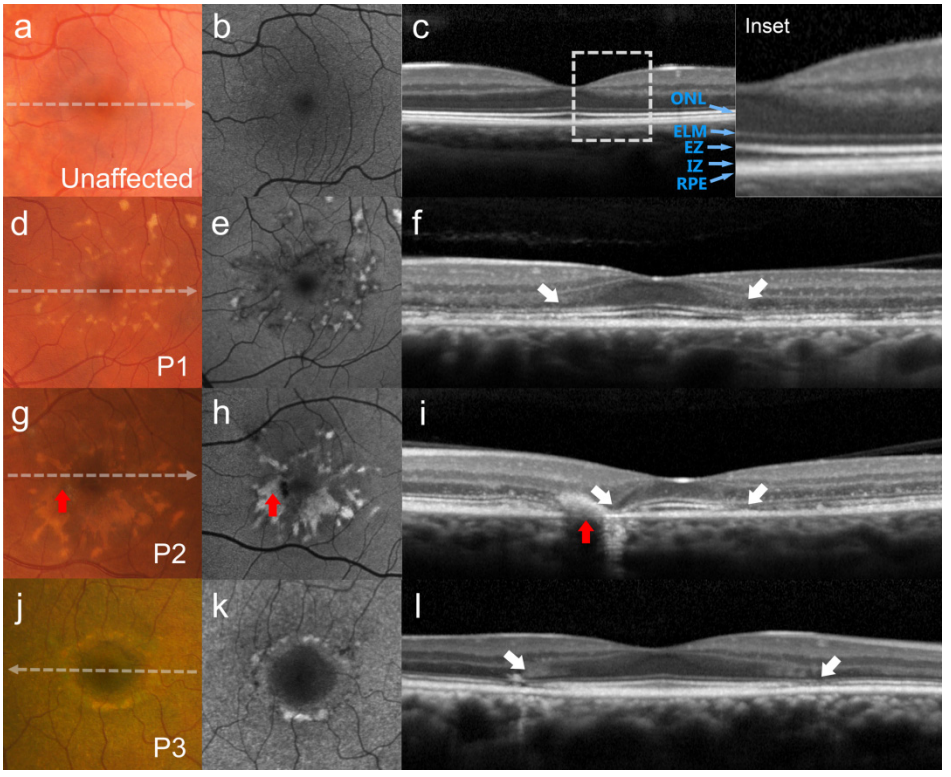

Figure 10. Thinning of the parafoveal region with relative foveal sparing presenting as the hydroxychloroquine retinopathy associated parafoveal outer retina thinning phenotype in patients with Stargardt disease. Color photograph (a), fundus autofluorescence (b), and spectral-domain optical coherence tomography (c) images of an unaffected individual with outer retinal layers defined: the outer nuclear layer (ONL), the external limiting membrane (ELM), the ellipsoid zone (EZ), the interdigitation zone (IZ) and the retinal pigment epithelium (RPE) (Inset). Yellow pisciform flecks accompanying mottling over in the central macula are apparent on color, FAF and SD-OCT (g, h, i; red arrows). Corresponding SD-OCT scans (f, i, l) reveal abrupt disruptions of the outer retinal layers in the parafoveal regions in each patient (white arrows).

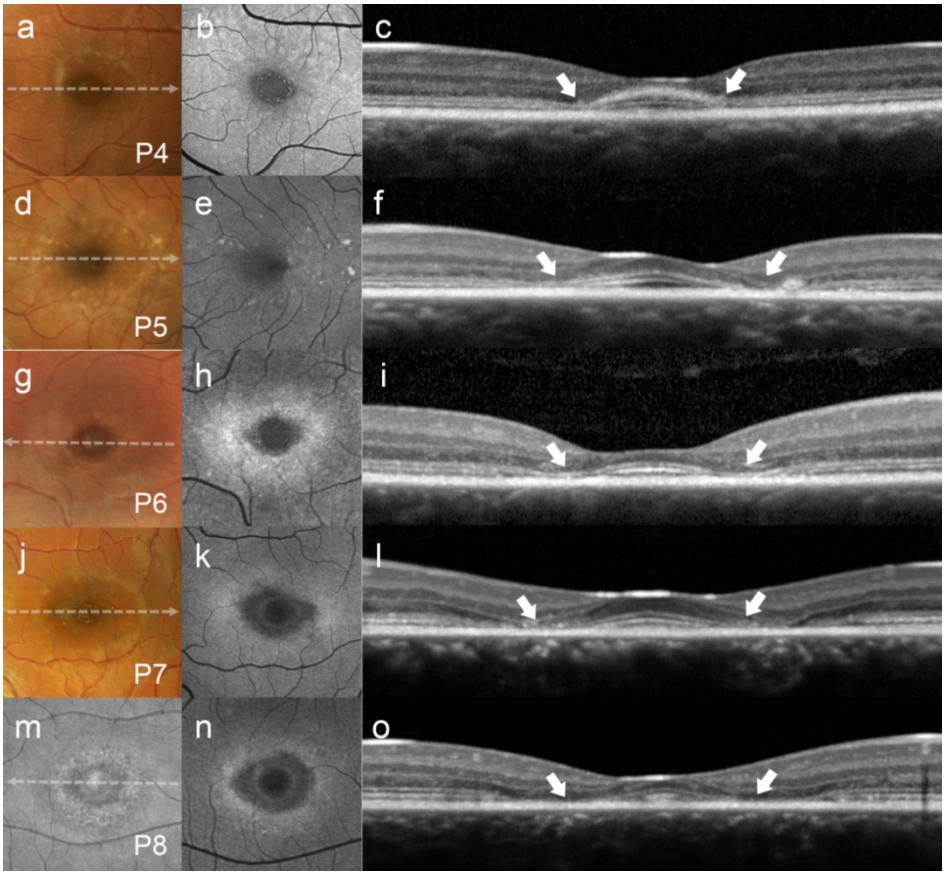

Figure 11. Abrupt thinning of the parafoveal region (white arrows), with relative foveal sparing, presenting as the hydroxychloroquine retinopathy associated parafoveal outer retina thinning phenotype with Stargardt disease, continued. Color photographs (a, d, g, j), fundus autofluorescence images (b, e, h, k, n), and spectral-domain optical coherence tomography images (c, f, i, l, o) in patients 4, 5, 6, 7 and 8; infrared reflectance image (m) in P8.

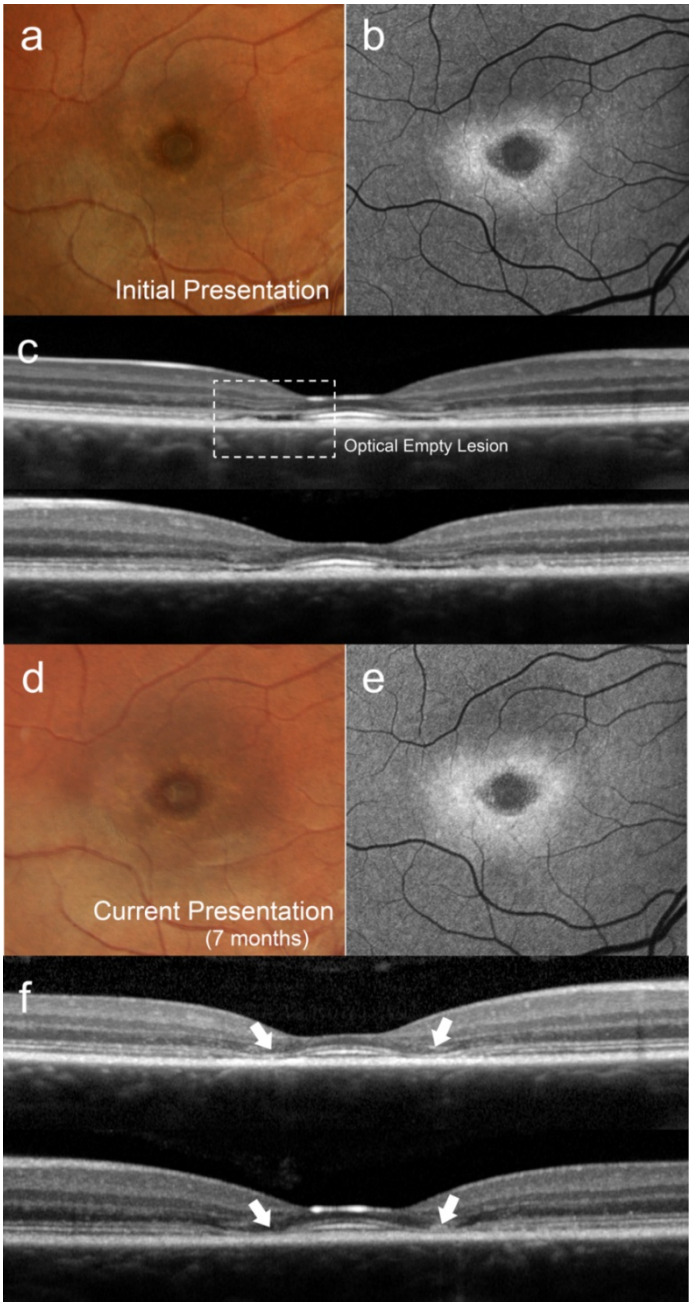

Figure 12. Structural development of a lesion resembling the HCQ associated parafoveal outer retina thinning phenotype in patient 6. Color (a) and autofluorescence (b) images presented with corresponding spectral domain-optical coherence tomography scans in both eyes (c). Parafoveal optically empty lesions in each eye (dotted box) are apparent bilaterally. A subsequent visit 7 months later (d, e, f) revealed an apparent collapse of the inner retinal layers forming abrupt thinning of the parafoveal region (white arrows), consistent with an HCQ-induced retinal toxicity presentation.

6. DISCUSSION

STGD1 is the most common inherited macular dystrophy caused by defective ABCA4 transporter leading to excessive lipofuscin accumulation, RPE cell and photoreceptor degeneration (Molday and Zhang, 2010). The classical phenotype in STGD1 is an atrophic-appearing macular lesion with pisciform yellowish flecks, but there is a remarkable phenotypic heterogeneity (Michaelides et al., 2003).

Today, the modern imaging methods provide us with new possibilities in studying the phenotypic expression of the disease (Keane and Sadda, 2014). One of such is SD-OCT, which enables to perform in vivo histology and detect even very fine structural changes in the retina.

All our studies used SD-OCT to assess the retinal structural changes and phenotypes in STGD1. The universal phenotypic feature in STGD1 is outer retinal degeneration and thinning detectable on SD-OCT (Duncker et al., 2014, Burke et al., 2011, Park et al., 2015, Ergun et al., 2005), however it has been shown that inner retinal changes accompany with photoreceptor loss indicating that retina is a complex tissue with different cell types and communications (Huang et al., 2014, Genead et al., 2011, Pasadhika et al., 2009).

6.1. Early stage retinal structural changes in STGD1

We have shown for the first time quantitatively in a cohort of patients that, in addition to atrophic outer retinal changes, there is an abnormal ELM thickening in young STGD1 patients. At the time of the study (Paper I) we found only 2 case reports in the literature mentioning the ELM thickening in patients with STGD1 (Burke et al., 2013, Fujinami et al., 2014). One of them reported a single case of a young patient with STGD1 exhibiting an unusual thickening of the ELM on SD-OCT in the absence of other functional and structural changes in the retina (Burke et al., 2013).

Our study included 26 young (< 20 years old) STGD1 patients, imaged relatively soon after the disease onset, and 30 age-matched controls. The quantitative analysis revealed that all patients, except two in whom quantitation was not possible, exhibited significantly thicker and hyper-reflective ELM but thinner EZ compared with the control individuals. The EZ thinning, representing photoreceptor abnormalities (Spaide and Curcio, 2011, Wong et al., 2012), was expected considering the pathogenesis of the disease, while the ELM thickening was somewhat surprising.

The exact source of band reflectivity on SD-OCT is largely unknown, but it has been suggested that mitochondria may partly contribute to the OCT visibility, among other structures. Ellipsoid zone represents the ellipsoids of photoreceptor inner segments, containing high volume of mitochondria (Spaide and Curcio, 2011). The band has been shown to correlate well with the health of photoreceptors and the visual function (Wong et al., 2012, Testa et al., 2012,

Ergun et al., 2005), while the hyper-reflective band above EZ is thought to represent the ELM, which is formed by the apical ends of Müller cells forming junctional complexes between each other and photoreceptors (Spaide and Curcio, 2011, Staurenghi et al., 2014, Ross and Pawlina, 2011). Therefore, several hypotheses can be generated from these findings. First, changes in the ELM can be attributed to the (mis)interaction between photoreceptors and Müller cell processes or homotypically between Müller cells (Burke et al., 2013). Secondly, it has been hypothesized that the ELM thickening and higher reflectivity could be caused by the mitochondria translocation and attachment to the ELM in the background of retinal degeneration (Litts et al., 2015).

Müller cells became reactive to many pathologic stimuli in the retina-weather extrinsic or intrinsic. In the background of photoreceptor degeneration and possible neuroinflammation (Radu et al., 2011, Kohno et al., 2013, Zhou et al., 2006) Müller cell activation is vital, protecting the surrounding neurons and restoring homeostasis in the retina via various mechanisms, including secretion of neurotropic factors, growth factors and cytokines (Reichenbach and Bringmann, 2013). Müller cell activation leads to their reactive gliosis (Bringmann et al., 2009, Bringmann et al., 2006), which involves hypertrophy, proliferation and migration of the glial cells and their processes (Bringmann et al., 2009, Vecino et al., 2016). It is known, that retinal degeneration does not cause only photoreceptor and RPE death, but the process is much more complex and certain pattern of retinal remodeling takes place, including glial seal formation composed of Müller cell distal processes (Jones and Marc, 2005). However, there are still limited data on Müller cell gliosis in retinal dystrophies. In STGD1 we found only one histopathological study on two enucleated eyes, which described the reactive Müller cell hypertrophy in addition to reduced number of photoreceptors and the RPE cells (Birnbach et al., 1994). However, some other *in vivo* studies with mammals have demonstrated early Müller cell activation and gliosis in retinitis pigmnetosa models. In retinitis pigmentosa RPE65 mutant dog model, transient Müller cell activation was noted, interestingly more intense in early stages and younger animals possibly due to less advanced degenerative changes (Vecino et al., 2016). Retinitis pigmentosa P23H (rhodopsin) rat model shows hypertrophy of both Müller cells and astroglia indicating to reactive gliosis in the retina (Fernandez-Sanchez et al., 2015). The hypertrophic Müller cell apical ends form firework-like structures into the ONL, which disappeared in later stages of retinal degeneration (Fernandez-Sanchez et al., 2015). All this indicates that the reactive response is probably a transient event in a background of less advanced atrophic changes. The same is supported by our clinical observation that the ELM prominence is noted in younger patients with generally less advanced atrophic changes. Furthermore, we found the ELM prominence gradually decrease with increasing patient age (downward sloping trend line, $r^2 = 0.21$).

Whether the extensive ELM thickening detectable on SD-OCT is specific to STGD1 needs to be investigated further, but existing studies show that despite

the universal reactive gliosis in retinal stress situations, the extent of the process is disease specific (Hippert et al., 2015).

Different retinal dystrophies share common cellular responses to stress, such as inflammatory response, oxidative stress and activation of apoptotic pathways (Cuenca et al., 2014), but each has also specific factors depending on the etiology and pathogenesis. These include rate of cell loss, intercellular interactions or local change in the chemical milieu which all may affect Müller cell responses. In STGD1 the characteristic pathologic event is increased lipofuscin accumulation, which may contribute to the ELM prominence, furthermore very recently the ELM thickening as an early stage abnormality was described in another Stargardt-like lipofuscin-associated retinopathy (Palejwala et al., 2016).

The study has some limitations. The quantitation method, including the spatially restricted area of the measurements, image quality, inter subject scan normalization, among others, is likely to introduce errors, further necessitating more extensive analyses in addition to those that have been previously described (Hood et al., 2011, Hood et al., 2009). However, comparable studies have confirmed the reproducibility of SD-OCT measurements with built-in caliber tool from the instrument (Heidelberg Engineering) used in this study (Yamashita et al., 2012). In addition, we calculated the intraclass correlation coefficients for the measurements, which showed acceptable agreement between two independent measurers, further indicating compatibility.

It has to be noted, that the patient age was strictly confined to < 20 years. Presuming that ELM abnormalities occur in early stages of STGD1, we examined a cohort of 26 clinically diagnosed and genetically confirmed patients soon after the disease onset. Symptomatic changes indicative of early-onset STGD1 typically begin within the first and second decades of life (Michaelides et al., 2003). Therefore, the inclusion criteria were limited to those patients first examined when aged younger than 20 years. At the time of imaging, most of the patients in our cohort had relatively early stage of the disease (Fishman 1 (54%) or 2 (46%)) with the mean disease duration of 3.2 years. Therefore, due to our selection criteria, we cannot extend these findings to the later-onset disease.

6.2. Sub-phenotypes in STGD1 detectable on SD-OCT

Optical gap phenotype in STGD1

There are several sub-phenotypes in STGD1 which are best detected on SD-OCT, one of which is the optical gap phenotype. It represents a focal loss of subfoveal photoreceptors leaving an optically empty space detectable by SD-OCT (Leng et al., 2012, Cella et al., 2009). The phenotype has been associated with retinal dystrophies mostly affecting cone photoreceptors, such as rod monochromatism (Greenberg et al., 2014) and maculopathies caused by mutations in *RP1L1* and *KCVN2* genes (Park et al., 2010, Sergouniotis et al., 2012). In the literature, only sporadic cases of the optical gap phenotype in

STGD1 have been published (Cella et al., 2009, Leng et al., 2012, Gomes et al., 2009, Ritter et al., 2013).

We conducted a study (Paper II), specifically looking for the optical gap phenotype in a large cohort of STGD1 patients to assess the structural development, possibly deciphering the early effects of ABCA4 dysfunction in this phenotypic subgroup, and the genetic background of the phenotype. Furthermore, we were interested in the association between the phenotype and the retinal function.

The analysis of this patient cohort suggests that the development of optical gap can be divided into three structural stages over several years. Stage 1 patients present with disorganization of photoreceptors and intermittent brakes in the EZ band forming gap lesion in the subfoveal region. A further spatial depletion of the EZ is seen in Stage 2 patients where an expansive subfoveal empty cavity is apparent with accompanying decline in visual acuity. Stage 3 represents a structural collapse of the inner retina into the gap lesion. The visibility of the EZ band has been attributed to the photoreceptor integrity correlating well with visual function (Wong et al., 2012, Testa et al., 2012), therefore patients with Stage 1 optical gap had relatively spared central vision, compared with patients exhibiting more severe EZ loss in Stages 2 and 3. All patients with the optical gap phenotype and available ffERG recordings had normal full-field ERG findings indicating a localized disease and better prognosis in terms of visual function (Fujinami et al., 2013a, Zahid et al., 2013, Lois et al., 1999).

Loss of ABCA4 function results in lipofuscin deposition in the RPE cells that have phototoxic effects on the RPE cells ultimately leading to its imminent death (Sparrow et al., 2000, Sparrow and Boulton, 2005). This mechanism supports the current understanding that structural degeneration of the RPE cells sequentially precedes that of photoreceptors in STGD1 (Sparrow and Boulton, 2005, Cideciyan et al., 2004, Glazer and Dryja, 2002). However, there are still some controversies in the understanding of exact sequence of disease process (Gomes et al., 2009, Duncker et al., 2014, Chen et al., 2011, Song et al., 2015, Glazer and Dryja, 2002). In addition to observation by other groups (Gomes et al., 2009, Cella et al., 2009, Leng et al., 2012), our study supports the finding that the photoreceptors degeneration precedes RPE death in this subgroup of patients. First of all, in Stages 1 and 2 the RPE seems relatively intact despite the EZ band disruption. Secondly, the mf ERG from nine eyes showed decreased responses in the 5° to 15° of retina in the posterior pole. Similar to other mfERG studies in STGD1 (Kretschmann et al., 1998, Gomes et al., 2009) the functionally affected areas were much larger than structural changes on SD-OCT or FAF, suggesting that functional loss precedes structural changes in these patients. Additionally, given that the decreases in mfERG responses have been attributed to the influence of the EZ band, a case can be made for early photoreceptor dysfunction preceding structural RPE loss in these patients (Testa et al., 2012, Gomes et al., 2009). This is further supported by the genetic background of the phenotype. We detected that the optical gap phenotype is associated with the

p.G1961E allele. The p.G1961E allele in homozygous or compound heterozygous state has been associated with a milder, localized disease process that is confined to the central macula, often as a bull's eye lesion, in conjunction with a characteristic absence of "dark choroid" on fluorescein angiography (Fishman et al., 1999, Cella et al., 2009, Simonelli et al., 2005). The absence of "dark choroid" reflects lower levels of lipofuscin accumulation, which was further demonstrated with quantitative autofluorescence imaging, showing that FAF levels are much lower in STGD1 patients carrying the p.G1961E allele compared to non-p.G1961E STGD1 patients (Burke et al., 2014). Low lipofuscin levels imply that cone dysfunction probably precedes RPE lipofuscin toxicity in the central maculae of p.G1961E patients indicating that a different pathogenetic mechanism compared to other STGD1 patients is possible (Burke et al., 2014).

Furthermore, there is increasing evidence that free all-trans retinal causes light-induced photoreceptor degeneration directly even without the presence of A2E (Maeda et al., 2009, Maeda et al., 2012, Chen et al., 2012, Maeda et al., 2014), therefore this pathogenic mechanism probably predominates in this subgroup of STGD1 patients**.** Our results of the structural behavior and the discussion of disease sequence were further supported by the findings from Sisk et al (Sisk and Leng, 2014), who published their study about the same time as we did, however their cohort was based on ophthalmoscopic findings and, in our opinion, contained only two patients with an evident optical gap phenotype.

A subtype of foveal sparing phenotype in STGD1

Another phenotype in STGD1 is foveal sparing, best detectable by SD-OCT. In contrast to the optical gap phenotype, where early foveal cone involvement takes place, foveal sparing phenotype on the contrary exhibits a relatively intact fovea, preserving cones and good visual function (van Huet et al., 2014, Fujinami et al., 2013d). We detected a variant of foveal sparing phenotype in STGD1 associated mostly with HCQ retinopathy. The phenotype is described as a thinning of the outer retinal layers around the preserved region of the ellipsoid zone forming "flying saucer" configuration. Therefore, the phenotype is colloquially called a "flying saucer" sign in HCQ retinopathy (Chen et al., 2010, Marmor, 2012, Ascaso et al., 2013, Tailor et al., 2012).

We detected 8 STGD1 patients with similar SD-OCT phenotype, 3 of whom exhibited also HCQ retinopathy-like BEM lesions on FAF and funduscopy, showing that Stargardt disease may phenocopy the HCQ retinopathy (Paper III). The majority of the patients did not report any visual symptoms and had excellent visual acuity, which is consistent with the relatively spared fovea with intact photoreceptors. Our study confirmed that despite similarities in SD-OCT imaging in these patients, a valuable imaging tool in differentiating STGD1 from HCQ retinopathy is FAF, because most of the patents exhibit characteristic flecks, although not always, as 3 patients revealed classical BEM lesion, without any apparent hyper-AF flecks.

Spectral-domain OCT revealed variable severity of retinal atrophy in the parafoveal region, while five younger patients (P4–8) showed also qualitatively thickened and hyper-reflective ELM, in consistent with the first study (Paper I), while in 3 older patients the prominence was not that obvious, indicating to the importance of this finding in younger STGD1 patients. Based on our clinical observation the ELM prominence is not evident in HCQ retinopathy, but it has to be noted that patients with HCQ toxic maculopathy are generally older. Furthermore, despite the relatively spared fovea in these STGD1 patients, all patients had the loss of IZand majority exhibited some degree of ONL thinning uncommon in an early or moderate stage of HCQ retinopathy (Marmor, 2012).

The development of the HCQ retinopathy-like SD-OCT phenotype was noted in one patient, where similar optically empty lesion as described in Paper 2 formed around a central island of preserved photoreceptors later collapsing and leaving a phenotype resembling the HCQ retinopathy.

The exact mechanism of HCQ retinal toxicity is not fully understood, however both, STGD1 and HCQ, share some common mechanistic features. It has been shown that HCQ may cause lysosomal dysfunction leading to lipofuscin accumulation (Mahon et al., 2004, Sundelin and Terman, 2002), while STGD1 is caused by a defective ABCA4 transporter, which similarly leads to lipofuscin accumulation (Molday and Zhang, 2010). The lipofuscin is toxic to the RPE cells and photoreceptors, leading to the outer retinal degeneration (Sparrow et al., 2000, Sparrow and Boulton, 2005). Both retinopathies show initially an increased FAF signal (Burke et al., 2014, Kellner et al., 2006, Kellner et al., 2008), referring to increased lipofuscin accumulation, and later bull's eye-like lesion, when the RPE atrophy develops. However, in HCQ retinopathy the photoreceptor loss precedes the RPE atrophy (Rodriguez-Padilla et al., 2007, Chen et al., 2010, Marmor, 2012, Kellner et al., 2009), while in STGD1, the precise sequence of RPE/photoreceptor loss is less clear (Cideciyan et al., 2004, Glazer and Dryja, 2002, Burke et al., 2011, Gomes et al., 2009). All patients from our cohort had some degree of visible RPE involvement, with pigment mottling, flecks or BEM, indicating much earlier RPE damage than would be expected in HCQ retinopathy.

It has been proposed, that the *ABCA4* gene could be involved in the development of HCQ-induced retinopathy (Shroyer et al., 2001). The incidence of toxic retinopathy in HCQ users is between 0.5–7.5% (Marmor et al., 2011, Melles and Marmor, 2014), and it is not fully understood why some users are predisposed to the toxicity. Shroyer et al found disease causing missense variants in the *ABCA4* gene in two of eight patients thought to have HCQ maculopathy due to the history of HCQ use and classical appearance of HCQ maculopathy lacking in STGD1-associated dark choroid and lipofuscin flecks. These variants were not present in the control group, suggesting that carrying an *ABCA4* mutation may increase the risk of HCQ retinopathy (Shroyer et al., 2001). In fact, one of the two patients was homozygous for missense mutation p.R2107H, but was thought to have HCQ maculopathy due to the classical appearance of this retinopathy. This mutation was also present in two of eight patients in our

cohort with phenotypes resembling HCQ retinopathy. Moreover, these patients in our study (Paper 3) are of African descent and the p.R2107H variant was recently described as the most prevalent disease causing mutation in African-American patients with STGD1, exhibiting disease with milder phenotype and later-onset (Zernant et al., 2014a). Interestingly, a more recent study has found, on the contrary, that some *ABCA4* missense variants may have a protective effect reducing the susceptibility to develop toxic retinopathy under chloroquine treatment (Grassmann et al., 2015).

6.3. Genotype-phenotype associations in STGD1

Genotype-phenotype associations are difficult to assess and detect in STGD1. First of all, there is remarkable allelic heterogeneity in STGD1 and secondly, harboring two different alleles in autosomal-recessive disorder makes it difficult to determine the combination effect, especially if the number of known *ABCA4* disease-associated alleles is >1000. Therefore, large databases are needed with genotype and phenotype information, and possibly also some functional studies to detect the effects of individual alleles. However, we detected genotype-phenotype association in the optical gap phenotype. By genetic analysis of patients with the optical gap phenotype we confirmed that all were compound heterozygous for *ABCA4* mutations. Interestingly, the p.G1961E variant was present in 10 of 11 unrelated cases (91%). The p.G1961E mutation is the most frequent disease associated *ABCA4* allele seen in approximately 10% of STGD1 patients of European origin (Burke et al., 2012a). This fraction was almost the same in our cohort of 179 patients, including 157 unrelated individuals (42/157; 13.4%), but remarkably higher in patients with the optical gap phenotype (46.7% vs. 13.4%, $p < 0.0001$). It has to be noted, however, that while the optical gap phenotype is definitely associated with the p.G1961E variant, the reverse is not the case since a larger fraction (32 unrelated individuals) who harbored the p.G1961E allele did not present with the optical gap. Fourteen of these individuals were clinically characterized at the same age after onset as the optical gap group. Of the other disease-associated *ABCA4* alleles compound heterozygous with p.G1961E, the p.L541P mutation, presenting alone or as a complex allele with the p.A1038V variant, was observed in seven cases (four unrelated) with the optical gap while only once in patients without the phenotype. However, due to a relatively small size of the optical gap cohort we cannot make an unequivocal conclusion about the association of this allele with the optical gap phenotype. With the exception of P13, the optical gap was not observed in the SD-OCT scans of any other non-p.G1961E patients (n = 131) whose age at time of examination, age of onset and estimated disease duration were not statistically different from those of the p.G1961E (n = 48) patients. Therefore the p.G1961E variant, maybe sometimes together with the p.L541P or p. (L541P; A1038V) allele, is associated with the optical gap phenotype. It is also interesting that p.L541P and p.(L541P; A1038V) alleles have been considered as severe alleles causing misfolding and reduction of ATPase activity of ABCA4 leading

to severe phenotypic expression (Zhang et al., 2015, Cideciyan et al., 2009), while in this case, the combination with p.G1961E allele, the phenotype in rather mild, indicating that the p.G1961E might have a "dominant" effect over the second mutation (Burke and Allikmets, 2013, Burke et al., 2014).

Genotype-phenotype association was not detected in the foveal sparing phenotype. However, the number of patients was very small. A study by Fujinami et al reported slightly higher frequency of p.R2030Q variant and lower incidence of p.G1961E *ABCA4* variant in STGD1 patients with foveal sparing phenotype, however the association was not statistically significant (Fujinami et al., 2013d). None of our patients as well as patients in another study (van Huet et al., 2014) harbored the p.R2030Q variant. An etiological connection between foveal sparing and *ABCA4* is further weakened by the incidence of foveal sparing phenotype in other genetically distinct retinal degenerative diseases such as *PRPH2* pattern dystrophy and AMD (Boon et al., 2008, Schmitz-Valckenberg et al., 2009, Duncker et al., 2015). In addition, two patients in this cohort harbored the p.G1961E allele, which would explain the milder course of the disease, but it was somewhat surprising in the foveal sparing phenotype, as the allele is associated predominantly with the central macular disease with cone involvement (Cella et al., 2009). The same was demonstrated in Paper 2 that the optical gap phenotype with cone-predominant change is associated with p.G1961E allele. Furthermore, in another study with foveal sparing phenotype (van Huet et al., 2014), none of the patients harbored p.G1961E allele and in a cohort of 40 patients with preserved foveal FAF only one patient carried the p.G1961E mutation as opposed to higher p.G1961E allele frequency in non-foveal sparing patients (1.6% vs 6.1%) (Fujinami et al., 2013d). Therefore, in agreement with other studies there are probably other genetic or non-genetic factors contributing to foveal sparing phenomenon, which need to be further determined (Fujinami et al., 2013d, van Huet et al., 2014).

7. CONCLUSIONS

1. In addition to significant thinning of the photoreceptor-associated ellipsoid zone layer, there is a statistically significant thickening of the external limiting membrane in young STGD1 patients compared to the age-matched controls. The finding probably reflects a transient hypertrophy of retinal Müller cells in response to cellular stress at the photoreceptor level, and could clinically be an important early stage disease marker, holding a diagnostic potential in early diagnosis of the STGD1.

2. The optical gap phenotype in STGD1 can be structurally divided into 3 progressive developmental stages. Initially there is mild subfoveal disruption of the EZ followed by progressive expansion of the EZ loss resulting in optically empty space devoid of foveal photoreceptors. At the later stage of the disease, the optically empty space collapses followed by progressive neuroretinal and the RPE cell atrophy. In contrast to the common understanding, that the first cells being affected in STGD1 are the RPE cells, our study seems to support the finding of some other groups, that in the STGD1-associated optical gap phenotype, photoreceptor loss sequentially precedes the RPE degeneration, suggesting a different pathogenetic mechanism in this subgroup of patients.

   The visual acuity in these patients correlated well with the EZ integrity, therefore patients with Stage 1 optical gap had relatively spared central vision, compared with the patients having more severe ellipsoid zone loss in Stage 2 and Stage 3. All patients with the optical gap phenotype and available ffERG recordings had normal ffERG responses, indicating a localized disease process and better prognosis in terms of visual function.

   We detected that STGD1 could phenocopy HCQ toxic retinopathy. A variant of foveal sparing phenotype in STGD1 mimics an OCT sign associated with HCQ retinal toxicity, also called a "flying-saucer" sign. Furthermore, in addition to the similar SD-OCT phenotype presentation, some of the patients presented with classical HCQ retinopathy-like bull's eye lesion on FAF and funduscopy lacking STGD1-characteristic flecks, therefore making phenotypic differentiation of these retinopathies difficult. Consequently, in more ambiguous cases *ABCA4* screening should be considered to prevent possible misdiagnosis.

   The majority of patients with the variant of "foveal sparing" phenotype were asymptomatic with very good visual acuity due to the preserved foveal photoreceptors. All the patients, with available ERG recordings, had normal ffERG responses.

3. The optical gap phenotype in STGD1 is highly associated with p.G1961E mutation in *ABCA4*. The allele frequency of p.G1961E allele in patients with the optical gap phenotype was 46.7%, while in the entire STGD1 cohort of 179 patients (157 unrelated individuals) it was 13.4%, showing statistically a highly significant difference ($p < 0.0001$).

Stargardt disease exhibits remarkable phenotypic heterogeneity. Despite Mendelian inheritance, genotype-phenotype associations are difficult to detect due to the large number of disease causing mutations. However, modern retinal imaging methods enable clinicians and researchers to expand the knowledge of disease expression, and increase the possibility to detect the genotype-phenotype associations. Detailed phenotypic descriptions and dynamic assessment via multimodal imaging as well as detecting new genotype-phenotype associations potentially improve the planning of pharmacological, gene- and stem cell-based treatment studies of STGD1.

8. REFERENCES

Adhi, M., Read, S. P., Ferrara, D., Weber, M., Duker, J. S. & Waheed, N. K. 2015. Morphology and Vascular Layers of the Choroid in Stargardt Disease Analyzed Using Spectral-Domain Optical Coherence Tomography. *Am J Ophthalmol,* 160, 1276–1284.e1.

Allikmets, R., Shroyer, N. F., Singh, N., Seddon, J. M., Lewis, R. A., Bernstein, P. S., Peiffer, A., Zabriskie, N. A., Li, Y., Hutchinson, A., Dean, M., Lupski, J. R. & Leppert, M. 1997a. Mutation of the Stargardt disease gene (ABCR) in age-related macular degeneration. *Science,* 277, 1805–7.

Allikmets, R., Singh, N., Sun, H., Shroyer, N. F., Hutchinson, A., Chidambaram, A., Gerrard, B., Baird, L., Stauffer, D., Peiffer, A., Rattner, A., Smallwood, P., Li, Y., Anderson, K. L., Lewis, R. A., Nathans, J., Leppert, M., Dean, M. & Lupski, J. R. 1997b. A photoreceptor cell-specific ATP-binding transporter gene (ABCR) is mutated in recessive Stargardt macular dystrophy. *Nat Genet,* 15, 236–46.

Ascaso, F. J., Rodriguez, N. A., San Miguel, R. & Huerva, V. 2013. The "flying saucer" sign on spectral domain optical coherence tomography in chloroquine retinopathy. *Arthritis Rheum,* 65, 2322.

Ben-Shabat, S., Parish, C. A., Vollmer, H. R., Itagaki, Y., Fishkin, N., Nakanishi, K. & Sparrow, J. R. 2002. Biosynthetic studies of A2E, a major fluorophore of retinal pigment epithelial lipofuscin. *J Biol Chem,* 277, 7183–90.

Birnbach, C. D., Jarvelainen, M., Possin, D. E. & Milam, A. H. 1994. Histopathology and immunocytochemistry of the neurosensory retina in fundus flavimaculatus. *Ophthalmology,* 101, 1211–9.

Boon, C. J., Jeroen Klevering, B., Keunen, J. E., Hoyng, C. B. & Theelen, T. 2008. Fundus autofluorescence imaging of retinal dystrophies. *Vision Res,* 48, 2569–77.

Boon, C. J., van Schooneveld, M. J., den Hollander, A. I., van Lith-Verhoeven, J. J., Zonneveld-Vrieling, M. N., Theelen, T., Cremers, F. P., Hoyng, C. B. & Klevering, B. J. 2007. Mutations in the peripherin/RDS gene are an important cause of multi-focal pattern dystrophy simulating STGD1/fundus flavimaculatus. *Br J Ophthalmol,* 91, 1504–11.

Boulton, M. & Dayhaw-Barker, P. 2001. The role of the retinal pigment epithelium: topographical variation and ageing changes. *Eye (Lond),* 15, 384–9.

Bringmann, A., Iandiev, I., Pannicke, T., Wurm, A., Hollborn, M., Wiedemann, P., Osborne, N. N. & Reichenbach, A. 2009. Cellular signaling and factors involved in Muller cell gliosis: neuroprotective and detrimental effects. *Prog Retin Eye Res,* 28, 423–51.

Bringmann, A., Pannicke, T., Grosche, J., Francke, M., Wiedemann, P., Skatchkov, S. N., Osborne, N. N. & Reichenbach, A. 2006. Muller cells in the healthy and diseased retina. *Prog Retin Eye Res,* 25, 397–424.

Burke, T. R. & Allikmets, R. 2013. Author response: Retinal phenotypes in patients homozygous for the G1961E mutation in the ABCA4 gene. *Invest Ophthalmol Vis Sci,* 54, 521.

Burke, T. R., Duncker, T., Woods, R. L., Greenberg, J. P., Zernant, J., Tsang, S. H., Smith, R. T., Allikmets, R., Sparrow, J. R. & Delori, F. C. 2014. Quantitative fundus autofluorescence in recessive Stargardt disease. *Invest Ophthalmol Vis Sci,* 55, 2841–52.

Burke, T. R., Fishman, G. A., Zernant, J., Schubert, C., Tsang, S. H., Smith, R. T., Ayyagari, R., Koenekoop, R. K., Umfress, A., Ciccarelli, M. L., Baldi, A., Iannac-

cone, A., Cremers, F. P., Klaver, C. C. & Allikmets, R. 2012a. Retinal phenotypes in patients homozygous for the G1961E mutation in the ABCA4 gene. *Invest Ophthalmol Vis Sci,* 53, 4458–67.

Burke, T. R., Rhee, D. W., Smith, R. T., Tsang, S. H., Allikmets, R., Chang, S., Lazow, M. A., Hood, D. C. & Greenstein, V. C. 2011. Quantification of peripapillary sparing and macular involvement in Stargardt disease (STGD1). *Invest Ophthalmol Vis Sci,* 52, 8006–15.

Burke, T. R. & Tsang, S. H. 2011. Allelic and phenotypic heterogeneity in ABCA4 mutations. *Ophthalmic Genet,* 32, 165–74.

Burke, T. R., Tsang, S. H., Zernant, J., Smith, R. T. & Allikmets, R. 2012b. Familial discordance in Stargardt disease. *Mol Vis,* 18, 227–33.

Burke, T. R., Yzer, S., Zernant, J., Smith, R. T., Tsang, S. H. & Allikmets, R. 2013. Abnormality in the external limiting membrane in early Stargardt disease. *Ophthalmic Genet,* 34, 75–7.

Cella, W., Greenstein, V. C., Zernant-Rajang, J., Smith, T. R., Barile, G., Allikmets, R. & Tsang, S. H. 2009. G1961E mutant allele in the Stargardt disease gene ABCA4 causes bull's eye maculopathy. *Exp Eye Res,* 89, 16–24.

Chan-Ling, T. 1994. Glial, neuronal and vascular interactions in the mammalian retina. *Progress in Retinal and Eye Research,* 13, 357–389.

Chen, C. C. & Heller, J. 1977. Uptake of retinol and retinoic acid from serum retinol-binding protein by retinal pigment epithelial cells. *J Biol Chem,* 252, 5216–21.

Chen, E., Brown, D. M., Benz, M. S., Fish, R. H., Wong, T. P., Kim, R. Y. & Major, J. C. 2010. Spectral domain optical coherence tomography as an effective screening test for hydroxychloroquine retinopathy (the "flying saucer" sign). *Clin Ophthalmol,* 4, 1151–8.

Chen, Y., Okano, K., Maeda, T., Chauhan, V., Golczak, M., Maeda, A. & Palczewski, K. 2012. Mechanism of all-trans-retinal toxicity with implications for stargardt disease and age-related macular degeneration. *J Biol Chem,* 287, 5059–69.

Chen, Y., Ratnam, K., Sundquist, S. M., Lujan, B., Ayyagari, R., Gudiseva, V. H., Roorda, A. & Duncan, J. L. 2011. Cone photoreceptor abnormalities correlate with vision loss in patients with Stargardt disease. *Invest Ophthalmol Vis Sci,* 52, 3281–92.

Cideciyan, A. V., Aleman, T. S., Swider, M., Schwartz, S. B., Steinberg, J. D., Brucker, A. J., Maguire, A. M., Bennett, J., Stone, E. M. & Jacobson, S. G. 2004. Mutations in ABCA4 result in accumulation of lipofuscin before slowing of the retinoid cycle: a reappraisal of the human disease sequence. *Hum Mol Genet,* 13, 525–34.

Cideciyan, A. V., Swider, M., Aleman, T. S., Tsybovsky, Y., Schwartz, S. B., Windsor, E. A., Roman, A. J., Sumaroka, A., Steinberg, J. D., Jacobson, S. G., Stone, E. M. & Palczewski, K. 2009. ABCA4 disease progression and a proposed strategy for gene therapy. *Hum Mol Genet,* 18, 931–41.

Cremers, F. P., van de Pol, D. J., van Driel, M., den Hollander, A. I., van Haren, F. J., Knoers, N. V., Tijmes, N., Bergen, A. A., Rohrschneider, K., Blankenagel, A., Pinckers, A. J., Deutman, A. F. & Hoyng, C. B. 1998. Autosomal recessive retinitis pigmentosa and cone-rod dystrophy caused by splice site mutations in the Stargardt's disease gene ABCR. *Hum Mol Genet,* 7, 355–62.

Cuenca, N., Fernandez–Sanchez, L., Campello, L., Maneu, V., De la Villa, P., Lax, P. & Pinilla, I. 2014. Cellular responses following retinal injuries and therapeutic approaches for neurodegenerative diseases. *Prog Retin Eye Res,* 43, 17–75.

Delori, F. C., Dorey, C. K., Staurenghi, G., Arend, O., Goger, D. G. & Weiter, J. J. 1995. In vivo fluorescence of the ocular fundus exhibits retinal pigment epithelium lipofuscin characteristics. *Invest Ophthalmol Vis Sci,* 36, 718–29.

Delori, F. C., Goger, D. G. & Dorey, C. K. 2001. Age-related accumulation and spatial distribution of lipofuscin in RPE of normal subjects. *Invest Ophthalmol Vis Sci,* 42, 1855–66.

Drexler, W. & Fujimoto, J. G. 2008. State-of-the-art retinal optical coherence tomography. *Prog Retin Eye Res,* 27, 45–88.

Duncker, T., Marsiglia, M., Lee, W., Zernant, J., Tsang, S. H., Allikmets, R., Greenstein, V. C. & Sparrow, J. R. 2014. Correlations among near-infrared and short-wavelength autofluorescence and spectral-domain optical coherence tomography in recessive Stargardt disease. *Invest Ophthalmol Vis Sci,* 55, 8134–43.

Duncker, T., Tsang, S. H., Woods, R. L., Lee, W., Zernant, J., Allikmets, R., Delori, F. C. & Sparrow, J. R. 2015. Quantitative Fundus Autofluorescence and Optical Coherence Tomography in PRPH2/RDS- and ABCA4-Associated Disease Exhibiting Phenotypic Overlap. *Invest Ophthalmol Vis Sci,* 56, 3159–70.

Ergun, E., Hermann, B., Wirtitsch, M., Unterhuber, A., Ko, T. H., Sattmann, H., Scholda, C., Fujimoto, J. G., Stur, M. & Drexler, W. 2005. Assessment of central visual function in Stargardt's disease/fundus flavimaculatus with ultrahigh-resolution optical coherence tomography. *Invest Ophthalmol Vis Sci,* 46, 310–6.

Fernandez-Sanchez, L., Lax, P., Campello, L., Pinilla, I. & Cuenca, N. 2015. Astrocytes and Muller Cell Alterations During Retinal Degeneration in a Transgenic Rat Model of Retinitis Pigmentosa. *Front Cell Neurosci,* 9, 484.

Fischer, A. J., Zelinka, C. & Scott, M. A. 2010. Heterogeneity of glia in the retina and optic nerve of birds and mammals. *PLoS One,* 5, e10774.

Fishman, G. A. 1976. Fundus flavimaculatus. A clinical classification. *Arch Ophthalmol,* 94, 2061–7.

Fishman, G. A., Farbman, J. S. & Alexander, K. R. 1991. Delayed rod dark adaptation in patients with Stargardt's disease. *Ophthalmology,* 98, 957–62.

Fishman, G. A., Stone, E. M., Grover, S., Derlacki, D. J., Haines, H. L. & Hockey, R. R. 1999. Variation of clinical expression in patients with Stargardt dystrophy and sequence variations in the ABCR gene. *Arch Ophthalmol,* 117, 504–10.

Forte, R., Querques, G., Querques, L., Leveziel, N., Benhamou, N. & Souied, E. H. 2013. Multimodal evaluation of foveal sparing in patients with geographicatrophy due to age-related macular degeneration. *Retina,* 33, 482–9.

Franceschetti, A. & Francois, J. 1965. [Fundus flavimaculatus]. *Arch Ophtalmol Rev Gen Ophtalmol,* 25, 505–30.

Franze, K., Grosche, J., Skatchkov, S. N., Schinkinger, S., Foja, C., Schild, D., Uckermann, O., Travis, K., Reichenbach, A. & Guck, J. 2007. Muller cells are living optical fibers in the vertebrate retina. *Proc Natl Acad Sci U S A,* 104, 8287–92.

Fujinami, K., Lois, N., Davidson, A. E., Mackay, D. S., Hogg, C. R., Stone, E. M., Tsunoda, K., Tsubota, K., Bunce, C., Robson, A. G., Moore, A. T., Webster, A. R., Holder, G. E. & Michaelides, M. 2013a. A longitudinal study of stargardt disease: clinical and electrophysiologic assessment, progression, and genotype correlations. *Am J Ophthalmol,* 155, 1075–1088.e13.

Fujinami, K., Lois, N., Mukherjee, R., McBain, V. A., Tsunoda, K., Tsubota, K., Stone, E. M., Fitzke, F. W., Bunce, C., Moore, A. T., Webster, A. R. & Michaelides, M. 2013b. A longitudinal study of Stargardt disease: quantitative assessment of fundus

autofluorescence, progression, and genotype correlations. *Invest Ophthalmol Vis Sci,* 54, 8181–90.

Fujinami, K., Sergouniotis, P. I., Davidson, A. E., Mackay, D. S., Tsunoda, K., Tsubota, K., Robson, A. G., Holder, G. E., Moore, A. T., Michaelides, M. & Webster, A. R. 2013c. The clinical effect of homozygous ABCA4 alleles in 18 patients. *Ophthalmology,* 120, 2324–31.

Fujinami, K., Sergouniotis, P. I., Davidson, A. E., Wright, G., Chana, R. K., Tsunoda, K., Tsubota, K., Egan, C. A., Robson, A. G., Moore, A. T., Holder, G. E., Michaelides, M. & Webster, A. R. 2013d. Clinical and molecular analysis of Stargardt disease with preserved foveal structure and function. *Am J Ophthalmol,* 156, 487–501 e1.

Fujinami, K., Singh, R., Carroll, J., Zernant, J., Allikmets, R., Michaelides, M. & Moore, A. T. 2014. Fine central macular dots associated with childhood-onset Stargardt Disease. *Acta Ophthalmol,* 92, e157–9.

Fujinami, K., Zernant, J., Chana, R. K., Wright, G. A., Tsunoda, K., Ozawa, Y., Tsubota, K., Robson, A. G., Holder, G. E., Allikmets, R., Michaelides, M. & Moore, A. T. 2015. Clinical and molecular characteristics of childhood-onset Stargardt disease. *Ophthalmology,* 122, 326–34.

Genead, M. A., Fishman, G. A. & Anastasakis, A. 2011. Spectral-domain OCT peripapillary retinal nerve fibre layer thickness measurements in patients with Stargardt disease. *Br J Ophthalmol,* 95, 689–93.

Glazer, L. C. & Dryja, T. P. 2002. Understanding the etiology of Stargardt's disease. *Ophthalmol Clin North Am,* 15, 93–100, viii.

Gomes, N. L., Greenstein, V. C., Carlson, J. N., Tsang, S. H., Smith, R. T., Carr, R. E., Hood, D. C. & Chang, S. 2009. A comparison of fundus autofluorescence and retinal structure in patients with Stargardt disease. *Invest Ophthalmol Vis Sci,* 50, 3953–9.

Grassmann, F., Bergholz, R., Mandl, J., Jagle, H., Ruether, K. & Weber, B. H. 2015. Common synonymous variants in ABCA4 are protective for chloroquine induced maculopathy (toxic maculopathy). *BMC Ophthalmol,* 15, 18.

Greenberg, J. P., Sherman, J., Zweifel, S. A., Chen, R. W., Duncker, T., Kohl, S., Baumann, B., Wissinger, B., Yannuzzi, L. A. & Tsang, S. H. 2014. Spectral-domain optical coherence tomography staging and autofluorescence imaging in achromatopsia. *JAMA Ophthalmol,* 132, 437–45.

Hattar, S., Liao, H. W., Takao, M., Berson, D. M. & Yau, K. W. 2002. Melanopsin-containing retinal ganglion cells: architecture, projections, and intrinsic photosensitivity. *Science,* 295, 1065–70.

Heathfield, L., Lacerda, M., Nossek, C., Roberts, L. & Ramesar, R. S. 2013. Stargardt disease: towards developing a model to predict phenotype. *Eur J Hum Genet,* 21, 1173–6.

Hippert, C., Graca, A. B., Barber, A. C., West, E. L., Smith, A. J., Ali, R. R. & Pearson, R. A. 2015. Muller glia activation in response to inherited retinal degeneration is highly varied and disease-specific. *PLoS One,* 10, e0120415.

Holder, G. E., Celesia, G. G., Miyake, Y., Tobimatsu, S. & Weleber, R. G. 2010. International Federation of Clinical Neurophysiology: recommendations for visual system testing. *Clin Neurophysiol,* 121, 1393–409.

Holz, F. G., Bellman, C., Staudt, S., Schutt, F. & Volcker, H. E. 2001. Fundus autofluorescence and development of geographic atrophy in age-related macular degeneration. *Invest Ophthalmol Vis Sci,* 42, 1051–6.

Holz, F. G., Schutt, F., Kopitz, J., Eldred, G. E., Kruse, F. E., Volcker, H. E. & Cantz, M. 1999. Inhibition of lysosomal degradative functions in RPE cells by a retinoid component of lipofuscin. *Invest Ophthalmol Vis Sci,* 40, 737–43.

Hood, D. C., Bach, M., Brigell, M., Keating, D., Kondo, M., Lyons, J. S., Marmor, M. F., McCulloch, D. L. & Palmowski-Wolfe, A. M. 2012. ISCEV standard for clinical multifocal electroretinography (mfERG) (2011 edition). *Doc Ophthalmol,* 124, 1–13.

Hood, D. C., Cho, J., Raza, A. S., Dale, E. A. & Wang, M. 2011. Reliability of a computer-aided manual procedure for segmenting optical coherence tomography scans. *Optom Vis Sci,* 88, 113–23.

Hood, D. C., Lin, C. E., Lazow, M. A., Locke, K. G., Zhang, X. & Birch, D. G. 2009. Thickness of receptor and post-receptor retinal layers in patients with retinitis pigmentosa measured with frequency-domain optical coherence tomography. *Invest Ophthalmol Vis Sci,* 50, 2328–36.

Hoyng, C. B., Heutink, P., Testers, L., Pinckers, A., Deutman, A. F. & Oostra, B. A. 1996. Autosomal dominant central areolar choroidal dystrophy caused by a mutation in codon 142 in the peripherin/RDS gene. *Am J Ophthalmol,* 121, 623–9.

Huang, W. C., Cideciyan, A. V., Roman, A. J., Sumaroka, A., Sheplock, R., Schwartz, S. B., Stone, E. M. & Jacobson, S. G. 2014. Inner and outer retinal changes in retinal degenerations associated with ABCA4 mutations. *Invest Ophthalmol Vis Sci,* 55, 1810–22.

Jain, A., Desai, R. U., Charalel, R. A., Quiram, P., Yannuzzi, L. & Sarraf, D. 2009. Solar retinopathy: comparison of optical coherence tomography (OCT) and fluorescein angiography (FA). *Retina,* 29, 1340–5.

Jones, B. W. & Marc, R. E. 2005. Retinal remodeling during retinal degeneration. *Exp Eye Res,* 81, 123–37.

Karampelas, M., Sim, D. A., Keane, P. A., Papastefanou, V. P., Sadda, S. R., Tufail, A. & Dowler, J. 2013. Evaluation of retinal pigment epithelium-Bruch's membrane complex thickness in dry age-related macular degeneration using optical coherence tomography. *Br J Ophthalmol,* 97, 1256–61.

Keane, P. A. & Sadda, S. R. 2014. Retinal imaging in the twenty-first century: state of the art and future directions. *Ophthalmology,* 121, 2489–500.

Kellner, S., Weinitz, S. & Kellner, U. 2009. Spectral domain optical coherence tomography detects early stages of chloroquine retinopathy similar to multifocal electroretinography, fundus autofluorescence and near-infrared autofluorescence. *Br J Ophthalmol,* 93, 1444–7.

Kellner, U., Kellner, S. & Weinitz, S. 2008. Chloroquine retinopathy: lipofuscin- and melanin-related fundus autofluorescence, optical coherence tomography and multifocal electroretinography. *Doc Ophthalmol,* 116, 119–27.

Kellner, U., Renner, A. B. & Tillack, H. 2006. Fundus autofluorescence and mfERG for early detection of retinal alterations in patients using chloroquine/hydroxychloroquine. *Invest Ophthalmol Vis Sci,* 47, 3531–8.

Kennedy, C. J., Rakoczy, P. E. & Constable, I. J. 1995. Lipofuscin of the retinal pigment epithelium: a review. *Eye (Lond),* 9 (Pt 6), 763–71.

Kniazeva, M., Chiang, M. F., Morgan, B., Anduze, A. L., Zack, D. J., Han, M. & Zhang, K. 1999. A new locus for autosomal dominant stargardt-like disease maps to chromosome 4. *Am J Hum Genet,* 64, 1394–9.

Kohno, H., Chen, Y., Kevany, B. M., Pearlman, E., Miyagi, M., Maeda, T., Palczewski, K. & Maeda, A. 2013. Photoreceptor proteins initiate microglial activation via Toll-like

receptor 4 in retinal degeneration mediated by all-trans-retinal. *J Biol Chem,* 288, 15326–41.

Kretschmann, U., Seeliger, M. W., Ruether, K., Usui, T., Apfelstedt-Sylla, E. & Zrenner, E. 1998. Multifocal electroretinography in patients with Stargardt's macular dystrophy. *Br J Ophthalmol,* 82, 267–75.

Lamb, T. D. & Pugh, E. N., Jr. 2006. Phototransduction, dark adaptation, and rhodopsin regeneration the proctor lecture. *Invest Ophthalmol Vis Sci,* 47, 5137–52.

Lambertus, S., van Huet, R. A., Bax, N. M., Hoefsloot, L. H., Cremers, F. P., Boon, C. J., Klevering, B. J. & Hoyng, C. B. 2015. Early-onset stargardt disease: phenotypic and genotypic characteristics. *Ophthalmology,* 122, 335–44.

Langmann, T. 2007. Microglia activation in retinal degeneration. *J Leukoc Biol,* 81, 1345–51.

Lei, L., Tzekov, R., Tang, S. & Kaushal, S. 2012. Accumulation and autofluorescence of phagocytized rod outer segment material in macrophages and microglial cells. *Mol Vis,* 18, 103–13.

Leng, T., Marmor, M. F., Kellner, U., Thompson, D. A., Renner, A. B., Moore, W. & Sowden, J. C. 2012. Foveal cavitation as an optical coherence tomography finding in central cone dysfunction. *Retina,* 32, 1411–9.

Litts, K. M., Messinger, J. D., Freund, K. B., Zhang, Y. & Curcio, C. A. 2015. Inner Segment Remodeling and Mitochondrial Translocation in Cone Photoreceptors in Age-Related Macular Degeneration With Outer Retinal Tubulation. *Invest Ophthalmol Vis Sci,* 56, 2243–53.

Lois, N., Halfyard, A. S., Bird, A. C., Holder, G. E. & Fitzke, F. W. 2004. Fundus autofluorescence in Stargardt macular dystrophy-fundus flavimaculatus. *Am J Ophthalmol,* 138, 55–63.

Lois, N., Holder, G. E., Bunce, C., Fitzke, F. W. & Bird, A. C. 2001. Phenotypic subtypes of Stargardt macular dystrophy-fundus flavimaculatus. *Arch Ophthalmol,* 119, 359–69.

Lois, N., Holder, G. E., Fitzke, F. W., Plant, C. & Bird, A. C. 1999. Intrafamilial variation of phenotype in Stargardt macular dystrophy-Fundus flavimaculatus. *Invest Ophthalmol Vis Sci,* 40, 2668–75.

Ma, W., Coon, S., Zhao, L., Fariss, R. N. & Wong, W. T. 2013. A2E accumulation influences retinal microglial activation and complement regulation. *Neurobiol Aging,* 34, 943–60.

Ma, W., Zhao, L., Fontainhas, A. M., Fariss, R. N. & Wong, W. T. 2009. Microglia in the mouse retina alter the structure and function of retinal pigmented epithelial cells: a potential cellular interaction relevant to AMD. *PLoS One,* 4, e7945.

Ma, W., Zhao, L. & Wong, W. T. 2012. *Microglia in the Outer Retina and Their Relevance to Pathogenesis of Age-Related Macular Degeneration*, Springer US.

Maeda, A., Golczak, M., Chen, Y., Okano, K., Kohno, H., Shiose, S., Ishikawa, K., Harte, W., Palczewska, G., Maeda, T. & Palczewski, K. 2012. Primary amines protect against retinal degeneration in mouse models of retinopathies. *Nat Chem Biol,* 8, 170–8.

Maeda, A., Maeda, T., Golczak, M., Chou, S., Desai, A., Hoppel, C. L., Matsuyama, S. & Palczewski, K. 2009. Involvement of all-trans-retinal in acute light-induced retinopathy of mice. *J Biol Chem,* 284, 15173–83.

Maeda, A., Palczewska, G., Golczak, M., Kohno, H., Dong, Z., Maeda, T. & Palczewski, K. 2014. Two-photon microscopy reveals early rod photoreceptor cell damage in light-exposed mutant mice. *Proc Natl Acad Sci U S A,* 111, E1428–37.

Mahon, G. J., Anderson, H. R., Gardiner, T. A., McFarlane, S., Archer, D. B. & Stitt, A. W. 2004. Chloroquine causes lysosomal dysfunction in neural retina and RPE: implications for retinopathy. *Curr Eye Res,* 28, 277–84.

Mantyjarvi, M. & Tuppurainen, K. 1992. Color vision in Stargardt's disease. *Int Ophthalmol,* 16, 423–8.

Marmor, M. F. 2012. Comparison of screening procedures in hydroxychloroquine toxicity. *Arch Ophthalmol,* 130, 461–9.

Marmor, M. F., Fulton, A. B., Holder, G. E., Miyake, Y., Brigell, M., Bach, M. & International Society for Clinical Electrophysiology of, V. 2009. ISCEV Standard for full-field clinical electroretinography (2008 update). *Doc Ophthalmol,* 118, 69–77.

Marmor, M. F., Kellner, U., Lai, T. Y., Lyons, J. S., Mieler, W. F. & American Academy of, O. 2011. Revised recommendations on screening for chloroquine and hydroxychloroquine retinopathy. *Ophthalmology,* 118, 415–22.

Marmor, M. F. & Wolfensberger, T. J. 1998. *The retinal pigment epithelium,* Oxford, Oxford University

Martinez-Mir, A., Paloma, E., Allikmets, R., Ayuso, C., del Rio, T., Dean, M., Vilageliu, L., Gonzalez-Duarte, R. & Balcells, S. 1998. Retinitis pigmentosa caused by a homozygous mutation in the Stargardt disease gene ABCR. *Nat Genet,* 18, 11–2.

Maugeri, A., Klevering, B. J., Rohrschneider, K., Blankenagel, A., Brunner, H. G., Deutman, A. F., Hoyng, C. B. & Cremers, F. P. 2000. Mutations in the ABCA4 (ABCR) gene are the major cause of autosomal recessive cone-rod dystrophy. *Am J Hum Genet,* 67, 960–6.

Melles, R. B. & Marmor, M. F. 2014. The risk of toxic retinopathy in patients on long-term hydroxychloroquine therapy. *JAMA Ophthalmol,* 132, 1453–60.

Michaelides, M., Chen, L. L., Brantley, M. A., Jr., Andorf, J. L., Isaak, E. M., Jenkins, S. A., Holder, G. E., Bird, A. C., Stone, E. M. & Webster, A. R. 2007. ABCA4 mutations and discordant ABCA4 alleles in patients and siblings with bull's-eye maculopathy. *Br J Ophthalmol,* 91, 1650–5.

Michaelides, M., Hunt, D. M. & Moore, A. T. 2003. The genetics of inherited macular dystrophies. *J Med Genet,* 40, 641–50.

Molday, L. L., Rabin, A. R. & Molday, R. S. 2000. ABCR expression in foveal cone photoreceptors and its role in stargardt macular dystrophy. *Am J Ophthalmol,* 130, 689.

Molday, R. S. & Zhang, K. 2010. Defective lipid transport and biosynthesis in recessive and dominant Stargardt macular degeneration. *Prog Lipid Res,* 49, 476–92.

Mustafi, D., Engel, A. H. & Palczewski, K. 2009. Structure of cone photoreceptors. *Prog Retin Eye Res,* 28, 289–302.

Noailles, A., Fernandez-Sanchez, L., Lax, P. & Cuenca, N. 2014. Microglia activation in a model of retinal degeneration and TUDCA neuroprotective effects. *J Neuroinflammation,* 11, 186.

O'Brien, B. J., Isayama, T., Richardson, R. & Berson, D. M. 2002. Intrinsic physiological properties of cat retinal ganglion cells. *J Physiol,* 538, 787–802.

Oh, K. T., Weleber, R. G., Stone, E. M., Oh, D. M., Rosenow, J. & Billingslea, A. M. 2004. Electroretinographic findings in patients with Stargardt disease and fundus flavimaculatus. *Retina,* 24, 920–8.

Palczewski, K. 2012. Chemistry and biology of vision. *J Biol Chem,* 287, 1612–9.

Palejwala, N. V., Gale, M. J., Clark, R. F., Schlechter, C., Weleber, R. G. & Pennesi, M. E. 2016. Insights into autosomal dominant Stargardt-like macular dystrophy through multimodality diagnostic imaging. *Retina,* 36, 119–30.

Park, J. C., Collison, F. T., Fishman, G. A., Allikmets, R., Zernant, J., Liu, M. & McAnany, J. J. 2015. Objective Analysis of Hyperreflective Outer Retinal Bands Imaged by Optical Coherence Tomography in Patients With Stargardt Disease. *Invest Ophthalmol Vis Sci,* 56, 4662–7.

Park, S. J., Woo, S. J., Park, K. H., Hwang, J. M. & Chung, H. 2010. Morphologic photoreceptor abnormality in occult macular dystrophy on spectral-domain optical coherence tomography. *Invest Ophthalmol Vis Sci,* 51, 3673–9.

Pasadhika, S., Fishman, G. A., Allikmets, R. & Stone, E. M. 2009. Peripapillary retinal nerve fiber layer thinning in patients with autosomal recessive cone-rod dystrophy. *Am J Ophthalmol,* 148, 260–265.e1.

Purves, D., Augustine, G. J., Fitzpatrick, D., Hall, W. C., LaMantia, A. S., McNamara, J. O. & Williams, S. M. 2004. *Neuroscience,* Saunderland, Massachusetts, USA, Sinauer Associates, Inc.

Quazi, F., Lenevich, S. & Molday, R. S. 2012. ABCA4 is an N-retinylidene-phosphatidylethanolamine and phosphatidylethanolamine importer. *Nat Commun,* 3, 925.

Quazi, F. & Molday, R. S. 2014. ATP-binding cassette transporter ABCA4 and chemical isomerization protect photoreceptor cells from the toxic accumulation of excess 11-cis-retinal. *Proc Natl Acad Sci U S A,* 111, 5024–9.

Querques, G., Kamami-Levy, C., Georges, A., Pedinielli, A., Capuano, V., Blanco-Garavito, R., Poulon, F. & Souied, E. H. 2016. Adaptive optics imaging of foveal sparing in geographic atrophy secondary to age-related macular degeneration. *Retina,* 36, 247–54.

Radu, R. A., Hu, J., Yuan, Q., Welch, D. L., Makshanoff, J., Lloyd, M., McMullen, S., Travis, G. H. & Bok, D. 2011. Complement system dysregulation and inflammation in the retinal pigment epithelium of a mouse model for Stargardt macular degeneration. *J Biol Chem,* 286, 18593–601.

Rattner, A., Smallwood, P. M. & Nathans, J. 2000. Identification and characterization of all-trans-retinol dehydrogenase from photoreceptor outer segments, the visual cycle enzyme that reduces all-trans-retinal to all-trans-retinol. *J Biol Chem,* 275, 11034–43.

Regillo, C., Chang, T. S., Mark, J. W., Kaiser, P. K., Scott, I. U., Spaide, R. F. & Griggs, P. B. 2007. *Basic and clinical science course,* San Fransisco, American Academy of Ophthamology (AAO).

Reichenbach, A. & Bringmann, A. 2013. New functions of Muller cells. *Glia,* 61, 651–78.

Reynolds, J. D. & Olitsky, S. E. 2011. *Pediatric retina,* New York, Springer-Verlag Berlin Heidelberg.

Ritter, M., Zotter, S., Schmidt, W. M., Bittner, R. E., Deak, G. G., Pircher, M., Sacu, S., Hitzenberger, C. K., Schmidt-Erfurth, U. M. & Macula Study Group, V. 2013. Characterization of stargardt disease using polarization-sensitive optical coherence tomography and fundus autofluorescence imaging. *Invest Ophthalmol Vis Sci,* 54, 6416–25.

Rodriguez-Padilla, J. A., Hedges, T. R., 3rd, Monson, B., Srinivasan, V., Wojtkowski, M., Reichel, E., Duker, J. S., Schuman, J. S. & Fujimoto, J. G. 2007. High-speed ultra-high-resolution optical coherence tomography findings in hydroxychloroquine retinopathy. *Arch Ophthalmol,* 125, 775–80.

Roosing, S., Thiadens, A. A., Hoyng, C. B., Klaver, C. C., den Hollander, A. I. & Cremers, F. P. 2014. Causes and consequences of inherited cone disorders. *Prog Retin Eye Res,* 42, 1–26.

Ross, M. H. & Pawlina, W. 2011. *Histology: a text and atlas: with correlated cell and molecular biology,* Baltmore, Lippincott Williams & Wilkins.
Saari, J. C. 2012. Vitamin A metabolism in rod and cone visual cycles. *Annu Rev Nutr,* 32, 125–45.
Sakata, L. M., Deleon-Ortega, J., Sakata, V. & Girkin, C. A. 2009. Optical coherence tomography of the retina and optic nerve – a review. *Clin Experiment Ophthalmol,* 37, 90–9.
Schindler, E. I., Nylen, E. L., Ko, A. C., Affatigato, L. M., Heggen, A. C., Wang, K., Sheffield, V. C. & Stone, E. M. 2010. Deducing the pathogenic contribution of recessive ABCA4 alleles in an outbred population. *Hum Mol Genet,* 19, 3693–701.
Schmidt, T. M., Chen, S. K. & Hattar, S. 2011. Intrinsically photosensitive retinal ganglion cells: many subtypes, diverse functions. *Trends Neurosci,* 34, 572–80.
Schmitz-Valckenberg, S., Fleckenstein, M., Helb, H. M., Charbel Issa, P., Scholl, H. P. & Holz, F. G. 2009. In vivo imaging of foveal sparing in geographic atrophy secondary to age-related macular degeneration. *Invest Ophthalmol Vis Sci,* 50, 3915–21.
Schmitz-Valckenberg, S., Holz, F. G., Bird, A. C. & Spaide, R. F. 2008. Fundus autofluorescence imaging: review and perspectives. *Retina,* 28, 385–409.
Schutt, F., Davies, S., Kopitz, J., Boulton, M. & Holz, F. G. 2000. [A retinoid constituent of lipofuscin, A2-E, is a photosensitizer in human retinal pigment epithelial cells]. *Ophthalmologe,* 97, 682–7.
Sergouniotis, P. I., Holder, G. E., Robson, A. G., Michaelides, M., Webster, A. R. & Moore, A. T. 2012. High-resolution optical coherence tomography imaging in KCNV2 retinopathy. *Br J Ophthalmol,* 96, 213–7.
Shamsi, F. A. & Boulton, M. 2001. Inhibition of RPE lysosomal and antioxidant activity by the age pigment lipofuscin. *Invest Ophthalmol Vis Sci,* 42, 3041–6.
Shroyer, N. F., Lewis, R. A., Allikmets, R., Singh, N., Dean, M., Leppert, M. & Lupski, J. R. 1999. The rod photoreceptor ATP-binding cassette transporter gene, ABCR, and retinal disease: from monogenic to multifactorial. *Vision Res,* 39, 2537–44.
Shroyer, N. F., Lewis, R. A. & Lupski, J. R. 2001. Analysis of the ABCR (ABCA4) gene in 4-aminoquinoline retinopathy: is retinal toxicity by chloroquine and hydroxychloroquine related to Stargardt disease? *Am J Ophthalmol,* 131, 761–6.
Simo, R., Villarroel, M., Corraliza, L., Hernandez, C. & Garcia-Ramirez, M. 2010. The retinal pigment epithelium: something more than a constituent of the blood-retinal barrier – implications for the pathogenesis of diabetic retinopathy. *J Biomed Biotechnol,* 2010, 190724.
Simonelli, F., Testa, F., Zernant, J., Nesti, A., Rossi, S., Allikmets, R. & Rinaldi, E. 2005. Genotype-phenotype correlation in Italian families with Stargardt disease. *Ophthalmic Res,* 37, 159–67.
Sisk, R. A. & Leng, T. 2014. Multimodal imaging and multifocal electroretinography demonstrate autosomal recessive Stargardt disease may present like occult macular dystrophy. *Retina,* 34, 1567–75.
Song, H., Rossi, E. A., Latchney, L., Bessette, A., Stone, E., Hunter, J. J., Williams, D. R. & Chung, M. 2015. Cone and rod loss in Stargardt disease revealed by adaptive optics scanning light ophthalmoscopy. *JAMA Ophthalmol,* 133, 1198–203.
Spaide, R. F. & Curcio, C. A. 2011. Anatomical correlates to the bands seen in the outer retina by optical coherence tomography: literature review and model. *Retina,* 31, 1609–19.

Sparrow, J. R. & Boulton, M. 2005. RPE lipofuscin and its role in retinal pathobiology. *Exp Eye Res,* 80, 595–606.
Sparrow, J. R., Kim, S. R., Cuervo, A. M. & Bandhyopadhyayand, U. 2008. A2E, a pigment of RPE lipofuscin, is generated from the precursor, A2PE by a lysosomal enzyme activity. *Adv Exp Med Biol,* 613, 393–8.
Sparrow, J. R., Nakanishi, K. & Parish, C. A. 2000. The lipofuscin fluorophore A2E mediates blue light-induced damage to retinal pigmented epithelial cells. *Invest Ophthalmol Vis Sci,* 41, 1981–9.
Sparrow, J. R., Parish, C. A., Hashimoto, M. & Nakanishi, K. 1999. A2E, a lipofuscin fluorophore, in human retinal pigmented epithelial cells in culture. *Invest Ophthalmol Vis Sci,* 40, 2988–95.
Sparrow, J. R., Zhou, J. & Cai, B. 2003. DNA is a target of the photodynamic effects elicited in A2E-laden RPE by blue-light illumination. *Invest Ophthalmol Vis Sci,* 44, 2245–51.
Stargardt, K. 1909. Uber familiare, progressive degeneration under makulagegend des augen. *Albrecht. von. Graefes Arch. Ophthalmol*, 534–550.
Staurenghi, G., Sadda, S., Chakravarthy, U. & Spaide, R. F. 2014. Proposed lexicon for anatomic landmarks in normal posterior segment spectral-domain optical coherence tomography: the IN*OCT consensus. *Ophthalmology,* 121, 1572–8.
Strauss, O. 2005. The retinal pigment epithelium in visual function. *Physiol Rev,* 85, 845–81.
Sun, H. & Nathans, J. 1997. Stargardt's ABCR is localized to the disc membrane of retinal rod outer segments. *Nat Genet,* 17, 15–6.
Sun, H., Smallwood, P. M. & Nathans, J. 2000. Biochemical defects in ABCR protein variants associated with human retinopathies. *Nat Genet,* 26, 242–6.
Sundelin, S. P. & Terman, A. 2002. Different effects of chloroquine and hydroxychloroquine on lysosomal function in cultured retinal pigment epithelial cells. *APMIS,* 110, 481–9.
Sung, C. H. & Chuang, J. Z. 2010. The cell biology of vision. *J Cell Biol,* 190, 953–63.
Zahid, S., Jayasundera, T., Rhoades, W., Branham, K., Khan, N., Niziol, L. M., Musch, D. C. & Heckenlively, J. R. 2013. Clinical phenotypes and prognostic full-field electroretinographic findings in Stargardt disease. *Am J Ophthalmol,* 155, 465–473.e3.
Zernant, J., Collison, F. T., Lee, W., Fishman, G. A., Noupuu, K., Yuan, B., Cai, C., Lupski, J. R., Yannuzzi, L. A., Tsang, S. H. & Allikmets, R. 2014a. Genetic and clinical analysis of ABCA4-associated disease in African American patients. *Hum Mutat,* 35, 1187–94.
Zernant, J., Schubert, C., Im, K. M., Burke, T., Brown, C. M., Fishman, G. A., Tsang, S. H., Gouras, P., Dean, M. & Allikmets, R. 2011. Analysis of the ABCA4 gene by next-generation sequencing. *Invest Ophthalmol Vis Sci,* 52, 8479–87.
Zernant, J., Xie, Y. A., Ayuso, C., Riveiro–Alvarez, R., Lopez-Martinez, M. A., Simonelli, F., Testa, F., Gorin, M. B., Strom, S. P., Bertelsen, M., Rosenberg, T., Boone, P. M., Yuan, B., Ayyagari, R., Nagy, P. L., Tsang, S. H., Gouras, P., Collison, F. T., Lupski, J. R., Fishman, G. A. & Allikmets, R. 2014b. Analysis of the ABCA4 genomic locus in Stargardt disease. *Hum Mol Genet,* 23, 6797–806.
Zhang, K., Kniazeva, M., Han, M., Li, W., Yu, Z., Yang, Z., Li, Y., Metzker, M. L., Allikmets, R., Zack, D. J., Kakuk, L. E., Lagali, P. S., Wong, P. W., MacDonald, I. M., Sieving, P. A., Figueroa, D. J., Austin, C. P., Gould, R. J., Ayyagari, R. &

Petrukhin, K. 2001. A 5-bp deletion in ELOVL4 is associated with two related forms of autosomal dominant macular dystrophy. *Nat Genet,* 27, 89–93.

Zhang, L., Zheng, A., Nie, H., Bhavsar, K. V., Xu, Y., Sliney, D. H., Trokel, S. L. & Tsang, S. H. 2016. Laser-Induced Photic Injury Phenocopies Macular Dystrophy. *Ophthalmic Genet,* 37, 59–67.

Zhang, N., Tsybovsky, Y., Kolesnikov, A. V., Rozanowska, M., Swider, M., Schwartz, S. B., Stone, E. M., Palczewska, G., Maeda, A., Kefalov, V. J., Jacobson, S. G., Cideciyan, A. V. & Palczewski, K. 2015. Protein misfolding and the pathogenesis of ABCA4-associated retinal degenerations. *Hum Mol Genet,* 24, 3220–37.

Zhou, J., Jang, Y. P., Kim, S. R. & Sparrow, J. R. 2006. Complement activation by photooxidation products of A2E, a lipofuscin constituent of the retinal pigment epithelium. *Proc Natl Acad Sci U S A,* 103, 16182–7.

Zhou, J., Kim, S. R., Westlund, B. S. & Sparrow, J. R. 2009. Complement activation by bisretinoid constituents of RPE lipofuscin. *Invest Ophthalmol Vis Sci,* 50, 1392–9.

Tailor, R., Elaraoud, I., Good, P., Hope-Ross, M. & Scott, R. A. 2012. A case of severe hydroxychloroquine-induced retinal toxicity in a patient with recent onset of renal impairment: a review of the literature on the use of hydroxychloroquine in renal impairment. *Case Rep Ophthalmol Med,* 2012, 182747.

Testa, F., Rossi, S., Sodi, A., Passerini, I., Di Iorio, V., Della Corte, M., Banfi, S., Surace, E. M., Menchini, U., Auricchio, A. & Simonelli, F. 2012. Correlation between photoreceptor layer integrity and visual function in patients with Stargardt disease: implications for gene therapy. *Invest Ophthalmol Vis Sci,* 53, 4409–15.

Tsybovsky, Y., Molday, R. S. & Palczewski, K. 2010. The ATP-binding cassette transporter ABCA4: structural and functional properties and role in retinal disease. *Adv Exp Med Biol,* 703, 105–25.

van Driel, M. A., Maugeri, A., Klevering, B. J., Hoyng, C. B. & Cremers, F. P. 1998. ABCR unites what ophthalmologists divide(s). *Ophthalmic Genet,* 19, 117–22.

van Huet, R. A., Bax, N. M., Westeneng-Van Haaften, S. C., Muhamad, M., Zonneveld-Vrieling, M. N., Hoefsloot, L. H., Cremers, F. P., Boon, C. J., Klevering, B. J. & Hoyng, C. B. 2014. Foveal sparing in Stargardt disease. *Invest Ophthalmol Vis Sci,* 55, 7467–78.

Vandenbroucke, T., Buyl, R., De Zaeytijd, J., Bauwens, M., Uvijls, A., De Baere, E. & Leroy, B. P. 2015. Colour Vision in Stargardt Disease. *Ophthalmic Res,* 54, 181–94.

Wang, J. S. & Kefalov, V. J. 2011. The cone-specific visual cycle. *Prog Retin Eye Res,* 30, 115–28.

Vecino, E., Rodriguez, F. D., Ruzafa, N., Pereiro, X. & Sharma, S. C. 2016. Glia-neuron interactions in the mammalian retina. *Prog Retin Eye Res,* 51, 1–40.

Westeneng-van Haaften, S. C., Boon, C. J., Cremers, F. P., Hoefsloot, L. H., den Hollander, A. I. & Hoyng, C. B. 2012. Clinical and genetic characteristics of late-onset Stargardt's disease. *Ophthalmology,* 119, 1199–210.

Wiszniewski, W., Zaremba, C. M., Yatsenko, A. N., Jamrich, M., Wensel, T. G., Lewis, R. A. & Lupski, J. R. 2005. ABCA4 mutations causing mislocalization are found frequently in patients with severe retinal dystrophies. *Hum Mol Genet,* 14, 2769–78.

Wong, I. Y., Iu, L. P., Koizumi, H. & Lai, W. W. 2012. The inner segment/outer segment junction: what have we learnt so far? *Curr Opin Ophthalmol,* 23, 210–8.

Wright, K. W., Spegel, P. H. & Thompson, L. S. 2006. *Handbook of pediatric retinal disease*, Springer-Verlag New York.

Xu, H., Chen, M. & Forrester, J. V. 2009. Para-inflammation in the aging retina. *Prog Retin Eye Res,* 28, 348–68.

Yamashita, T., Yamashita, T., Shirasawa, M., Arimura, N., Terasaki, H. & Sakamoto, T. 2012. Repeatability and reproducibility of subfoveal choroidal thickness in normal eyes of Japanese using different SD-OCT devices. *Invest Ophthalmol Vis Sci,* 53, 1102–7.

Yanoff, M. & Duker, J. S. 2004. *Ophthalmology,* St Louis, Mosby.

Yatsenko, A. N., Shroyer, N. F., Lewis, R. A. & Lupski, J. R. 2001. Late-onset Stargardt disease is associated with missense mutations that map outside known functional regions of ABCR (ABCA4). *Hum Genet,* 108, 346–55.

Yau, K. W. 1994. Phototransduction mechanism in retinal rods and cones. The Friedenwald Lecture. *Invest Ophthalmol Vis Sci,* 35, 9–32.

Yau, K. W. & Hardie, R. C. 2009. Phototransduction motifs and variations. *Cell,* 139, 246–64.

9. SUMMARY IN ESTONIAN

Autosoom-retsessiivne Stargardti tõbi: fenotüübiline heterogeensus ja genotüübi-fenotüübi seosed

Stargardti tõbi (STGD1) on kõige sagedasem pärilik kollatähni düstroofia, mille esinemissageduseks hinnatakse olevat 1:8000–1:10 000 (Michaelides et al., 2003). Haigus on põhjustatud *ABCA4* geeni defektist, mille tulemusena häirub fotoretseptorites paikneva ning visuaaltsüklis olulise ABCA4 transporteri töö (Allikmets et al., 1997b, Molday and Zhang, 2010). Haiguse tulemusena koguneb võrkkesta pigmentepiteeli (RPE) rakkudesse toksiline ühend (lipofustsiin), mis viib RPE rakkude ja fotoretseptorite kaole. Samas on siiani diskussiooniks, kas primaarselt hävivad RPE rakud, viies sekundaarselt fotoretseptorite kaole, või toimub fotoretseptorites juba varem destruktiivseid kahjustusi (Cideciyan et al., 2004, Sparrow and Boulton, 2005, Duncker et al., 2014, Gomes et al., 2009).

Arvestades, et STGD1 on autosoom-retsessiivse pärilikkusega haigus ning kirjeldatud on enam kui 1000 haigustekkelise mutatsiooni, esineb kliinilises pildis ja haiguse väljakujunemise eas väga suur varieeruvus (Burke and Tsang, 2011). Fenotüübiliselt on STGD1 haigeid jaotatud vastavalt võrkkesta haaratusele nelja staadiumisse, kus esimene staadium väljendub isoleeritud kollatähni haigusena ja neljas staadium laiaulatusliku korioretinaalse atroofiana (Fishman, 1976). Elektrofüsioloogiliselt on samuti kirjeldatud erinevaid STGD1 fenotüüpe (Lois et al., 2001). Esineb haigeid, kellel on normaalne kepikeste ja kolvikeste massvastus, kuid ka neid, kellel kolvikeste või nii kolvikeste kui ka kepikeste funktsioon on oluliselt langenud (Lois et al., 2001). Haigus on enamasti varajase algusega ning sümptomid tekkivad tavaliselt teisel eludekaadil, kuid esineb ka hilis-algusega STGD1, kus haiguse sümptomid avalduvad tunduvalt hiljem (Westeneng-van Haaften et al., 2012).

Võrkkesta muutuste detailseks hindamiseks on kasutusel mitmeid võrkkesta kuvamisuuringuid, millest olulisemad on optiline koherentne tomograafia (SD-OCT) ja silmapõhja autofluorestsents- uuring (FAF). Esimene võimaldab visualiseerida erinevaid võrkkesta kihte, kuvades *in vivo* histoloogilise pildi, ning teine, autofluorestsents kuvamisuuring, võimaldab hinnata lipofustsiini distributsiooni ja RPE rakkude terviklikkust (Boon et al., 2008). Klassikaliselt on varajasteks STGD1 iseloomulikeks kliinilisteks leidudeks tähnilised kollakad ladestused ja kollatähni atroofia, mis võrkkesta kuvamisuuringutel väljenduvad lipofustsiini kogunemisest tekkiva autofluorestsents-signaali intensiivistumisena ja kollatähni piirkonna välisreetina atroofiana (Michaelides et al., 2003, Cideciyan et al., 2004, Huang et al., 2014). Samas võimaldavad detailsed kuvamisuuringud laiendada STGD1 fenotüübilist spektrit veelgi. Nüüdseks on STGD1 puhul kirjeldatud nii „foveat säilitavat“ (ingl.k *foveal sparing*) fenotüüpi kui ka fovea tühimikku (ingl.k *optical gap; foveal cavitation*) (Fujinami et al., 2013d, van Huet et al., 2014, Leng et al., 2012). Kumbki fenotüüp ei ole spetsiifiline STGD1, vaid on kirjeldatud mitmete erinevate võrkkesta düstroofiate korral

(Greenberg et al., 2014, Park et al., 2010, Sergouniotis et al., 2012). Foveat säilitava fenotüübi korral püsib võrkkesta terava nägemise punkt (fovea) suhteliselt kaua muutumatuna, vaatamata küllalt väljendunud leiule mujal võrkkestas, mistõttu säilib nägemisteravus suhteliselt kaua (van Huet et al., 2014). Fovea tühimik on aga SD-OCT-l ilmestuv fenotüüp, kus fovea fotoretseptorite kaost tekkib struktuurne tühimik fovea piirkonna võrkkesta väliskihti (Leng et al., 2012).

Genotüübi-fenotüübi seoseid on STGD1 puhul keeruline leida ja analüüsida, kuna esineb väga suur alleelne heterogeensus ning sama alleelse kombinatsiooniga patsiente esineb harva. Lisaks võib fenotüüp olla küllalt erinev ka sama alleelse kombinatsiooniga patsientidel, viidates haigust modifitseerivatele geenidele või keskkonna faktoritele (Lois et al., 1999, Michaelides et al., 2007). Varasemad uuringud on viidanud, et fenotüübi raskuse määrab ära mutatsiooni mõju ABCA4 aktiivsusele, samas ei pea funktsiooni hüpotees alati paika (Sun et al., 2000, Shroyer et al., 1999, van Driel et al., 1998, Cideciyan et al., 2009, Burke et al., 2012b).

Üks enim uuritud ja levinumaid *ABCA4* mutatsioone on p.G1961E. Kliinilised uuringud on näidanud, et kirjeldatud mutatsioon põhjustab nii liitheterosügootses kui ka homosügootses olekus enamasti tagasihoidlikumat kliinilist leidu (Cella et al., 2009, Burke et al., 2012a). Nendel haigetel algab haigus tavaliselt vanemas eas, avaldudes enamasti nn „härjasilma" meenutava kollatähni atroofiana, kusjuures kepikeste ja kolvikeste massvastus on normis (Cella et al., 2009). Kvantitatiivse autofluorestsentsuuringuga on näidatud, et p.G1961E mutatsiooniga esineb tagasihoidlikum lipofustsiini kogunemine, viidates võimalikule alternatiivsele patogeneesi mehhanismile (Burke et al., 2014).

Uurimistöö eesmärgid

- Analüüsida varaseid võrkkesta struktuurimuutuseid noortel STGD1 haigetel.
- Leida, kirjeldada ja analüüsida optilisel koherentsel tomograafial ilmestuvaid STGD1 fenotüüpe ja hinnata nende fenotüüpidega kaasnevat võrkkesta funktsiooni.
- Leida ja kirjeldada võimalikke Stargardti tõvega esinevaid genotüübi-fenotüübi seoseid.

Patsiendid ja meetodid

Uurimustöös kasutati Columbia Ülikooli silmakliiniku pärilike võrkkesta ehk reetina düstroofiate andmebaasi, mis sisaldab endas ka geneetiliselt kinnitatud STGD1 haigeid. Andmebaasis oli kahe esimese uuringu teostamise ajaks 179 STDG1 haiget, kellele olid teostatud nii SD-OCT kui ka FAF uuringud. Kuna andmebaas on ajas pidevalt täienev, siis kolmanda uuringu teostamise ajaks oli vastavate võrkkesta kuvamisuuringutega STGD1 haigete arv 200.

Võrkkesta struktuuri analüüsimiseks kasutasime silmapõhja fotosid, SD-OCT ja FAF kuvamisuuringuid. Funktsiooni hindamiseks kasutasime nägemis-

teravuse määramist, multifokaalset ja täisvälja elektroretinograafiat (ERG). Geenianalüüs oli esimesesse uuringusse kaasatud patsientidel teostatud *ABCA4* geenikiibiga või järgmise põlvkonna ja Sangeri sekveneerimisega. Teise ja kolmandasse uuringusse kaasatud patsientidel oli geenianalüüs teostatud vaid järgmise põlvkonna ja Sangeri sekveneerimisega.

Kuna esimeses uuringus soovisime hinnata varaseid võrkkesta struktuurimuutuseid ning STGD1 puhused sümptomid kujunevad välja tavaliselt 20ndateks eluaastateks, siis kaasasime uuringusse kõik STGD1 haiged, kelle võrkkesta struktuurianalüüsiks vajalikud kuvamisuuringud olid teostatud enne 20. eluaastat (keskmine haiguskestvus oli 3,2 a) . Kokku leidsime 179st haigest 26 vastava kriteeriumile vastavat STGD1 juhtu (keskmine vanus 12,9 a; vahemik 5–19 a). Haigetel mõõdeti ja analüüsiti SD-OCT piltidel võrkkesta ellipsoidtsooni (iseloomustab fotoretseptorite terviklikkust) ja välise piirimembraani paksust ja reflektiivsust kasutades Heidelberg Explorer tarkvara ja ImageJ programmi. Tulemusi võrreldi 30 kontrolluuritava (keskmine vanus 12,5 a; vahemik 4–20 a) võrkkesta vastavate parameetritega.

Teises uuringus uurisime fovea tühimikuga STGD1 haigete fenotüübi dünaamilist kujunemist, mõju võrkkesta funktsioonile ning mutatsioonide profiili (ehk genotüübi-fenotüübi seost). Vaadates läbi 179 STGD1 haige SD-OCT ülesvõtted, leidsime 15 haiget, kellel esines kirjeldatud fenotüüp.

Kolmandas uuringus kirjeldasime ja analüüsisime SD-OCT ilmestuvat foveat säilitava fenotüübi varianti, mida siiani on seostatud hüdroksüklorokviin (HCQ) toksilise võrkkesta muutusega (retinopaatiaga). Vaadates läbi 200 STGD1 haige SD-OCT pildid, leidsime 8 vastava fenotüübiga haiget. Analüüsisime ja kirjeldasime leitud haigete kuvamisuuringute, funktsiooni ja *ABCA4* geeniuuringute tulemusi.

Peamised tulemused ja järeldused

1) Lisaks klassikalisele seisukohale, kus STGD1 haigetel tekkib võrkkesta väliskihtide atroofia, näitasime, et noortel STGD1 haigetel esineb lisaks võrkkesta fotoretseptoreid iseloomustava kihi (ellipsoidtsooni) õhenemisele võrkkesta välise piirimembraani statistiliselt oluline paksenemine võrreldes kontrollgrupiga. Leid võib viidata võrkkesta Mülleri rakkude mööduvale hüpertroofiale vastusena fotoretseptorite tasandil esinevale stressile. Välise piirimembraani paksenemine võib olla STGD1 varajaseks kliiniliseks markeriks, mis omab kliinilist potentsiaali diagnoosimaks haigust varases faasis, kui tüüpiline STGD1 iseloomulik fenotüüp ei pruugi olla veel välja kujunenud.

2) Võrkkesta kuvamisuuringute analüüsil saab STGD1 esinevat fovea tühimikku jaotada 3 arengustaadiumisse. Algfaasis esineb kerge fovea aluse ellipsoidtsooni granulaarsus, mis progresseerudes viib selge tühimiku moodustumiseni. Lõppfaasis tühimik kaob, millele järgneb neuroreetina ja RPE atroofia. Sarnaselt mitmetele teistele uuringutele näitasime ka meie, et klassikaline arusaam STGD1 patogeneesist, kus primaarselt esineb lipofust-

siinist põhjustatud RPE atroofia, millele järgneb sekundaarne fotoretseptorite kadu, ei kehti kõikidele STGD1 haigetele. Kirjeldatud fenotüübiga haigetel esineb primaarselt just fotoretseptorite kadu, viidates võimalikule alternatiivsele patogeneesimehhanismile.

Kirjeldatud struktuuimuutusega patsientidel korelleerub nägemisteravus ellipsoidtsooni terviklikkusega, seetõttu on 1. staadiumi fovea tühimikuga patsientidel nägemisteravus suhteliselt vähe langenud erinevalt 2. ja 3. staadiumist, kus ellipsoidtsoon on rohkem haaratud. Kõigil fovea tühimikuga STGD1 haigetel, kellel oli ERG tehtud, olid täisvälja ERG vastused normis, viidates lokaalsele haigusprotsessile ning paremale haiguse prognoosile.

Stargardti tõbi võib fenokopeerida HCQ toksilist võrkkesta muutust, omades SD-OCT uuringul iseloomulikku konformatsiooni. Tekkib nn „foveat säilitava" fenotüübi variant, mille tulemusena on kollatähni teravanägemise punktis võrkkest suhteliselt hästi säilinud, kusjuures patsiendid on avastamise hetkel enamasti sümptomivabad ja väga hea nägemisteravusega. Kolmel patsiendil esines ka klassikaline „härjasilma" meenutav atroofiline ala ilma nähtavate STGD1 iseloomulike lipofustsiini ladestusteta, mistõttu võib haiguse diferentseerimine toksilisest HCQ retinopaatiast fenotüübiliselt olla pea võimatu. Sellest tulenevalt tuleks keerukamatel juhtudel kaaluda ka *ABCA4* skriinimist, et välistada STGD1. Kõigil haigetel, kelle oli tehtud ERG, olid täisvälja ERG vastused normis.

3) Fovea tühimik on STGD1 korral tugevalt seotud p.G1961E mutatsiooniga *ABCA4* geenis. Fovea tühimikuga haigete hulgas oli p.G1961E alleeli sagedus 46,7%, samas kui kogu STGD1 kohordis oli alleeli sagedus 13,4% ($p < 0.0001$).

Stargardti tõve iseloomustab märkimisväärne fenotüübiline heterogeensus. Kasutades kaasaegseid võrkkesta kuvamisuuringuid, analüüsisime võrkkesta väliskihtide varajasi struktuurimuutuseid, SD-OCT-l ilmestuvaid fenotüüpe ja kirjeldasime genotüübi-fenotüübi seost STGD1 haigetel. Fenotüüpide detailne iseloomustamine, dünaamika hindamine ja genotüübi-fenotüübi seoste kirjeldamine võiks potentsiaalset paremini aidata planeerida ja analüüsida ravimi, geeniteraapia ja tüvirakuteraapia uuringuid ning nende tulemusi STGD1 kontekstis.

10. ACKNOWLEDGEMENTS

The current studies were carried out at the Department of Ophthalmology, Columbia University, during my stay there as a research fellow. Working and studying in such a motivated, inspiring and supporting environment has been truly a lifetime experience.

This study was supported by grants from the National Eye Institute/National Institutes of Health (Bethesda, MD, USA) EY021163, EY019861, and EY019007 (Core Support for Vision Research), Foundation Fighting Blindness (Owings Mills, MD, USA), and an unrestricted funds from Research to Prevent Blindness (New York, NY, USA) to the Department of Ophthalmology, Columbia University.

I wish to thank Tartu University Hospital for supporting my PhD studies by nominating me for Tartu University Hospital PhD project scholarship.

I wish to express my sincere gratitude to all the people who have helped me in the present work, special thanks to:

- My supervisor Professor Rando Allikmets, who brought me to Stargardt disease enabling me to work with his team at the Columbia University. His mentorship has been vital for the present work and I wholeheartedly thank him for the opportunities he has given me.
- My supervisor Doctor Kuldar Kaljurand for the support and advice during my studies in the PhD program as well as in ophthalmology training in general. I would not have accomplished many things in my career without his support.
- My colleague and a good friend Winston Lee, without his help, support and motivation this work would not have been accomplished.
- Associate Professor Stephen H Tsang and Professor Stanley Chang from Columbia University Medical Center for enabling me to work with them. I learned a lot from them, their attitude towards research in general has been an important motivator.
- My colleagues in the Eye Clinic of Tarty University Hospital for their support and encouragement.
- Medical and research stuff at Columbia University, Department of Ophthalmology, for their kindest help and support.
- Professor Marina Aunapuu and Professor Andres Arend for introducing me the scientific work during my undergraduate studies by making it a very pleasant experience.
- Professor Pille Taba and Professor Katrin Õunap for reading and commenting on the thesis.
- My beloved Paula, my parents and sister for their support, patience and understanding during my PhD studies in Estonia and abroad.
- My lovely Emma, who has turned a new page in my life.

11. PUBLICATIONS

CURRICULUM VITAE

Name: Kalev Nõupuu
Date of birth: 09.06.1985, Tallinn, Estonia
Citizenship: Estonian
Address: 8 L. Puusepa Street, 51014, Tartu, Estonia
Phone: 7319 762
E-mail: kalev.noupuu@kliinikum.ee

Education and employment:

1993–2004	Tallinna Üldgümnaasium (Gold medal)
2004–2010	University of Tartu, Faculty of Medicine, Degree in Medicine
2010–2013	University of Tartu, Faculty of Medicine, Residency training in ophthalmology
2013	European Board of Ophthalmology (EBO) exam passed, Paris, France
2013–	University of Tartu, Faculty of Medicine, PhD studies in ophthalmology
2013–2014	Columbia University, Edward S. Harkness Eye Institute, Postdoctoral Research Fellow, New York, the United States
2015–	University of Tartu, Faculty of Medicine, Residency training in ophthalmic surgery subspecialty

Scientific work and professional organizations

Research fields: Retinal imaging, retinal dystrophies, Stargardt disease
Publications: 5 international
Membership: Estonian Ophthalmology Society
Fellow of European Board of Ophthalmology (FEBO)

List of publications

Nõupuu, K., Lee, W., Zernant, J., Greenstein, V. C., Tsang, S. H., Allikmets, R. 2016. Recessive Stargardt Disease Phenocopying Hydroxychloroquine Retinopathy. *Graefes Arch Clin Exp Ophthalmol*, 254, 865–72.

Lee, W*., Nõupuu, K*., Oll, M., Duncker, T., Burke, T., Zernant, J., Bearelly, S., Tsang, S. H., Sparrow, J. R., Allikmets, R. 2014. The External Limiting Membrane in Early-Onset Stargardt Disease. *Invest Ophthalmol Vis Sci*, 55, 6139–49
*Equivalent authors

Nõupuu, K., Lee, W., Zernant, J., Tsang, S. H., Allikmets, R. 2014. Structural and Genetic Assessment of the *ABCA4*- Associated Optical Gap Phenotype. *Invest Ophthalmol Vis Sci,* 55, 7217–26

Zernant, J., Collison, F. T., Lee, W., Fishman, G. A., Nõupuu, K., Yuang, B., Cai, C., Lupski, J. R., Yannuzzi, L. A., Tsang, S. H., Allikmets, R. 2014. Genetic and Clinical Analysis of ABCA4-Associated Disease in African American Patients. *Hum Mutat*, 35, 1187–94

Xie, Y. A., Lee, W., Cai, C., Gambin, T., Nõupuu, K., Sujirakul, T., Ayuso, C., Jhangiani, S., Muzny, D., Boerwinkle, E., Gibbs, R., Greenstein, V. C., Lupski, J. R., Tsang, S. H., Allikmets, R. 2014. New Syndrome with Retinitis Pigmentosa is Caused by Nonsense Mutations in Retinol Dehydrogenase RDH 11. *Hum Mol Genet*, 23, 5774–78

ELULOOKIRJELDUS

Nimi: Kalev Nõupuu
Sünniaeg: 09.06.1985, Tallinn, Eesti
Kodakondsus: Eesti
Aadress: L. Puusepa 8, Tartu 51014, Eesti
Telefon: 7319 762
E-post: kalev.noupuu@kliinikum.ee

Haridus- ja ametikäik:

1993–2004	Tallinna Üldgümnaasium (kuldmedal)
2004–2010	Tartu Ülikool, arstiteaduskond, arstiõpe
2010–2013	Tartu Ülikool, arstiteaduskond, silmahaiguste residentuur
2013	Euroopa Oftalmoloogia Erialaseltsi eksami sooritus, Pariis, Prantsusmaa
2013–	Tartu Ülikool, arstiteaduskond, doktoriõpe silmahaiguste erialal
2013–2014	Columbia Ülikool, Edward S. Harkness Eye Institute, õppe- ja teadustöö, New York, USA
2015–	Tartu Ülikool, arstiteaduskond, silmakirurgia kõrvaleriala residentuur

Teadus- ja erialane tegevus

Valdkonnad:	Reetina kuvamisuuringud, reetina düstroofiad, Stargardti tõbi
Publikatsioonid:	5 rahvusvahelist eriala publikatsiooni
Liikmelisus:	Eesti Oftalmoloogide Selts Euroopa Oftalmoloogia Erialaseltsi liige

Publikatsioonide nimekiri:

Nõupuu, K., Lee, W., Zernant, J., Greenstein, V. C., Tsang, S. H., Allikmets, R. 2016. Recessive Stargardt Disease Phenocopying Hydroxychloroquine Retinopathy. *Graefes Arch Clin Exp Ophthalmol*, 254, 865–72.

Lee, W*., Nõupuu, K*., Oll, M., Duncker, T., Burke, T., Zernant, J., Bearelly, S., Tsang, S. H., Sparrow, J. R., Allikmets, R. 2014. The External Limiting Membrane in Early-Onset Stargardt Disease. *Invest Ophthalmol Vis Sci*, 55, 6139–49

*Equivalent authors

Nõupuu, K., Lee, W., Zernant, J., Tsang, S. H., Allikmets, R. 2014. Structural and Genetic Assessment of the *ABCA4*- Associated Optical Gap Phenotype. *Invest Ophthalmol Vis Sci,* 55, 7217–26

Zernant, J., Collison, F. T., Lee, W., Fishman, G. A., Nõupuu, K., Yuang, B., Cai, C., Lupski, J. R., Yannuzzi, L. A., Tsang, S. H., Allikmets, R. 2014. Genetic and Clinical Analysis of ABCA4-Associated Disease in African American Patients. *Hum Mutat*, 35, 1187–94

Xie, Y. A., Lee, W., Cai, C., Gambin, T., Nõupuu, K., Sujirakul, T., Ayuso, C., Jhangiani, S., Muzny, D., Boerwinkle, E., Gibbs, R., Greenstein, V. C., Lupski, J. R., Tsang, S. H., Allikmets, R. 2014. New Syndrome with Retinitis Pigmentosa is Caused by Nonsense Mutations in Retinol Dehydrogenase RDH 11. *Hum Mol Genet*, 23, 5774–78

DISSERTATIONES MEDICINAE UNIVERSITATIS TARTUENSIS

1. **Heidi-Ingrid Maaroos**. The natural course of gastric ulcer in connection with chronic gastritis and *Helicobacter pylori*. Tartu, 1991.
2. **Mihkel Zilmer**. Na-pump in normal and tumorous brain tissues: Structural, functional and tumorigenesis aspects. Tartu, 1991.
3. **Eero Vasar**. Role of cholecystokinin receptors in the regulation of behaviour and in the action of haloperidol and diazepam. Tartu, 1992.
4. **Tiina Talvik**. Hypoxic-ischaemic brain damage in neonates (clinical, biochemical and brain computed tomographical investigation). Tartu, 1992.
5. **Ants Peetsalu**. Vagotomy in duodenal ulcer disease: A study of gastric acidity, serum pepsinogen I, gastric mucosal histology and *Helicobacter pylori*. Tartu, 1992.
6. **Marika Mikelsaar**. Evaluation of the gastrointestinal microbial ecosystem in health and disease. Tartu, 1992.
7. **Hele Everaus**. Immuno-hormonal interactions in chronic lymphocytic leukaemia and multiple myeloma. Tartu, 1993.
8. **Ruth Mikelsaar**. Etiological factors of diseases in genetically consulted children and newborn screening: dissertation for the commencement of the degree of doctor of medical sciences. Tartu, 1993.
9. **Agu Tamm**. On metabolic action of intestinal microflora: clinical aspects. Tartu, 1993.
10. **Katrin Gross**. Multiple sclerosis in South-Estonia (epidemiological and computed tomographical investigations). Tartu, 1993.
11. **Oivi Uibo**. Childhood coeliac disease in Estonia: occurrence, screening, diagnosis and clinical characterization. Tartu, 1994.
12. **Viiu Tuulik**. The functional disorders of central nervous system of chemistry workers. Tartu, 1994.
13. **Margus Viigimaa**. Primary haemostasis, antiaggregative and anticoagulant treatment of acute myocardial infarction. Tartu, 1994.
14. **Rein Kolk**. Atrial versus ventricular pacing in patients with sick sinus syndrome. Tartu, 1994.
15. **Toomas Podar**. Incidence of childhood onset type 1 diabetes mellitus in Estonia. Tartu, 1994.
16. **Kiira Subi**. The laboratory surveillance of the acute respiratory viral infections in Estonia. Tartu, 1995.
17. **Irja Lutsar**. Infections of the central nervous system in children (epidemiologic, diagnostic and therapeutic aspects, long term outcome). Tartu, 1995.
18. **Aavo Lang**. The role of dopamine, 5-hydroxytryptamine, sigma and NMDA receptors in the action of antipsychotic drugs. Tartu, 1995.
19. **Andrus Arak**. Factors influencing the survival of patients after radical surgery for gastric cancer. Tartu, 1996.

20. **Tõnis Karki**. Quantitative composition of the human lactoflora and method for its examination. Tartu, 1996.
21. **Reet Mändar**. Vaginal microflora during pregnancy and its transmission to newborn. Tartu, 1996.
22. **Triin Remmel**. Primary biliary cirrhosis in Estonia: epidemiology, clinical characterization and prognostication of the course of the disease. Tartu, 1996.
23. **Toomas Kivastik**. Mechanisms of drug addiction: focus on positive reinforcing properties of morphine. Tartu, 1996.
24. **Paavo Pokk**. Stress due to sleep deprivation: focus on $GABA_A$ receptor-chloride ionophore complex. Tartu, 1996.
25. **Kristina Allikmets**. Renin system activity in essential hypertension. Associations with atherothrombogenic cardiovascular risk factors and with the efficacy of calcium antagonist treatment. Tartu, 1996.
26. **Triin Parik**. Oxidative stress in essential hypertension: Associations with metabolic disturbances and the effects of calcium antagonist treatment. Tartu, 1996.
27. **Svetlana Päi**. Factors promoting heterogeneity of the course of rheumatoid arthritis. Tartu, 1997.
28. **Maarike Sallo**. Studies on habitual physical activity and aerobic fitness in 4 to 10 years old children. Tartu, 1997.
29. **Paul Naaber**. *Clostridium difficile* infection and intestinal microbial ecology. Tartu, 1997.
30. **Rein Pähkla**. Studies in pinoline pharmacology. Tartu, 1997.
31. **Andrus Juhan Voitk**. Outpatient laparoscopic cholecystectomy. Tartu, 1997.
32. **Joel Starkopf**. Oxidative stress and ischaemia-reperfusion of the heart. Tartu, 1997.
33. **Janika Kõrv**. Incidence, case-fatality and outcome of stroke. Tartu, 1998.
34. **Ülla Linnamägi**. Changes in local cerebral blood flow and lipid peroxidation following lead exposure in experiment. Tartu, 1998.
35. **Ave Minajeva**. Sarcoplasmic reticulum function: comparison of atrial and ventricular myocardium. Tartu, 1998.
36. **Oleg Milenin**. Reconstruction of cervical part of esophagus by revascularised ileal autografts in dogs. A new complex multistage method. Tartu, 1998.
37. **Sergei Pakriev**. Prevalence of depression, harmful use of alcohol and alcohol dependence among rural population in Udmurtia. Tartu, 1998.
38. **Allen Kaasik**. Thyroid hormone control over β-adrenergic signalling system in rat atria. Tartu, 1998.
39. **Vallo Matto**. Pharmacological studies on anxiogenic and antiaggressive properties of antidepressants. Tartu, 1998.
40. **Maire Vasar**. Allergic diseases and bronchial hyperreactivity in Estonian children in relation to environmental influences. Tartu, 1998.
41. **Kaja Julge**. Humoral immune responses to allergens in early childhood. Tartu, 1998.

42. **Heli Grünberg**. The cardiovascular risk of Estonian schoolchildren. A cross-sectional study of 9-, 12- and 15-year-old children. Tartu, 1998.
43. **Epp Sepp**. Formation of intestinal microbial ecosystem in children. Tartu, 1998.
44. **Mai Ots**. Characteristics of the progression of human and experimental glomerulopathies. Tartu, 1998.
45. **Tiina Ristimäe**. Heart rate variability in patients with coronary artery disease. Tartu, 1998.
46. **Leho Kõiv**. Reaction of the sympatho-adrenal and hypothalamo-pituitary-adrenocortical system in the acute stage of head injury. Tartu, 1998.
47. **Bela Adojaan**. Immune and genetic factors of childhood onset IDDM in Estonia. An epidemiological study. Tartu, 1999.
48. **Jakov Shlik**. Psychophysiological effects of cholecystokinin in humans. Tartu, 1999.
49. **Kai Kisand**. Autoantibodies against dehydrogenases of α-ketoacids. Tartu, 1999.
50. **Toomas Marandi**. Drug treatment of depression in Estonia. Tartu, 1999.
51. **Ants Kask**. Behavioural studies on neuropeptide Y. Tartu, 1999.
52. **Ello-Rahel Karelson**. Modulation of adenylate cyclase activity in the rat hippocampus by neuropeptide galanin and its chimeric analogs. Tartu, 1999.
53. **Tanel Laisaar**. Treatment of pleural empyema — special reference to intrapleural therapy with streptokinase and surgical treatment modalities. Tartu, 1999.
54. **Eve Pihl**. Cardiovascular risk factors in middle-aged former athletes. Tartu, 1999.
55. **Katrin Õunap**. Phenylketonuria in Estonia: incidence, newborn screening, diagnosis, clinical characterization and genotype/phenotype correlation. Tartu, 1999.
56. **Siiri Kõljalg**. *Acinetobacter* – an important nosocomial pathogen. Tartu, 1999.
57. **Helle Karro**. Reproductive health and pregnancy outcome in Estonia: association with different factors. Tartu, 1999.
58. **Heili Varendi**. Behavioral effects observed in human newborns during exposure to naturally occurring odors. Tartu, 1999.
59. **Anneli Beilmann**. Epidemiology of epilepsy in children and adolescents in Estonia. Prevalence, incidence, and clinical characteristics. Tartu, 1999.
60. **Vallo Volke**. Pharmacological and biochemical studies on nitric oxide in the regulation of behaviour. Tartu, 1999.
61. **Pilvi Ilves**. Hypoxic-ischaemic encephalopathy in asphyxiated term infants. A prospective clinical, biochemical, ultrasonographical study. Tartu, 1999.
62. **Anti Kalda**. Oxygen-glucose deprivation-induced neuronal death and its pharmacological prevention in cerebellar granule cells. Tartu, 1999.
63. **Eve-Irene Lepist**. Oral peptide prodrugs – studies on stability and absorption. Tartu, 2000.

64. **Jana Kivastik**. Lung function in Estonian schoolchildren: relationship with anthropometric indices and respiratory symptomas, reference values for dynamic spirometry. Tartu, 2000.
65. **Karin Kull**. Inflammatory bowel disease: an immunogenetic study. Tartu, 2000.
66. **Kaire Innos**. Epidemiological resources in Estonia: data sources, their quality and feasibility of cohort studies. Tartu, 2000.
67. **Tamara Vorobjova**. Immune response to *Helicobacter pylori* and its association with dynamics of chronic gastritis and epithelial cell turnover in antrum and corpus. Tartu, 2001.
68. **Ruth Kalda**. Structure and outcome of family practice quality in the changing health care system of Estonia. Tartu, 2001.
69. **Annika Krüüner**. *Mycobacterium tuberculosis* – spread and drug resistance in Estonia. Tartu, 2001.
70. **Marlit Veldi**. Obstructive Sleep Apnoea: Computerized Endopharyngeal Myotonometry of the Soft Palate and Lingual Musculature. Tartu, 2001.
71. **Anneli Uusküla**. Epidemiology of sexually transmitted diseases in Estonia in 1990–2000. Tartu, 2001.
72. **Ade Kallas**. Characterization of antibodies to coagulation factor VIII. Tartu, 2002.
73. **Heidi Annuk**. Selection of medicinal plants and intestinal lactobacilli as antimicrobil components for functional foods. Tartu, 2002.
74. **Aet Lukmann**. Early rehabilitation of patients with ischaemic heart disease after surgical revascularization of the myocardium: assessment of health-related quality of life, cardiopulmonary reserve and oxidative stress. A clinical study. Tartu, 2002.
75. **Maigi Eisen**. Pathogenesis of Contact Dermatitis: participation of Oxidative Stress. A clinical – biochemical study. Tartu, 2002.
76. **Piret Hussar**. Histology of the post-traumatic bone repair in rats. Elaboration and use of a new standardized experimental model – bicortical perforation of tibia compared to internal fracture and resection osteotomy. Tartu, 2002.
77. **Tõnu Rätsep**. Aneurysmal subarachnoid haemorrhage: Noninvasive monitoring of cerebral haemodynamics. Tartu, 2002.
78. **Marju Herodes**. Quality of life of people with epilepsy in Estonia. Tartu, 2003.
79. **Katre Maasalu**. Changes in bone quality due to age and genetic disorders and their clinical expressions in Estonia. Tartu, 2003.
80. **Toomas Sillakivi**. Perforated peptic ulcer in Estonia: epidemiology, risk factors and relations with *Helicobacter pylori*. Tartu, 2003.
81. **Leena Puksa**. Late responses in motor nerve conduction studies. F and A waves in normal subjects and patients with neuropathies. Tartu, 2003.
82. **Krista Lõivukene**. *Helicobacter pylori* in gastric microbial ecology and its antimicrobial susceptibility pattern. Tartu, 2003.

83. **Helgi Kolk**. Dyspepsia and *Helicobacter pylori* infection: the diagnostic value of symptoms, treatment and follow-up of patients referred for upper gastrointestinal endoscopy by family physicians. Tartu, 2003.
84. **Helena Soomer**. Validation of identification and age estimation methods in forensic odontology. Tartu, 2003.
85. **Kersti Oselin**. Studies on the human MDR1, MRP1, and MRP2 ABC transporters: functional relevance of the genetic polymorphisms in the *MDR1* and *MRP1* gene. Tartu, 2003.
86. **Jaan Soplepmann**. Peptic ulcer haemorrhage in Estonia: epidemiology, prognostic factors, treatment and outcome. Tartu, 2003.
87. **Margot Peetsalu**. Long-term follow-up after vagotomy in duodenal ulcer disease: recurrent ulcer, changes in the function, morphology and *Helicobacter pylori* colonisation of the gastric mucosa. Tartu, 2003.
88. **Kersti Klaamas**. Humoral immune response to *Helicobacter pylori* a study of host-dependent and microbial factors. Tartu, 2003.
89. **Pille Taba**. Epidemiology of Parkinson's disease in Tartu, Estonia. Prevalence, incidence, clinical characteristics, and pharmacoepidemiology. Tartu, 2003.
90. **Alar Veraksitš**. Characterization of behavioural and biochemical phenotype of cholecystokinin-2 receptor deficient mice: changes in the function of the dopamine and endopioidergic system. Tartu, 2003.
91. **Ingrid Kalev**. CC-chemokine receptor 5 (CCR5) gene polymorphism in Estonians and in patients with Type I and Type II diabetes mellitus. Tartu, 2003.
92. **Lumme Kadaja**. Molecular approach to the regulation of mitochondrial function in oxidative muscle cells. Tartu, 2003.
93. **Aive Liigant**. Epidemiology of primary central nervous system tumours in Estonia from 1986 to 1996. Clinical characteristics, incidence, survival and prognostic factors. Tartu, 2004.
94. **Andres, Kulla**. Molecular characteristics of mesenchymal stroma in human astrocytic gliomas. Tartu, 2004.
95. **Mari Järvelaid**. Health damaging risk behaviours in adolescence. Tartu, 2004.
96. **Ülle Pechter**. Progression prevention strategies in chronic renal failure and hypertension. An experimental and clinical study. Tartu, 2004.
97. **Gunnar Tasa**. Polymorphic glutathione S-transferases – biology and role in modifying genetic susceptibility to senile cataract and primary open angle glaucoma. Tartu, 2004.
98. **Tuuli Käämbre**. Intracellular energetic unit: structural and functional aspects. Tartu, 2004.
99. **Vitali Vassiljev**. Influence of nitric oxide syntase inhibitors on the effects of ethanol after acute and chronic ethanol administration and withdrawal. Tartu, 2004.

100. **Aune Rehema**. Assessment of nonhaem ferrous iron and glutathione redox ratio as markers of pathogeneticity of oxidative stress in different clinical groups. Tartu, 2004.
101. **Evelin Seppet**. Interaction of mitochondria and ATPases in oxidative muscle cells in normal and pathological conditions. Tartu, 2004.
102. **Eduard Maron**. Serotonin function in panic disorder: from clinical experiments to brain imaging and genetics. Tartu, 2004.
103. **Marje Oona**. *Helicobacter pylori* infection in children: epidemiological and therapeutic aspects. Tartu, 2004.
104. **Kersti Kokk**. Regulation of active and passive molecular transport in the testis. Tartu, 2005.
105. **Vladimir Järv**. Cross-sectional imaging for pretreatment evaluation and follow-up of pelvic malignant tumours. Tartu, 2005.
106. **Andre Õun**. Epidemiology of adult epilepsy in Tartu, Estonia. Incidence, prevalence and medical treatment. Tartu, 2005.
107. **Piibe Muda**. Homocysteine and hypertension: associations between homocysteine and essential hypertension in treated and untreated hypertensive patients with and without coronary artery disease. Tartu, 2005.
108. **Külli Kingo**. The interleukin-10 family cytokines gene polymorphisms in plaque psoriasis. Tartu, 2005.
109. **Mati Merila**. Anatomy and clinical relevance of the glenohumeral joint capsule and ligaments. Tartu, 2005.
110. **Epp Songisepp**. Evaluation of technological and functional properties of the new probiotic *Lactobacillus fermentum* ME-3. Tartu, 2005.
111. **Tiia Ainla**. Acute myocardial infarction in Estonia: clinical characteristics, management and outcome. Tartu, 2005.
112. **Andres Sell**. Determining the minimum local anaesthetic requirements for hip replacement surgery under spinal anaesthesia – a study employing a spinal catheter. Tartu, 2005.
113. **Tiia Tamme**. Epidemiology of odontogenic tumours in Estonia. Pathogenesis and clinical behaviour of ameloblastoma. Tartu, 2005.
114. **Triine Annus**. Allergy in Estonian schoolchildren: time trends and characteristics. Tartu, 2005.
115. **Tiia Voor**. Microorganisms in infancy and development of allergy: comparison of Estonian and Swedish children. Tartu, 2005.
116. **Priit Kasenõmm**. Indicators for tonsillectomy in adults with recurrent tonsillitis – clinical, microbiological and pathomorphological investigations. Tartu, 2005.
117. **Eva Zusinaite**. Hepatitis C virus: genotype identification and interactions between viral proteases. Tartu, 2005.
118. **Piret Kõll**. Oral lactoflora in chronic periodontitis and periodontal health. Tartu, 2006.
119. **Tiina Stelmach**. Epidemiology of cerebral palsy and unfavourable neurodevelopmental outcome in child population of Tartu city and county, Estonia Prevalence, clinical features and risk factors. Tartu, 2006.

120. **Katrin Pudersell**. Tropane alkaloid production and riboflavine excretion in the field and tissue cultures of henbane (*Hyoscyamus niger* L.). Tartu, 2006.
121. **Külli Jaako**. Studies on the role of neurogenesis in brain plasticity. Tartu, 2006.
122. **Aare Märtson**. Lower limb lengthening: experimental studies of bone regeneration and long-term clinical results. Tartu, 2006.
123. **Heli Tähepõld**. Patient consultation in family medicine. Tartu, 2006.
124. **Stanislav Liskmann**. Peri-implant disease: pathogenesis, diagnosis and treatment in view of both inflammation and oxidative stress profiling. Tartu, 2006.
125. **Ruth Rudissaar**. Neuropharmacology of atypical antipsychotics and an animal model of psychosis. Tartu, 2006.
126. **Helena Andreson**. Diversity of *Helicobacter pylori* genotypes in Estonian patients with chronic inflammatory gastric diseases. Tartu, 2006.
127. **Katrin Pruus**. Mechanism of action of antidepressants: aspects of serotoninergic system and its interaction with glutamate. Tartu, 2006.
128. **Priit Põder**. Clinical and experimental investigation: relationship of ischaemia/reperfusion injury with oxidative stress in abdominal aortic aneurysm repair and in extracranial brain artery endarterectomy and possibilities of protection against ischaemia using a glutathione analogue in a rat model of global brain ischaemia. Tartu, 2006.
129. **Marika Tammaru**. Patient-reported outcome measurement in rheumatoid arthritis. Tartu, 2006.
130. **Tiia Reimand**. Down syndrome in Estonia. Tartu, 2006.
131. **Diva Eensoo**. Risk-taking in traffic and Markers of Risk-Taking Behaviour in Schoolchildren and Car Drivers. Tartu, 2007.
132. **Riina Vibo**. The third stroke registry in Tartu, Estonia from 2001 to 2003: incidence, case-fatality, risk factors and long-term outcome. Tartu, 2007.
133. **Chris Pruunsild**. Juvenile idiopathic arthritis in children in Estonia. Tartu, 2007.
134. **Eve Õiglane-Šlik**. Angelman and Prader-Willi syndromes in Estonia. Tartu, 2007.
135. **Kadri Haller**. Antibodies to follicle stimulating hormone. Significance in female infertility. Tartu, 2007.
136. **Pille Ööpik**. Management of depression in family medicine. Tartu, 2007.
137. **Jaak Kals**. Endothelial function and arterial stiffness in patients with atherosclerosis and in healthy subjects. Tartu, 2007.
138. **Priit Kampus**. Impact of inflammation, oxidative stress and age on arterial stiffness and carotid artery intima-media thickness. Tartu, 2007.
139. **Margus Punab**. Male fertility and its risk factors in Estonia. Tartu, 2007.
140. **Alar Toom**. Heterotopic ossification after total hip arthroplasty: clinical and pathogenetic investigation. Tartu, 2007.

141. **Lea Pehme**. Epidemiology of tuberculosis in Estonia 1991–2003 with special regard to extrapulmonary tuberculosis and delay in diagnosis of pulmonary tuberculosis. Tartu, 2007.
142. **Juri Karjagin**. The pharmacokinetics of metronidazole and meropenem in septic shock. Tartu, 2007.
143. **Inga Talvik**. Inflicted traumatic brain injury shaken baby syndrome in Estonia – epidemiology and outcome. Tartu, 2007.
144. **Tarvo Rajasalu**. Autoimmune diabetes: an immunological study of type 1 diabetes in humans and in a model of experimental diabetes (in RIP-B7.1 mice). Tartu, 2007.
145. **Inga Karu**. Ischaemia-reperfusion injury of the heart during coronary surgery: a clinical study investigating the effect of hyperoxia. Tartu, 2007.
146. **Peeter Padrik**. Renal cell carcinoma: Changes in natural history and treatment of metastatic disease. Tartu, 2007.
147. **Neve Vendt**. Iron deficiency and iron deficiency anaemia in infants aged 9 to 12 months in Estonia. Tartu, 2008.
148. **Lenne-Triin Heidmets**. The effects of neurotoxins on brain plasticity: focus on neural Cell Adhesion Molecule. Tartu, 2008.
149. **Paul Korrovits**. Asymptomatic inflammatory prostatitis: prevalence, etiological factors, diagnostic tools. Tartu, 2008.
150. **Annika Reintam**. Gastrointestinal failure in intensive care patients. Tartu, 2008.
151. **Kristiina Roots**. Cationic regulation of Na-pump in the normal, Alzheimer's and CCK_2 receptor-deficient brain. Tartu, 2008.
152. **Helen Puusepp**. The genetic causes of mental retardation in Estonia: fragile X syndrome and creatine transporter defect. Tartu, 2009.
153. **Kristiina Rull**. Human chorionic gonadotropin beta genes and recurrent miscarriage: expression and variation study. Tartu, 2009.
154. **Margus Eimre**. Organization of energy transfer and feedback regulation in oxidative muscle cells. Tartu, 2009.
155. **Maire Link**. Transcription factors FoxP3 and AIRE: autoantibody associations. Tartu, 2009.
156. **Kai Haldre**. Sexual health and behaviour of young women in Estonia. Tartu, 2009.
157. **Kaur Liivak**. Classical form of congenital adrenal hyperplasia due to 21-hydroxylase deficiency in Estonia: incidence, genotype and phenotype with special attention to short-term growth and 24-hour blood pressure. Tartu, 2009.
158. **Kersti Ehrlich**. Antioxidative glutathione analogues (UPF peptides) – molecular design, structure-activity relationships and testing the protective properties. Tartu, 2009.
159. **Anneli Rätsep**. Type 2 diabetes care in family medicine. Tartu, 2009.
160. **Silver Türk**. Etiopathogenetic aspects of chronic prostatitis: role of mycoplasmas, coryneform bacteria and oxidative stress. Tartu, 2009.

161. **Kaire Heilman**. Risk markers for cardiovascular disease and low bone mineral density in children with type 1 diabetes. Tartu, 2009.
162. **Kristi Rüütel**. HIV-epidemic in Estonia: injecting drug use and quality of life of people living with HIV. Tartu, 2009.
163. **Triin Eller**. Immune markers in major depression and in antidepressive treatment. Tartu, 2009.
164. **Siim Suutre**. The role of TGF-β isoforms and osteoprogenitor cells in the pathogenesis of heterotopic ossification. An experimental and clinical study of hip arthroplasty. Tartu, 2010.
165. **Kai Kliiman**. Highly drug-resistant tuberculosis in Estonia: Risk factors and predictors of poor treatment outcome. Tartu, 2010.
166. **Inga Villa**. Cardiovascular health-related nutrition, physical activity and fitness in Estonia. Tartu, 2010.
167. **Tõnis Org**. Molecular function of the first PHD finger domain of Autoimmune Regulator protein. Tartu, 2010.
168. **Tuuli Metsvaht**. Optimal antibacterial therapy of neonates at risk of early onset sepsis. Tartu, 2010.
169. **Jaanus Kahu**. Kidney transplantation: Studies on donor risk factors and mycophenolate mofetil. Tartu, 2010.
170. **Koit Reimand**. Autoimmunity in reproductive failure: A study on associated autoantibodies and autoantigens. Tartu, 2010.
171. **Mart Kull**. Impact of vitamin D and hypolactasia on bone mineral density: a population based study in Estonia. Tartu, 2010.
172. **Rael Laugesaar**. Stroke in children – epidemiology and risk factors. Tartu, 2010.
173. **Mark Braschinsky**. Epidemiology and quality of life issues of hereditary spastic paraplegia in Estonia and implemention of genetic analysis in everyday neurologic practice. Tartu, 2010.
174. **Kadri Suija**. Major depression in family medicine: associated factors, recurrence and possible intervention. Tartu, 2010.
175. **Jarno Habicht**. Health care utilisation in Estonia: socioeconomic determinants and financial burden of out-of-pocket payments. Tartu, 2010.
176. **Kristi Abram**. The prevalence and risk factors of rosacea. Subjective disease perception of rosacea patients. Tartu, 2010.
177. **Malle Kuum**. Mitochondrial and endoplasmic reticulum cation fluxes: Novel roles in cellular physiology. Tartu, 2010.
178. **Rita Teek**. The genetic causes of early onset hearing loss in Estonian children. Tartu, 2010.
179. **Daisy Volmer**. The development of community pharmacy services in Estonia – public and professional perceptions 1993–2006. Tartu, 2010.
180. **Jelena Lissitsina**. Cytogenetic causes in male infertility. Tartu, 2011.
181. **Delia Lepik**. Comparison of gunshot injuries caused from Tokarev, Makarov and Glock 19 pistols at different firing distances. Tartu, 2011.
182. **Ene-Renate Pähkla**. Factors related to the efficiency of treatment of advanced periodontitis. Tartu, 2011.

183. **Maarja Krass**. L-Arginine pathways and antidepressant action. Tartu, 2011.
184. **Taavi Lai**. Population health measures to support evidence-based health policy in Estonia. Tartu, 2011.
185. **Tiit Salum**. Similarity and difference of temperature-dependence of the brain sodium pump in normal, different neuropathological, and aberrant conditions and its possible reasons. Tartu, 2011.
186. **Tõnu Vooder**. Molecular differences and similarities between histological subtypes of non-small cell lung cancer. Tartu, 2011.
187. **Jelena Štšepetova**. The characterisation of intestinal lactic acid bacteria using bacteriological, biochemical and molecular approaches. Tartu, 2011.
188. **Radko Avi**. Natural polymorphisms and transmitted drug resistance in Estonian HIV-1 CRF06_cpx and its recombinant viruses. Tartu, 2011, 116 p.
189. **Edward Laane**. Multiparameter flow cytometry in haematological malignancies. Tartu, 2011, 152 p.
190. **Triin Jagomägi**. A study of the genetic etiology of nonsyndromic cleft lip and palate. Tartu, 2011, 158 p.
191. **Ivo Laidmäe**. Fibrin glue of fish (*Salmo salar*) origin: immunological study and development of new pharmaceutical preparation. Tartu, 2012, 150 p.
192. **Ülle Parm**. Early mucosal colonisation and its role in prediction of invasive infection in neonates at risk of early onset sepsis. Tartu, 2012, 168 p.
193. **Kaupo Teesalu**. Autoantibodies against desmin and transglutaminase 2 in celiac disease: diagnostic and functional significance. Tartu, 2012, 142 p.
194. **Maksim Zagura**. Biochemical, functional and structural profiling of arterial damage in atherosclerosis. Tartu, 2012, 162 p.
195. **Vivian Kont**. Autoimmune regulator: characterization of thymic gene regulation and promoter methylation. Tartu, 2012, 134 p.
196. **Pirje Hütt**. Functional properties, persistence, safety and efficacy of potential probiotic lactobacilli. Tartu, 2012, 246 p.
197. **Innar Tõru**. Serotonergic modulation of CCK-4- induced panic. Tartu, 2012, 132 p.
198. **Sigrid Vorobjov**. Drug use, related risk behaviour and harm reduction interventions utilization among injecting drug users in Estonia: implications for drug policy. Tartu, 2012, 120 p.
199. **Martin Serg**. Therapeutic aspects of central haemodynamics, arterial stiffness and oxidative stress in hypertension. Tartu, 2012, 156 p.
200. **Jaanika Kumm**. Molecular markers of articular tissues in early knee osteoarthritis: a population-based longitudinal study in middle-aged subjects. Tartu, 2012, 159 p.
201. **Kertu Rünkorg**. Functional changes of dopamine, endopioid and endocannabinoid systems in CCK2 receptor deficient mice. Tartu, 2012, 125 p.
202. **Mai Blöndal**. Changes in the baseline characteristics, management and outcomes of acute myocardial infarction in Estonia. Tartu, 2012, 127 p.

203. **Jana Lass**. Epidemiological and clinical aspects of medicines use in children in Estonia. Tartu, 2012, 170 p.
204. **Kai Truusalu**. Probiotic lactobacilli in experimental persistent *Salmonella* infection. Tartu, 2013, 139 p.
205. **Oksana Jagur**. Temporomandibular joint diagnostic imaging in relation to pain and bone characteristics. Long-term results of arthroscopic treatment. Tartu, 2013, 126 p.
206. **Katrin Sikk**. Manganese-ephedrone intoxication – pathogenesis of neurological damage and clinical symptomatology. Tartu, 2013, 125 p.
207. **Kai Blöndal**. Tuberculosis in Estonia with special emphasis on drug-resistant tuberculosis: Notification rate, disease recurrence and mortality. Tartu, 2013, 151 p.
208. **Marju Puurand**. Oxidative phosphorylation in different diseases of gastric mucosa. Tartu, 2013, 123 p.
209. **Aili Tagoma**. Immune activation in female infertility: Significance of autoantibodies and inflammatory mediators. Tartu, 2013, 135 p.
210. **Liis Sabre**. Epidemiology of traumatic spinal cord injury in Estonia. Brain activation in the acute phase of traumatic spinal cord injury. Tartu, 2013, 135 p.
211. **Merit Lamp**. Genetic susceptibility factors in endometriosis. Tartu, 2013, 125 p.
212. **Erik Salum**. Beneficial effects of vitamin D and angiotensin II receptor blocker on arterial damage. Tartu, 2013, 167 p.
213. **Maire Karelson**. Vitiligo: clinical aspects, quality of life and the role of melanocortin system in pathogenesis. Tartu, 2013, 153 p.
214. **Kuldar Kaljurand**. Prevalence of exfoliation syndrome in Estonia and its clinical significance. Tartu, 2013, 113 p.
215. **Raido Paasma**. Clinical study of methanol poisoning: handling large outbreaks, treatment with antidotes, and long-term outcomes. Tartu, 2013, 96 p.
216. **Anne Kleinberg**. Major depression in Estonia: prevalence, associated factors, and use of health services. Tartu, 2013, 129 p.
217. **Triin Eglit**. Obesity, impaired glucose regulation, metabolic syndrome and their associations with high-molecular-weight adiponectin levels. Tartu, 2014, 115 p.
218. **Kristo Ausmees**. Reproductive function in middle-aged males: Associations with prostate, lifestyle and couple infertility status. Tartu, 2014, 125 p.
219. **Kristi Huik**. The influence of host genetic factors on the susceptibility to HIV and HCV infections among intravenous drug users. Tartu, 2014, 144 p.
220. **Liina Tserel**. Epigenetic profiles of monocytes, monocyte-derived macrophages and dendritic cells. Tartu, 2014, 143 p.
221. **Irina Kerna**. The contribution of *ADAM12* and *CILP* genes to the development of knee osteoarthritis. Tartu, 2014, 152 p.

222. **Ingrit Liiv**. Autoimmune regulator protein interaction with DNA-dependent protein kinase and its role in apoptosis. Tartu, 2014, 143 p.
223. **Liivi Maddison**. Tissue perfusion and metabolism during intra-abdominal hypertension. Tartu, 2014, 103 p.
224. **Krista Ress**. Childhood coeliac disease in Estonia, prevalence in atopic dermatitis and immunological characterisation of coexistence. Tartu, 2014, 124 p.
225. **Kai Muru**. Prenatal screening strategies, long-term outcome of children with marked changes in maternal screening tests and the most common syndromic heart anomalies in Estonia. Tartu, 2014, 189 p.
226. **Kaja Rahu**. Morbidity and mortality among Baltic Chernobyl cleanup workers: a register-based cohort study. Tartu, 2014, 155 p.
227. **Klari Noormets**. The development of diabetes mellitus, fertility and energy metabolism disturbances in a Wfs1-deficient mouse model of Wolfram syndrome. Tartu, 2014, 132 p.
228. **Liis Toome**. Very low gestational age infants in Estonia. Tartu, 2014, 183 p.
229. **Ceith Nikkolo**. Impact of different mesh parameters on chronic pain and foreign body feeling after open inguinal hernia repair. Tartu, 2014, 132 p.
230. **Vadim Brjalin**. Chronic hepatitis C: predictors of treatment response in Estonian patients. Tartu, 2014, 122 p.
231. **Vahur Metsna**. Anterior knee pain in patients following total knee arthroplasty: the prevalence, correlation with patellar cartilage impairment and aspects of patellofemoral congruence. Tartu, 2014, 130 p.
232. **Marju Kase**. Glioblastoma multiforme: possibilities to improve treatment efficacy. Tartu, 2015, 137 p.
233. **Riina Runnel**. Oral health among elementary school children and the effects of polyol candies on the prevention of dental caries. Tartu, 2015, 112 p.
234. **Made Laanpere**. Factors influencing women's sexual health and reproductive choices in Estonia. Tartu, 2015, 176 p.
235. **Andres Lust**. Water mediated solid state transformations of a polymorphic drug – effect on pharmaceutical product performance. Tartu, 2015, 134 p.
236. **Anna Klugman**. Functionality related characterization of pretreated wood lignin, cellulose and polyvinylpyrrolidone for pharmaceutical applications. Tartu, 2015, 156 p.
237. **Triin Laisk-Podar**. Genetic variation as a modulator of susceptibility to female infertility and a source for potential biomarkers. Tartu, 2015, 155 p.
238. **Mailis Tõnisson**. Clinical picture and biochemical changes in blood in children with acute alcohol intoxication. Tartu, 2015, 100 p.
239. **Kadri Tamme**. High volume haemodiafiltration in treatment of severe sepsis – impact on pharmacokinetics of antibiotics and inflammatory response. Tartu, 2015, 133 p.

240. **Kai Part**. Sexual health of young people in Estonia in a social context: the role of school-based sexuality education and youth-friendly counseling services. Tartu, 2015, 203 p.
241. **Urve Paaver**. New perspectives for the amorphization and physical stabilization of poorly water-soluble drugs and understanding their dissolution behavior. Tartu, 2015, 139 p.
242. **Aleksandr Peet**. Intrauterine and postnatal growth in children with HLA-conferred susceptibility to type 1 diabetes. Tartu. 2015, 146 p.
243. **Piret Mitt**. Healthcare-associated infections in Estonia – epidemiology and surveillance of bloodstream and surgical site infections. Tartu, 2015, 145 p.
244. **Merli Saare**. Molecular Profiling of Endometriotic Lesions and Endometria of Endometriosis Patients. Tartu, 2016, 129 p.
245. **Kaja-Triin Laisaar**. People living with HIV in Estonia: Engagement in medical care and methods of increasing adherence to antiretroviral therapy and safe sexual behavior. Tartu, 2016, 132 p.
246. **Eero Merilind**. Primary health care performance: impact of payment and practice-based characteristics. Tartu, 2016, 120 p.
247. **Jaanika Kärner**. Cytokine-specific autoantibodies in AIRE deficiency. Tartu, 2016, 182 p.
248. **Kaido Paapstel**. Metabolomic profile of arterial stiffness and early biomarkers of renal damage in atherosclerosis. Tartu, 2016, 173 p.
249. **Liidia Kiisk.** Long-term nutritional study: anthropometrical and clinico-laboratory assessments in renal replacement therapy patients after intensive nutritional counselling. Tartu, 2016, 207 p.
250. **Georgi Nellis**. The use of excipients in medicines administered to neonates in Europe. Tartu, 2017, 159 p.
251. **Aleksei Rakitin**. Metabolic effects of acute and chronic treatment with valproic acid in people with epilepsy. Tartu, 2017, 125 p.
252. **Eveli Kallas**. The influence of immunological markers to susceptibility to HIV, HBV, and HCV infections among persons who inject drugs. Tartu, 2017, 138 p.
253. **Tiina Freimann.** Musculoskeletal pain among nurses: prevalence, risk factors, and intervention. Tartu, 2017, 125 p.
254. **Evelyn Aaviksoo.** Sickness absence in Estonia: determinants and influence of the sick-pay cut reform. Tartu, 2017, 121 p.